ON THE PHENOMENOLOGICAL THEORY OF LINEAR RELAXATION PROCESSES

J. SCHRAMA

ON THE PHENOMENOLOGICAL THEORY OF LINEAR RELAXATION PROCESSES

ON THE PHENOMENOLOGICAL THEORY OF LINEAR RELAXATION PROCESSES

PROEFSCHRIFT

TER VERKRIJGING VAN DE GRAAD VAN DOCTOR IN DE WIS- EN NATUURKUNDE AAN DE RIJKSUNIVERSITEIT TE LEIDEN OP GEZAG VAN DE RECTOR MAGNIFICUS Dr. S. E. DE JONGH, HOOGLERAAR IN DE FACULTEIT DER GENEESKUNDE, TEGEN DE BEDENKINGEN VAN DE FACULTEIT DER WIS- EN NATUURKUNDE TE VERDEDIGEN OP WOENSDAG 25 SEPTEMBER 1957 TE 15 UUR

DOOR

JACOBUS SCHRAMA
GEBOREN TE LEIDEN IN 1924

UITGEVERIJ EXCELSIOR - ORANJEPLEIN 96 - 'S-GRAVENHAGE

Promotor: Prof. Dr. C.J.F.Böttcher

Aan mijn Moeder
Aan de nagedachtenis van mijn Vader
Aan mijn Vrouw

INTRODUCTION

A large number of publications dealing with mechanical and dielectric relaxation processes has appeared in the physicochemical literature of the last two decades. Although the fundamental similarity of all linear relaxational behaviour has repeatedly been pointed out and a fairly complete phenomenological theory of mechanical relaxation was formulated by Gross, Schwarzl, Alfrey, and others, it may be stated that the explicit transcription of this theory to dielectric and other relaxation processes has not received the attention it deserves.

One of the objects of the present investigation was to transcribe the existing theory into the symbolism of dielectric dispersion and loss. As might be expected, this explicit formulation of the dielectric theory was partly found to be a trivial task; the adaptation to the description of other relaxation phenomena proved to be equally straightforward. However, a non-trivial aspect of the unified phenomenological theory is that the duality in the description of mechanical relaxational behaviour finds no counterpart in the description of other relaxation processes. This subject is discussed in some detail in the following pages.

Other objects of the investigation were, first, to attain a better understanding of the Cole-Cole diagram, which is especially important in the phenomenology of dielectric relaxation, and the discussion of which is somewhat neglected in the mechanical theory; second, to give a critical analysis of the significance of the distribution functions; third, to develop a method for the numerical evaluation of the distribution functions from experimental data.

The present subject is concerned with the physical behaviour of a special class of *linear systems*. Probably the best known representatives of linear systems are those described in network theory; consequently, frequent use is made of both the concepts and the mathematical tools of the theories of electric and mechanical networks. A general discussion and formulation of the theory of linear systems falls outside the scope of the present thesis, however.

In the first three chapters considerable attention is given to

the exposition of the mathematical methods. This includes the discussion of physical analogies the author found helpful for the understanding of the mathematical aspects of relaxational behaviour. In the author's opinion, the dissemination of many valuable ideas contained in papers on the macroscopic theory of relaxation processes has been impeded by the excessively concise and abstract form of these publications. This should be kept in mind whenever, in the following pages, the argument appears unnecessarily long to those experienced in the mathematical theory of linear systems.

A few words should be said to justify the rather one-sided macroscopic treatment of relaxation processes in the present thesis. There is a general feeling that one achieves a deeper insight into the nature of these processes by the methods of statistical mechanics and kinetic theory. However, the following two quotations from P.W. Bridgman's *The Nature of Thermodynamics*: "The small-scale stuff is only a model, obtained by extrapolation of the large-scale stuff." and "The only check on the extrapolation is that when worked backward it shall again produce the large-scale stuff." aptly describe the state of affairs in the molecular theory of relaxation processes. Specific problems encountered in the microscopic interpretation of relaxational behaviour are those inherent in the small-scale understanding of dissipative processes and the difficulties associated with the internal field concept. The latter are well-known from the theory of electric polarization and have as yet not been solved even for equilibrium systems. Nevertheless, some relaxation processes have been completely elucidated through unambiguous correlation with other molecular processes.

Hypothetical views as to the constitution of relaxational systems or the nature of energy dissipation are not used in the first four chapters. This restriction has ensured generality of the discussion and expression of the results in terms of quantities which can be determined directly by experiment. Some molecular mechanisms of relaxational behaviour are reviewed in Chapter 5.

Another limitation of the present thesis is that it does not deal with the experimentally important situations arising in the measurements of relaxational behaviour by means of standing and travelling wave techniques. It was felt, however, that a necessarily lengthy discussion on this subject would not be relevant to the main objects of the investigation, and that it would have detracted from the generality of the argument.

Owing to the variety of physical systems mentioned in the following pages, the nomenclature presented some difficulties. The final choice of the symbols has been governed by the requirements of conformity with at least one nomenclature in the theory of mechanical relaxation, and of avoidance of proximity in the text of the same symbol for different physical quantities.

Chapter 1

VISCOELASTICITY

1.1. The linear viscoelastic body: transient phenomena

Many solids show a striking behaviour when suddenly subjected to a constant mechanical tension: after an instantaneous elongation at the moment of application of the stress a retarded deformation occurs at a continually decreasing rate. Although the rate of the time dependent process is sometimes found to approach a positive constant value, we will be concerned primarily with those instances in which the constant value is zero, that is, in which the ultimate deformation is finite. When the process has come to an end, from the experimental point of view, and the load is suddenly removed, it is found that the above phenomena are reversed. One observes an instantaneous contraction followed by a continually slower decrease in length.

Similarly, application of a sudden shear stress or an isotropic pressure gives rise to analogous changes in time of the angle of shear or the volume, respectively. Although these four quantities are more fundamental for the description of the mechanical behaviour of solids, we prefer to keep the following discussion as simple as possible and to speak in terms of linear tension and deformation. The specimen may then be imagined to be a slender rod or fibre of uniform cross-section. For reasons that will presently become obvious, it is essential that all the experiments to be described be made on systems that have been left to themselves for a long time.

The two experiments which have just been qualitatively described are examples of *viscoelastic* behaviour of solids. This type of behaviour is especially pronounced in many high polymers.

A method frequently used for the quantitative analysis of viscoelastic behaviour is based on the first experiment: at $t = o$ the system is subjected to the instantaneous stress

$$\sigma(t) = \sigma_o \, S_1(t) \tag{1}$$

its *response* to this *stimulus* is the time dependent strain

$$\varepsilon(t) = E_{\infty}^{-1} \{1 + \Psi(t)\} \sigma_o S_1(t) . \qquad (2)$$

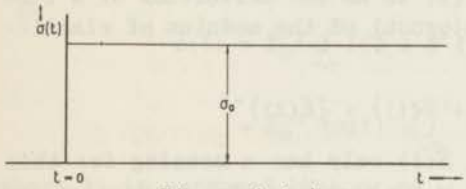

Figure 1.1.1

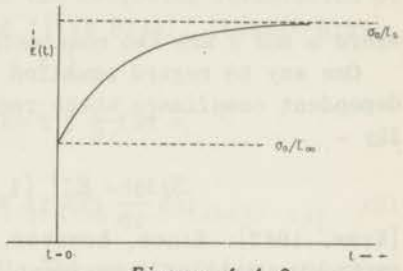

Figure 1.1.2

The following denotations are used:
σ, the stress, i.e., the force per unit area of cross-section,
ε, the strain, i.e., the ratio of the deformation Δl to the initial length l_o,
E_∞, the instantaneous modulus of elasticity,
E_s, the static modulus of the material,
$S_1(t)$, the unit step function (Heaviside's unit function), defined by

$$S_1(t) \begin{matrix} = 0 , & t < 0 , \\ = 1 , & t \geq 0 , \end{matrix} \qquad (3)$$

$\Psi(t)$, the *retardation* or *creep* function, a characteristic function of the material. The retardation function has the following general appearance:

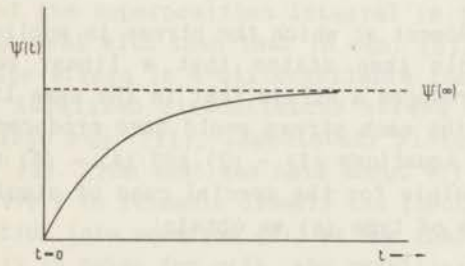

Figure 1.1.3

$\Psi(t) \geq 0$ if $t \geq 0$,
$\Psi(t)$ undetermined if $t < 0$,
$\Psi(0) = 0$,
$\Psi'(0) < \infty$,
$\Psi(\infty) < \infty$,
$\Psi(t_2) > \Psi(t_1)$ if $t_2 > t_1$.

In short, $\Psi(t)$ closely resembles the exponential function

$$\beta\ (1 - e^{-\alpha t}) , \qquad t \geqq 0 ,$$

where α and β are two constants *).

One way to regard equation (2) is as the definition of a time dependent *compliance* – the reciprocal of the modulus of elasticity –

$$S(t) = E_\infty^{-1}\ \{1 + \Psi(t)\} = \{E(t)\}^{-1}$$

[KUHN, 1947]. Since, however, $S(t)$ only has a meaning for this particular type of experiment, it is more fruitful to develop the theory first so as to include the response of viscoelastic systems to arbitrary stresses. As yet, this is only possible for *linear* systems, i.e., systems governed by *Boltzmann's principle of superposition*. Accordingly, non-linear systems are not considered in the present thesis.

Provisionally, we may use the experimental fact that mechanical systems of the kind considered here always show linear behaviour when stress and strain are sufficiently small.

In order to formulate the superposition principle we notice that the stress in (1) contains two parameters, its magnitude and its time of application. A more general starting point would therefore have been:

If $$\sigma(t) = \sigma_o\ S_1\ (t - t_o) , \tag{4}$$

then $$\varepsilon(t) = E_\infty^{-1}\ \{1 + \Psi\ (t - t_o)\}\ \sigma_o\ S_1\ (t - t_o) , \tag{5}$$

where t_o is the moment at which the stress is applied. The superposition principle then states that a linear combination of stresses $\sigma_i(t)$ produces a strain that is the same linear combination of the strains each stress would have produced had it acted alone. Evidently equations (1) – (2) and (4) – (5) already incorporate this principle for the special case of simultaneous stimuli. For stresses of type (4) we obtain:

a stress $$\sigma(t) = \sum_i \sigma_i\ S_1\ (t - t_i) \tag{6}$$

causes a strain

$$\varepsilon(t) = E_\infty^{-1} \sum_i \{1 + \Psi\ (t - t_i)\}\ \sigma_i\ S_1\ (t - t_i) . \tag{7}$$

*) Although many other functions might be used to summarize the properties of $\Psi(t)$, the exponential function is the most appropriate illustration (cf. Section 1.3).

Clearly, there is no reason to restrict this formulation to a finite number of finite contributions to the compound stress (6). The proper limiting process leads to the following formulation of Boltzmann's superposition principle ([TER HAAR], [KÁRMÁN-BIOT], [STAVERMAN-SCHWARZL, 1956]):

$$\varepsilon(t) = E_\infty^{-1} \int_{-\infty}^{t} \{1 + \Psi(t-\tau)\} \frac{d\sigma}{dt} d\tau =$$

$$= E_\infty^{-1} \{\sigma(t) + \int_{-\infty}^{t} \Psi(t-\tau) \frac{d\sigma}{dt} d\tau\} , \qquad (8)$$

where it is supposed that $\sigma(-\infty) = 0$. The *superposition integral* (8) connects the strain at any time with the whole preceding stress history of which it is the result. By partial integration equation (8) becomes

$$\varepsilon(t) = E_\infty^{-1} \{\sigma(t) + \int_{-\infty}^{t} \sigma(\tau)\, \Psi(t-\tau)\, d\tau\} , \qquad (9)$$

where

$$\psi(t) = \frac{d\Psi}{dt} \qquad (10)$$

is another characteristic function of the system which will be called the *rate of retardation* or the *rate of creep*.

The integral in (9) may once again be changed by introduction of the new variable $t-\tau$, to give

$$\varepsilon(t) = E_\infty^{-1} \{\sigma(t) + \int_{0}^{\infty} \sigma(t-\tau)\, \psi(\tau)\, d\tau\} . \qquad (11)$$

The forms of the superposition integral in (9) and (11) are often easier to deal with than that in eqn. (8), in which it is implied that the stress is a differentiable function of t. For instance, the idealized discontinuous stress of eqn. (1), on substitution into eqn. (11), immediately yields the attendant strain of eqn. (2). From what was said about $\Psi(t)$, we may expect $\psi(t)$ for positive t to resemble closely the function $\gamma e^{-\alpha t}$.

On substitution into equation (9), we see that if Dirac's delta function $\delta(t)$ is taken for $\sigma(t)$, the resulting strain is

$$\varepsilon(t) = E_\infty^{-1} \{\delta(t) + \psi(t)\} . \qquad (12)$$

Although the smallness of $\sigma(t)$ (required for linearity) has been ignored here, we may expect that a sharp narrow pulse of tension applied to the system results in a strain whose retarded part, apart from a factor, closely resembles $\psi(t)$.

The derivation of the superposition integral would have been simpler if this elementary response of the system had been taken

as a starting point for the theory. The then obvious meaning of $\psi(t)$ as a *memory* or *heredity function* [VOLTERRA, 1954] throws another light upon its nature.

It should be realized that the pair of functions $\{\varepsilon(t), \sigma(t)\}$ appearing in the superposition integral is uniquely determined by either function of the pair if E_∞ and $\psi(t)$ are given quantities. A logical consequence is that nothing in the mathematical formulation decides which function is the cause and which the effect. This decision is only determined by the apparatus used to produce the phenomena and by the point of view of the experimenter.

The superposition integral is an integral transformation that yields $\varepsilon(t)$ if $\sigma(t)$ is given. On the other hand, if $\varepsilon(t)$ is given, it may equally well be regarded as an integral equation the solution of which is $\sigma(t)$. Hence, we now turn to the problem of how to invert the integral equation so as to make $\sigma(t)$ easily accessible when $\varepsilon(t)$ is prescribed.

The formulae (8) – (11) are based upon the unit step experiment described by equations (1) and (2). We may, therefore, expect to find the inversion of the superposition integral by considering the outcome of the inverse unit step experiment in which

$$\varepsilon(t) = \varepsilon_o \, S_1(t) \; . \tag{13}$$

The attendant stress is certainly zero for negative t; also, it should consist of the simultaneous response,

$$E_\infty \, \varepsilon_o \, S_1(t) \; ,$$

added to a retarded one. Without loss of generality, we may assume that

$$\sigma(t) = E_\infty \, \varepsilon_o \, S_1(t) \, \{1 - \Phi(t)\} \tag{14}$$

is the stress in the system belonging to the strain (13). Furthermore, the same reasoning that led from equation (2) to, say, (11), yields

$$\sigma(t) = E_\infty \left\{\varepsilon(t) - \int_o^\infty \varepsilon(t-\tau) \, \varphi(\tau) \, d\tau\right\} \; . \tag{15}$$

for the required inversion of (11). Here

$$\varphi(t) = \frac{d\Phi}{dt} \tag{16}$$

corresponds to the rate of retardation given in equation (10).

Of course, equation (15) is useless as long as we do not have further information about $\Phi(t)$ or $\varphi(t)$. This information may be

obtained experimentally, by subjecting the viscoelastic system to the strain (13) and observing the resultant stress (14). It may, however, also be obtained from the form of the pair of reciprocal integral equations (11) and (15) if $\Psi(t)$ is experimentally known. To show this, we take the slightly less general equations

$$\varepsilon(t) = E_\infty^{-1} \{\sigma(t) + \int_0^t \sigma(t-\tau)\ \psi(\tau)\ d\tau\} \text{ , zero initial conditions,} \tag{17}$$

$$\sigma(t) = E_\infty \{\varepsilon(t) - \int_0^t \varepsilon(t-\tau)\ \varphi(\tau)\ d\tau\} \text{ , zero initial conditions,} \tag{18}$$

for otherwise arbitrary stress and strain which are zero before $t = 0$. The kind of integral in these modified forms of the equations is well-known in mathematical analysis as the *convolution* of the functions $\sigma(t)$ and $\psi(t)$, and $\varepsilon(t)$ and $\varphi(t)$, respectively; its most important property is that its Laplace transform is the product of the Laplace transforms of the functions of which it is the convolution ([Churchill], [Sneddon, 1955], [Widder]). Hence

$$\bar{\varepsilon}(p) = E_\infty^{-1} \{1 + \bar{\psi}(p)\}\ \bar{\sigma}(p) , \tag{19}$$

$$\bar{\sigma}(p) = E_\infty \{1 - \bar{\varphi}(p)\}\ \bar{\varepsilon}(p) , \tag{20}$$

both under zero initial conditions. The abbreviated notation

$$\bar{u}(p) = \int_0^\infty e^{-pt}\ u(t)\ dt \tag{21}$$

represents the Laplace transform of a function $u(t)$ ([Jaeger], [Sneddon, 1955], [Tranter]). From equations (19) and (20) it follows that the Laplace transforms of $\psi(t)$ and $\varphi(t)$ are related by the equation

$$\{1 + \bar{\psi}(p)\}\ \{1 - \bar{\varphi}(p)\} = 1 . \tag{22}$$

It should be noted that the restricted validity of (17) and (18) does not apply to eqn. (22). Both numerical evaluation of $\varphi(t)$ from this relation, when $\psi(t)$ is known, and direct measurement of $\Phi(t)$ followed by differentiation yield the same result, and vice versa [Gross, 1947]. The properties of $\Phi(t)$ and $\varphi(t)$ found in either way are identical with those provisionally given for $\Psi(t)$ and $\psi(t)$, although it is clear that the same function cannot be both retardation function and relaxation function for one system.

It is customary to denote phenomena in which the stress is a given function of time as retardation or creep processes; those

in which the strain is prescribed are called relaxation processes. Accordingly, $\Phi(t)$ is called the *relaxation function*, $\varphi(t)$ the *rate of relaxation*.

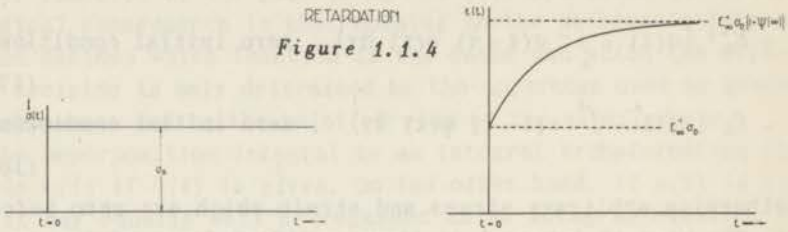

Figure 1.1.4

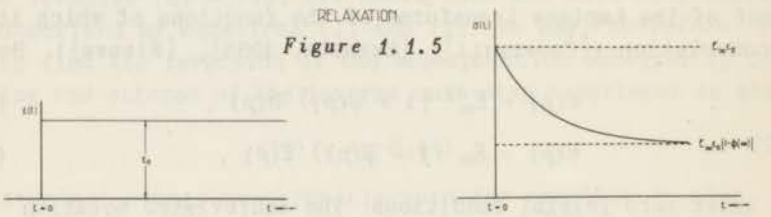

Figure 1.1.5

As such, of course, this nomenclature is as good as any other one. There is, however, a tendency in the literature on linear viscoelastic behaviour to regard the concept of relaxation as a more fundamental one than that of retardation [Kuhn, 1939, 1947]. Alternatively, creep and relaxation are presented as different, although related, phenomena [Gross, 1947, 1948].

There has also been discussion as to whether the molecular processes in which viscoelastic behaviour originates should be interpreted as retardation or relaxation processes [Alfrey-Doty]. On the other hand the treatment of other linear relaxation phenomena (to be considered in the following Chapters) is invariably made in terms of functions belonging to the retardation family of functions, and the alternative description is ignored. In all this, nothing more fundamental is involved than the arbitrary choice between either one of the pair of reciprocal integral equations (11) or (15), each of which gives the same relationship, characteristic for the system, between a pair of functions $\sigma(t)$ and $\varepsilon(t)$. The choice may be influenced by the experimental

method used to study the phenomena, but certainly is unimportant as far as the intrinsic properties of the system are concerned.

Eqn. (22) may be rewritten as

$$\overline{\psi}\overline{\varphi} = \overline{\psi} - \overline{\varphi} \ , \tag{22a}$$

which, because of the properties of the convolution and the uniqueness of the Laplace transform, is equivalent to

$$\int_0^t \psi(t-\tau)\ \varphi(\tau)\ d\tau = \psi(t) - \varphi(t) \ . \tag{23}$$

Then some generalities about the interrelationship of $\psi(t)$ and $\varphi(t)$ are obvious:
since the left-hand side of the equation is non-negative, $\psi(t)$ and $\varphi(t)$ being non-negative functions, we conclude that

$$\varphi(t) \leqq \psi(t) \ , \tag{24}$$

more precisely, that

$$\varphi(t) < \psi(t) \ , \quad t > 0 \ , \tag{24a}$$

$$\varphi(0) = \psi(0) \ , \tag{24b}$$

$$\varphi(\infty) = \psi(\infty) = 0 \ . \tag{24c}$$

Another relation, between the creep and relaxation function for $t \to \infty$, follows directly from eqn. (22); since

$$\overline{\Psi}(0) = \Psi(\infty) \qquad \text{and} \qquad \overline{\Phi}(0) = \Phi(\infty) \ ,$$

we have that

$$\{1 - \Phi(\infty)\}\ \{1 + \Psi(\infty)\} = 1 \ .$$

Although, according to the data of Figs. 4 and 5, this equation is a trivial one, since

$$E_\infty^{-1}\ \{1 + \Psi(\infty)\} = E_s^{-1} \ , \tag{25}$$

$$E_\infty\ \{1 - \Phi(\infty)\} = E_s \ , \tag{26}$$

it provides a check upon the internal consistency of the theory.

Another check is obtained by substituting $\sigma(t) = \varphi(t)$ into eqn. (11): Because of eqn. (23), one obtains $\varepsilon(t) = E_\infty^{-1}\psi(t)$; if $\varepsilon(t) = \psi(t)$ is inserted in eqn. (15), there results $\sigma(t) = E_\infty\varphi(t)$.

1.2. The linear viscoelastic body: sinusoidal stimuli

The unit step stimuli and their responses treated in Sect. 1.1 are, apart from their usefulness for the theory, of practical importance in the experimental study of viscoelasticity. Another experimental approach to the investigation of viscoelastic behaviour is by means of sinusoidal stimuli and their responses. What happens when a viscoelastic system is exposed to a sinusoidal stress is easily derived from the superposition integral (1.1.11):
inserting the stress in its complex form

$$\sigma(i\omega t) = \sigma_o \, e^{i\omega t} \tag{1}$$

leads to

$$\varepsilon(i\omega t) = E_\infty^{-1} \{1 + \bar{\psi}(i\omega)\} \, \sigma(i\omega t) \, . \tag{2}$$

The response of the system to a sinusoidal strain

$$\varepsilon(i\omega t) = \varepsilon_o \, e^{i\omega t} \tag{3}$$

is, by substitution into (1.1.15), found to be

$$\sigma(i\omega t) = E_\infty \{1 - \bar{\varphi}(i\omega)\} \, \varepsilon(i\omega t) \, . \tag{4}$$

The functions $\bar{\psi}(i\omega)$ and $\bar{\varphi}(i\omega)$ are the Laplace transforms of eqns. (1.1.19) and (1.1.20) for purely imaginary argument. It should be added that eqns. (1) – (4) apply to the steady state behaviour of the viscoelastic system. An important consequence of the superposition principle is seen to be contained in these equations: a sinusoidal stimulus to a linear viscoelastic system produces a response which is also purely sinusoidal and of the same frequency. Our definition of linearity obviously coincides with that of electric circuit theory, in which it is defined as the absence of harmonics upon application of a sinusoidal signal [GOLDMAN].

Eqns. (2) and (4) define the following two complex functions of the radian frequency or *pulsatance*:

$$S(i\omega) = E_\infty^{-1} \{1 + \bar{\psi}(i\omega)\} \, , \tag{5}$$

the dynamic or complex compliance, and

$$E(i\omega) = E_\infty \{1 - \bar{\varphi}(i\omega)\} \, , \tag{6}$$

the dynamic or complex modulus of elasticity. These quantities are related by

$$S(i\omega)\, E(i\omega) = 1 \,, \tag{7}$$

evidently an analogue, for purely imaginary argument, of eqn. (1.1.22).

The dynamical experiments show in a particularly striking way that retardation and relaxation are really two aspects of the same phenomenon. Although we can still choose between the complex compliance, belonging to the retardation group of functions, and the dynamic modulus, a member of the relaxation group of functions, these choices are equivalent because of eqn. (7).

Apart from the conventional physical meaning of these complex quantities, inherent in the use of the complex notation for sinusoidal functions, they are important because of their bearing on the energetical behaviour of the viscoelastic body.

This aspect of viscoelasticity is approached by considering

$$W = \int_{t_1}^{t_2} \sigma(t)\, d\varepsilon(t) \tag{8}$$

the amount of mechanical energy entering unit volume of the system during the interval $t_1 \ldots t_2$. When substituting the complex stress and strain of eqns. (1) – (4) into this equation, one should remember that only their real (or imaginary) parts have a physical meaning; accordingly

$$W = \int_{t_1}^{t_2} \mathrm{Re}\ \sigma \,.\, \mathrm{Re}\,\frac{d\varepsilon}{dt}\, dt = \omega \int_{t_1}^{t_2} \frac{\sigma + \sigma^*}{2}\, \frac{\varepsilon^* - \varepsilon}{2i}\, dt \,, \tag{9}$$

where the starred symbols stand for the complex conjugate quantities. In particular, using the pair (1) and (2) together with the definition (5), we obtain

$$W = \frac{\omega\sigma_o^2}{4i} \int_{t_1}^{t_2} (e^{i\omega t} + e^{-i\omega t})\,(S^*\, e^{-i\omega t} - S\, e^{i\omega t})\, dt =$$

$$= -\tfrac{1}{2}\omega\sigma_o^2 \,.\, \mathrm{Im}\, S(i\omega) \,.\, (t_2 - t_1) + \frac{\omega\sigma_o^2}{4} \left[\frac{S^*\, e^{-2i\omega t} + S\, e^{2i\omega t}}{2}\right]_{t_1}^{t_2} \tag{10}$$

Hence, during one complete cycle, e.g., from $t_1 = 0$ to $t_2 = 2\pi/\omega$, the input of mechanical energy per unit volume is

$$W = -\pi\sigma_o^2\, \mathrm{Im}\, S(i\omega) \,. \tag{11}$$

From eqn. (1.1.21) it follows that

$$\bar{\psi}(i\omega) = \int_0^\infty e^{-i\omega t}\, \psi(t)\, dt =$$

$$= \int_0^\infty \psi(t) \cos \omega t\, dt - i \int_0^\infty \psi(t) \sin \omega t\, dt \,; \tag{12}$$

therefore

$$\text{Re } S(i\omega) = S'(\omega) = S_\infty \{1 + \int_0^\infty \psi(t) \cos \omega t \, dt\} \qquad (13)$$

$$\text{Im } S(i\omega) = S''(\omega) = - S_\infty \int_0^\infty \psi(t) \sin \omega t \, dt \, , \qquad (14)$$

where $S_\infty = E_\infty^{-1}$ is the compliance at infinite frequency. According to eqns. (11) and (14) there is a continuous flow of energy *into* the viscoelastic body. This cannot mean anything else than a continuous conversion of mechanical work into heat during the steady state process. We meet here an essential aspect of viscoelastic behaviour, viz. its inherently dissipative character, a property that it has in common with all other relaxation phenomena.

On reconsidering eqn. (10), we see that the particular choice of the limits of integration incidentally annihilates the second term on the right hand side. The more general limits 0 and t lead, after elimination of the complex notation, to the relation

$$W(t) = -\tfrac{1}{2} \omega \sigma_o^2 S'' \, . \, t + \tfrac{1}{4} \sigma_o^2 \{S' (\cos 2\omega t - 1) - S'' \sin 2\omega t\} \qquad (15)$$

for the amount of mechanical energy entering unit volume of the linear viscoelastic body during the stated interval of time. Eqn. (15) shows that the influx of mechanical energy is a linear function of time, superposed on which there is a sinusoidal component of frequency 2ω. The latter function represents an alternative delivery and storage, during successive quarter cycles, of an amount of energy

$$\tfrac{1}{2} S' \sigma_o^2 \qquad (15a)$$

We conclude from eqns. (15a) and (11) that the real and negative imaginary part of the complex compliance are energy storage and dissipation factors, respectively. A completely analogous reasoning shows that the real and imaginary parts of the dynamic modulus have the same physical significance: the energy dissipation per cycle per unit volume is

$$- \pi \varepsilon_o^2 E'' \, ,$$

and the energy storage per unit volume per quarter cycle is

$$\tfrac{1}{2} E' \varepsilon_o^2 \, .$$

Although the analytical expressions for energy dissipation and storage were derived here for the special case of sinusoidal processes, similar energetical behaviour is typical of all processes

in a viscoelastic system that are not infinitely slow or infinitely fast. This will become obvious in the next Section, when the representation of viscoelastic behaviour in terms of mechanical models is discussed. Because of the energy dissipation, the systems will rise in temperature under adiabatic conditions.

Since the viscoelastic properties are temperature dependent, it is essential to state here that all relaxation processes in the present thesis are understood to take place under isothermal conditions.

A further analysis of the interdependence of the real and imaginary parts of the dynamic compliance, which follows, e.g., from eqns. (13) and (14), will be given in Chapter 3. As such, this interdependence could be treated here, since its existence is ultimately a consequence of the superposition principle alone, independent of the more specific properties of linear viscoelastic systems. In view of the introductory nature of the present Chapter, however, we will first discuss, in the next Section, what effect the special types of function that characterize a viscoelastic body have upon its physical properties.

1.3. Survey of the mathematical methods *). Mechanical models

Another way of looking upon the fundamental equations (1.1.11) and (1.1.15) is as implicit formulae defining a linear operator, the *compliance operator* S_{op}, and its reciprocal, the *elastic modulus operator* E_{op} [ALFREY, 1944, 1945]:

$$\varepsilon(t) = S_{op}\, \sigma(t) \,, \tag{1}$$

$$\sigma(t) = E_{op}\, \varepsilon(t) \,. \tag{2}$$

The aims of the phenomenological theory of viscoelasticity are to define and describe these operators, and to draw all possible physical consequences from their existence and nature.

In investigating the properties of an operator, one may proceed along various lines.

In Section 1.1 we started from the action of the operators upon the unit step function which led to the superposition equations

*) Note added in proof. – In a recent publication an extensive review has been given of the integral transform relations in linear systems [MACDONALD-BRACHMAN].

$$\varepsilon(t) = S_\infty \{\sigma(t) + \int_0^\infty \sigma(t-\tau)\ \psi(\tau)\ d\tau\} \tag{1a}$$

and
$$\sigma(t) = E_\infty \{\varepsilon(t) - \int_0^\infty \varepsilon(t-\tau)\ \varphi(\tau)\ d\tau\} . \tag{2a}$$

Any simple, versatile, function would have been equally suitable for this analysis of the operators. The usefulness of another transient, the delta function, has already been pointed out. In Chapter 2, it will be shown that the use of sinusoids leads to the same results.

A second method for analyzing operator equations of the present type makes use of the relations between the Laplace transforms of stress and strain. Relations of this kind were already encountered in equations (1.1.19) and (1.1.20):

$$\bar{\varepsilon}(p) = S_\infty \{1 + \bar{\psi}(p)\}\ \bar{\sigma}(p) , \qquad \text{z.i.c.,} \tag{3}$$

$$\bar{\sigma}(p) = E_\infty \{1 - \bar{\varphi}(p)\}\ \bar{\varepsilon}(p) , \qquad \text{z.i.c.,} \tag{4}$$

where z.i.c. stands for zero initial conditions. The quantities

$$S(p) = S_\infty \{1 + \bar{\psi}(p)\} \tag{5}$$

and
$$E(p) = E_\infty \{1 - \bar{\varphi}(p)\} \tag{6}$$

will be called the *generalized compliance* and *generalized elastic modulus* of the viscoelastic system. The generalized compliance may be interpreted as follows: if the Laplace transform of the stress applied to the system at rest is unity, $S(p)$ is the Laplace transform of the resulting strain. A similar interpretation may be given to $E(p)$. Since

$$\int_0^\infty e^{-pt}\ \delta(t)\ dt = 1 \tag{7}$$

(cf. (1.4.10)), the stress and strain used in these interpretations of $S(p)$ and $E(p)$, respectively, must be delta functions.

It is shown in the literature cited below eqn. (1.1.18) that (3) and (4) are necessary and sufficient for

$$\varepsilon(t) = S_\infty \{\sigma(t) + \int_0^t \sigma(t-\tau)\ \psi(\tau)\ d\tau\} , \qquad \text{z.i.c.,} \tag{8}$$

and
$$\sigma(t) = E_\infty \{\varepsilon(t) - \int_0^t \varepsilon(t-\tau)\ \varphi(\tau)\ d\tau\} , \qquad \text{z.i.c.,} \tag{9}$$

The restriction to zero initial conditions can be lifted by shifting the origin of the time axis to $t = -a$. We then obtain

$$\varepsilon(t) = S_\infty \{\sigma(t) + \int_0^{t+a} \sigma(t-\tau)\ \psi(\tau)\ d\tau\} \tag{8a}$$

and $$\sigma(t) = E_\infty \{\varepsilon(t) - \int_0^{t+a} \varepsilon(t-\tau)\ \varphi(\tau)\ d\tau\}\ , \tag{9a}$$

for a linear system which is at rest in $t = -a$ and afterwards is subjected to arbitrary stimuli. It is clear that eqns. (1a) and (2a) are obtained from this pair of equations for $a \to \infty$.

We conclude that the pairs of equations (3), (4) and (1a), (2a) contain the same amount of information about the operators. All the results obtained from the superposition integrals can also – and often more conveniently – be derived from the relations between the Laplace transforms.

Examples of the application of Laplace transformation – the so-called *operational* method – were encountered in eqns. (1.1.22) and (1.2.7) connecting the retardation and relaxation family of functions, and in the above-mentioned interpretation of $S(p)$ as the Laplace transform of the strain resulting from the application of a stress that is the delta function (cf. eqn. (1.1.12)). Other examples are:

a) If

$$\sigma(t) = \sigma_o\ S_1(t)\ , \qquad \overline{\sigma}(p) = \sigma_o/p\ , \tag{10}$$

which, upon substitution into eqn. (3), yields

$$\overline{\varepsilon}(p) = S_\infty \{1 + \overline{\psi}(p)\}\ \sigma_o/p\ , \tag{11}$$

for the Laplace transform of the strain of the system resulting from the stimulus (10). Inversion of (11) gives

$$\varepsilon(t) = S_\infty \{1 + \int_0^t \psi(\tau)\, d\tau\}\ \sigma_o\ S_1(t) = S_\infty \{1 + \Psi(t)\}\ \sigma_o\ S_1(t)\ , \tag{12}$$

which is identical with eqn. (1.1.2).

b) If

$$\sigma(t) = \sigma_o\ e^{i\omega t}\ , \qquad \overline{\sigma}(p) = \frac{\sigma_o}{p - i\omega}; \tag{13}$$

therefore

$$\overline{\varepsilon}(p) = S_\infty \frac{\sigma_o\ \{1 + \overline{\psi}(p)\}}{p - i\omega}\ , \tag{14}$$

which, upon inversion and application of the convolution theorem, gives

$$\varepsilon(t) = S_\infty \sigma_0 e^{i\omega t} + S_\infty \sigma_0 \int_0^t \psi(\tau)\, e^{i\omega(t-\tau)}\, d\tau =$$

$$= S_\infty \{1 + \int_0^t \psi(\tau)\, e^{-i\omega\tau}\, d\tau\}\, \sigma_0\, e^{i\omega\tau} =$$

$$= S_\infty \{1 + \overline{\psi}(i\omega) - \int_t^\infty \psi(\tau)\, e^{-i\omega\tau}\, d\tau\}\, \sigma_0\, e^{i\omega t} . \qquad (15)$$

The integral in (15) is a transient deformation not present in the steady state equation (1.2.2). Its presence here is a consequence of the restriction of the present method to zero initial conditions. After a sufficiently long time the transient decays and the former steady state solution is once again obtained.

We see that the operational method is not as abstract as it may have seemed at first: the generalized compliance and modulus have direct physical significance for purely imaginary values of p (cf. Sect. 1.2).

The variable p was hitherto tacitly assumed to be a purely real quantity. However, in all the formulae in which it has been used so far it may be replaced by the complex variable

$$z = p + i\omega , \qquad (16)$$

provided that p is large enough to ensure the convergence of the integrals. The introduction of z leads not only to greater generality, but also enables us to make concise statements about the nature of the operators. For, subject to conditions on the functions, the Laplace transforms are analytic functions of z in that part of the z-plane lying to the right of an abscissa of convergence. Since the dynamic compliance and modulus exist for all values of the frequency, we conclude that $S(z)$ and $E(z)$ must have their abscissa of convergence to the left of the imaginary axis of the z-plane, in other words, that their singularities must be located in the left half of this plane. It will presently be found that the most characteristic property of viscoelastic systems, apart from their linearity, is the fact that $S(z)$ and $E(z)$ have positive singularities on the negative real axis of the complex plane and *nowhere else*.

After z, which will be called the *complex frequency* [Bode], is introduced, we note that (1.1.22) and (1.2.7) are really the same equation. The name complex frequency becomes clear when (13) is regarded as a special instance of the stress

$$\sigma(t) = \sigma_0\, e^{zt} , \qquad (17)$$

i.e., as an exponentially increasing or decreasing sinusoidal function of the time. Eqn. (1a) yields

$$\varepsilon(t) = S_\infty \{1 + \bar{\psi}(z)\} \sigma_o e^{zt} = S(z) \sigma_o e^{zt} \qquad (18)$$

for the strain resulting from the application of this stress. It should be noted that the use of the superposition integral implies that the system has been subjected to (17) from $t = -\infty$ onwards.

Eqn. (18) shows yet another aspect of the nature of the generalized compliance $S(z)$: apart from its formal meaning as the Laplace transform of the strain resulting from the application of an impulsive stress to the system at rest, it has an immediate physical significance when z lies on the imaginary axis of the complex frequency plane and, according to (18), this physical meaning may be extended to regions of the complex plane in which the generalized compliance is a regular function of z. If the complex frequency in (18) happens to coincide with a singular point of $S(z)$, we formally obtain an infinite value for the strain, a phenomenon commonly designated as resonance in mechanical systems having singularities on the imaginary axis.

In the above examples we repeatedly mentioned inversion of the Laplace transformation. In practice inversion can very often be effected by simply using one of the existing tables ([Churchill], [Hodgman], [McLachlan], [Magnus-Oberhettinger]). Transforms not contained in these tables can usually be inverted by means of the complex inversion formula for the Laplace transformation: subject to conditions which are almost always fulfilled for the simple functions considered here.

$$y(t) = \frac{1}{2\pi i} \int_{c-i\infty}^{c+i\infty} \bar{y}(z)\, e^{tz}\, dz \qquad (19)$$

is the required inversion of

$$\bar{y}(z) = \int_o^\infty y(t)\, e^{-zt}\, dt\ .$$

The integration in (19) is to be carried out along a line $z = c$ parallel to the imaginary axis of the z-plane. If the line lies to the right of the singularities of $\bar{y}(z)$, the integration yields a $y(t)$ independent of the value of c. The line integral can usually be evaluated by transforming it into an integral along a closed contour and by making use of the calculus of residues (cf. the discussion of the *Bromwich-Wagner* integral in [McLachlan] and [Jeffreys-Jeffreys]).

The third and most easily visualized method for describing and predicting the properties of the operators governing linear viscoelastic behaviour is the one that uses *mechanical models*. These models are defined as mechanical structures having the same force-deformation behaviour as a unit cube of the viscoelastic body perpendicular to the direction of stress and strain. According to the previous definition of stress and strain the deformation of the model is then identical with the strain of the viscoelastic body and the force on the model is identical with the stress. The same relations with the same denotations will therefore be used interchangeably for models and viscoelastic systems, $\sigma(t)$ denoting either force or stress, $\varepsilon(t)$ deformation or strain.

How such a model is to be physically realized will emerge from the subsequent discussion; apart from being governed by the equations for the viscoelastic system it represents we require only that a model be equipped with two *terminals*, i.e., physical points constrained to move along a straight line. The force acts on one of the terminals, its reaction force – to prevent acceleration of the model as a whole – on the other terminal. The deformation is defined as the change of the distance between the terminals. Because of

$$\psi(\infty) = \varphi(\infty) = 0 \qquad (1.1.24c)$$

a zero point of the deformation is defined.

The models will be treated as linear mechanical networks ([KÁRMÁN-BIOT], [KEGEL]). Just as in the theory of linear electric two-terminal networks, only three basic mechanical two-terminal *elements* and two combination rules suffice for the construction of the mechanical networks.

According to these rules two elements (or combinations of elements) may only be combined by

(a) series connection, in which the deformations of the elements add, and the forces upon them are the same, and by

(b) parallel connection, in which the forces must be added, but the deformations of the elements are equal.

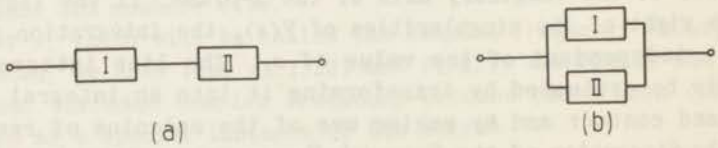

Figure 1.3.1

Although the theories of both mechanical and electric linear networks are identical in all essential aspects, there are some superficial differences. One instance is found in the combination rules, which, for mechanical networks, are the opposites of those for electric networks. Another difference is the following peculiarity of mechanical networks: the deformation is a geometrical parameter which imposes geometrical limitations on the construction and consequently on the diagrams. The straight lines in the diagrams should be imagined to be infinitely rigid connecting rods having a negligible mass. These connecting rods actually occupy the places and positions in which they are drawn; they are forced to stay parallel and perpendicular to one another by suitably placed frictionless guiding rails not included in the diagrams.

Again, operational methods will be used for the description of the mechanical networks. We start from the perfectly general assumption that the mechanical elements are governed by the linear operator equations

$$\varepsilon(t) = Y_{op}\, \sigma(t) \tag{20}$$

and

$$\sigma(t) = Z_{op}\, \varepsilon(t) \ . \tag{21}$$

These operators are called the *mechanical admittance operator* and the *mechanical impedance operator*, respectively, and are, of course, equivalent to the compliance and modulus operator of eqns. (1) and (2). Evidently, the admittance operator of a series combination is obtained by addition of the individual admittance operators, the impedance operator of a parallel combination by addition of the individual impedance operators. The same rule applies to the *generalized* mechanical admittance and impedance, two quantities whose definitions are identical with those of $S(z)$ and $E(z)$.

As the simplest possible linear elements we may regard those governed by

$$Z_{op} = \text{const.} \left(\frac{d}{dt}\right)^n , \qquad n = 0, 1, 2, \ldots , \tag{22}$$

$$Y_{op} = \text{const.} \left(\frac{d}{dt}\right)^m , \qquad m = 1, 2, \ldots . \tag{23}$$

Using the abbreviated notation

$$D = \frac{d}{dt} ,$$

we obtain

$$\int_0^\infty D^n\, y(t)\, e^{-zt}\, dt = z^n\, \bar{y}(z) \tag{24}$$

for the Laplace transform of the n-th derivative of a function $y(t)$ having the properties

a) $D^p\, y(0) = 0,\ p = 0,1,\ldots,n-1,$

b) $e^{-zt}\, y(t)$ tends to zero if $z \to \infty$.

Therefore, the generalized mechanical impedance and admittance of the elements of (22) and (23) are

$$Z(z) = \text{const.}\ z^n\ , \qquad n = 0,1,2,\ldots \tag{25}$$

and

$$Y(z) = \text{const.}\ z^m\ , \qquad m = 1,2,\ldots\ . \tag{26}$$

It may be easily shown that, when elements defined by the latter equations are connected in accordance with the above combination rules, there result mechanical structures whose generalized admittances and impedances are rational functions of z. We may therefore assume that a theory of linear mechanical two-terminal networks, based upon these elements and the two combination rules, is sufficiently general to account for all $Y(z)$ and $Z(z)$, and hence $S(z)$ and $E(z)$, that might possibly result from actual measurements. It is well-known from electric network theory, however, that the present foundation of the theory is much too general: of all the elements defined by eqns. (22) and (23), only three are physically possible and realizable. One of these is evident from eqn. (22): for $n = 0$ it defines the *ideal spring*, an element which obeys Hooke's Law

$$\sigma(t) = E\ \varepsilon(t)\ . \tag{27}$$

The two other possible elements are obtained by connecting the elements of eqn. (22) in parallel with an ideal spring.

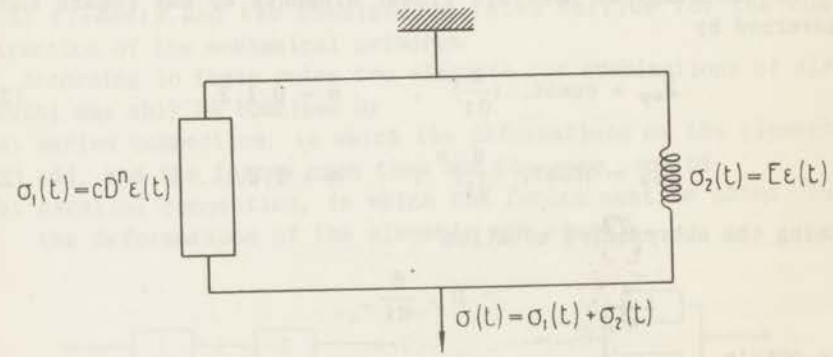

Figure 1.3.2

The generalized admittance of the resulting network is

$$Y(z) = \frac{1}{c\ z^n + E} . \tag{28}$$

We saw that this is the Laplace transform of the deformation resulting from the application of an impulsive stress to the system at rest in $t = 0$. Inversion of (28) is most easily accomplished by partial fractions expansion:

$$Y(z) = \frac{1}{c\ (z - z_1)\ (z - z_2)\ \ldots\ (z - z_n)}$$

$$= \sum_1^n \frac{A_k}{z - z_k} , \tag{29}$$

where the z_k's are the complex roots of the denominator:

$$z_k = (E/c)^{1/n}\ e^{i(\frac{\pi}{n} + k\frac{2\pi}{n})} , \qquad k = 1,2,\ldots,n . \tag{30}$$

(The images of the z_k's in the complex plane obviously are n equally spaced points upon the circumference of the circle about the origin

$$|z| = (E/c)^{1/n} .)$$

The A_k's are, by a well-known method, found to be

$$A_k = 1/[\frac{d}{dz}\ (c\ z^n + E)]_{z=z_k} = 1/(n\ c\ z_k^{n-1}) . \tag{31}$$

Eqn. (29) can then be immediately inverted to give for the deformation

$$\varepsilon(t) = \sum_1^n A_k\ e^{z_k t} . \tag{32}$$

It will be clear that if the denominator has any roots with positive real parts, $\varepsilon(t)$ includes sinusoidal terms of exponentially increasing amplitude, which means that the element in question is physically unstable [Bode]. Only when n has the values 1 or 2 do these terms not occur in eqn. (32). For completeness, the value $n = 0$ must be added; it has already been treated as the ideal spring.

The elements defined by $n = 1$ and 2 are, of course, well-known: they are called the *ideal dashpot* and the *ideal mass*, respectively, and obey the relations

$$\sigma(t) = \eta\ D\ \varepsilon(t) \tag{33}$$

and

$$\sigma(t) = m\ D^2\ \varepsilon(t) . \tag{34}$$

In the following diagrams, the ideal spring, dashpot and mass are represented by the symbols of Fig. 3, a, b and c, respectively.

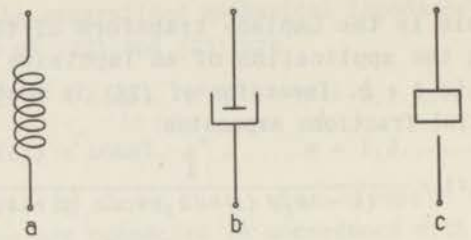

Figure 1.3.3

Actual examples of non-ideal dashpots may, e.g., be found in most modern balances, in which they are constructed as magnetic, air, or viscous dampers. A mass, of course, needs no further exemplification; it's two terminals may be chosen to be its centre of gravity and some fixed reference point outside the model upon the straight line along which the other terminal moves [KEGEL].

The non-existence of the elements of eqn. (23) may be proved in an entirely analogous way by analyzing the physical behaviour of such an element with an ideal mass attached to it. It is found that the resulting combination is physically stable only for $m = 0$, -1, and -2 and not for any of the indicated values of m in eqn. (23); hence, one again obtains the ideal spring, dashpot and mass as the only three possible mechanical elements. Even without this analysis, we conclude that it is improbable for any of the elements of eqn. (23) to exist: to maintain a constant deformation, the force acting on such an element would have to be a polynomial of degree m in time. Any polynomial of lower degree would not lead to any deformation at all. The argument used in these proofs leads to an important property of linear systems [BODE].

The complex functions $Y(z)$ and $Z(z)$ may have no singularities to the right of the imaginary axis of the complex frequency plane.

Another consequence is that, if $Z(z)$ is a rational function, the degree of its numerator may at most exceed the degree of its denominator by two. Only then, the behaviour of the system for very large values of z approximates the behaviour of one of the three possible elements. Another limitation upon the form of $Z(z)$ is obtained from the same requirement for very small values of z.

In the foregoing we have chosen the "force/displacement" rather than the "force/velocity" type of mechanical impedance

and admittance (cf. [KÁRMÁN-BIOT]). The distinction is that the *imaginary* parts of the steady-state impedances and admittances of the former type and the *real* parts of those of the latter type determine the energy dissipation in a system. The force-velocity quantities are, of course, the analogous of the impedances and admittances used in electric circuit theory. The author's attention was drawn to the fact that conformity with the definitions of electric network theory offers some advantages for a general formulation of the theory of linear systems [MEIXNER, private communication], since the generalized quantities thus defined are always found to be *positive* *) functions in the complex frequency plane [MEIXNER, 1954, 1957/8]. However, in view of the fact that the two kinds of generalized impedance and admittance are simply obtained from one another through multiplication or division by the complex frequency, the generalized quantities in the present thesis have been chosen so as to be closely connected with the physical quantities in terms of which relaxational behaviour is usually described.

We shall exclude the occurrence of masses in the mechanical models. This assumption is, explicitly or implicitly, made in practically the whole literature on viscoelasticity, since it is invariably found that all experimental results can be satisfactorily represented by means of models exclusively constructed from ideal springs and ideal dashpots. It can easily be proved by total induction that this is equivalent to the assumption that the singularities of $Y(z)$ and $Z(z)$ have positive residues and are located on the negative real axis of the complex frequency plane.

Clearly, the number of mechanical models having the same generalized admittance and impedance increases very rapidly with increasing complexity of these functions. Two kinds of mechanical networks, however, are distinguished by a particularly simple relationship between their structure and the functions $Y(z)$ and $Z(z)$. These networks are constructed from a number of units in such a way that each unit contributes a simple pole to these functions. The first model, variously known as the *Voigt-* or *Kelvin-model*, consists of a string of n parallel combinations of one ideal spring and one ideal dashpot called *Voigt-* or *Kelvin-*elements.

*) A positive function has the following properties: (i) it is regular and has a positive real part when the real part of its argument is positive; (ii) it is real for positive real values of its argument.

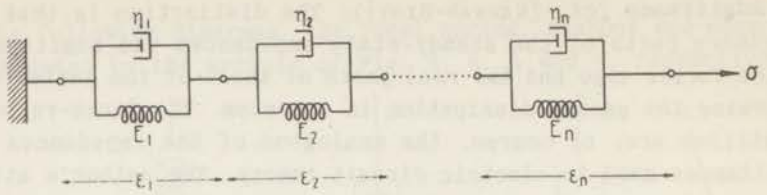

Figure 1.3.4

Application of the combination rules shows its generalized admittance to be

$$Y(z) = \sum_{1}^{n} \frac{1}{E_k + \eta_k z}. \tag{35}$$

The other model consists of n series combinations of one spring and one dashpot and is called the *Maxwell-model*.

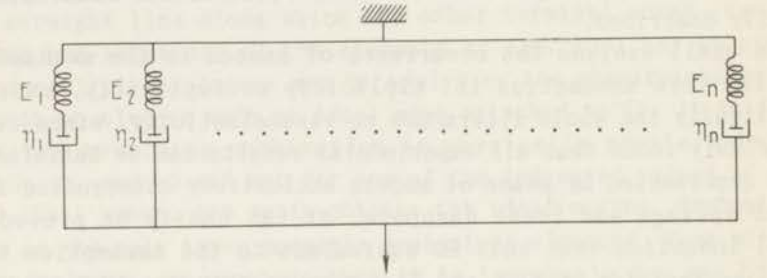

Figure 1.3.5

The generalized mechanical impedance of the Maxwell-model is easily found to be

$$Z(z) = \sum_{1}^{n} \frac{1}{(E_k)^{-1} + (\eta_k z)^{-1}} = \sum_{1}^{n} \frac{E_k \eta_k z}{E_k + \eta_k z}. \tag{36}$$

Obviously, the behaviour of these models does not yet conform to the qualitative description of the linear viscoelastic body given in the first two Sections: the Voigt-model, e.g., has no instantaneous part in its response to any stimulus that is not infinitely slow; the Maxwell-model does not have a definite length. Both deviations from the actual behaviour may be removed in the same way, viz. by letting one Voigt-element and one Maxwell-element in the respective models degenerate to a single ideal spring. We may arbitrarily assign the index 1 to the degenerate element, since the order in which the elements are arranged has no influence upon the mechanical behaviour of Voigt- and Max-

well-models – a reminder of the fact that a multitude of different models may represent the same viscoelastic behaviour. Note that degeneration to a spring has a different meaning for Voigt- and Maxwell-elements: for the former element, the dashpot should be removed, i.e., $\eta_1 \to 0$; the dashpot of the latter element, however, must become a rigid connecting rod, that is, $\eta_1 \to \infty$.

The generalized admittance and impedance of the modified Voigt- and Maxwell-models then become

$$Y(z) = 1/E_1 + \sum_2^n \frac{1}{E_k + \eta_k z} \tag{37}$$

and

$$Z(z) = E_1 + \sum_2^n \frac{E_k \eta_k z}{E_k + \eta_k z}, \tag{38}$$

respectively. It should be added that the two functions defined by these equations are not reciprocal to one another if the models consist of the same springs and dashpots. Both functions, however, obviously are quotients of polynomials of degree n in z. Hence, it is possible, using different springs and dashpots, to construct a Maxwell-model that shows the same behaviour as the Voigt-model defined by eqn. (37), and a Voigt-model whose behaviour is identical with that of the Maxwell-model of eqn. (38).

The equations (37) and (38) will be used as a *definition* of the linear viscoelastic body provisionally described in the first two Sections. It is indeed found that, apart from two minor modifications, these equations are sufficiently general to account for all viscoelastic phenomena. The consequences of this definition for the other phenomenological quantities will be the subject of the next Section.

1.4. The distribution functions

Since the meaning of the generalized admittance $Y(z)$ and the generalized compliance $S(z)$ is identical, the definition given at the end of the preceding Section yields

$$S(z) = S_\infty \left(1 + \sum_k \frac{f_k}{s_k + z}\right) \tag{1}$$

with $S_\infty = 1/E_1$, $f_k = E_1/\eta_k$, and $s_k = E_k/\eta_k$, (1a)

as the typical expression for the generalized compliance of the linear viscoelastic body. It is indeed obvious that the compli-

ance of the single spring in the Voigt-model determines its compliance with respect to infinitely fast processes, since the dashpots behave as rigid bodies under those conditions. The constants s_k have the proper dimension of a reciprocal time; they will be called the *retardation frequencies*.

It was mentioned at the end of Sect. 1.3 that it is useful to modify the above equation somewhat. The modification is suggested by the fact that the experimentally observed viscoelastic behaviour of many systems is conveniently represented by models containing a very large number of elements. The parameters s_k and f_k of these elements lie so close together as to suggest a continuous sequence. Accordingly, the Voigt-model defined by equation (1) is generalized to a *continuous* one and the generalized compliance becomes

$$S(z) = S_\infty \left(1 + \int_0^\infty \frac{f(s)\ ds}{s + z}\right) . \tag{2}$$

The non-negative function $f(s)$ defined by this equation will be called the *distribution function* of retardation frequencies ([Gross, 1947], [Ter Haar]); both continuous and discrete distributions are included in eqn. (2) if we also allow $f(s)$ to be a sum of weighted delta functions. The distribution function is said to define a continuous or discrete *spectrum* of retardation frequencies. From its definition it is seen that $f(s)\ ds$ is a weight factor for the contribution to $S(z)$ of those elements of the Voigt-model whose parameters η/E lie in an infinitesimal region ds containing s.

It is clear that experimental methods cannot decide between a discrete and a continuous distribution function. Hence, one might be inclined to regard the introduction of continuous distribution functions as an artifice having the sole purpose of facilitating the discussion; one should realize, however, that the same is true for the discrete spectra, which are based on the equally artificial notion of the discrete models.

The modification of the models has a profound influence upon the nature of the singularities of $S(z)$ in the complex frequency plane. The essential part of $S(z)$, from this point of view, is the function $\Psi(z)$ of eqn. (1.3.18):

$$\Psi(z) = \sum_k \frac{f_k}{s_k + z} \qquad \text{(discrete spectrum)} \tag{3}$$

$$= \int_0^\infty \frac{f(s)\ ds}{s + z} \qquad \text{(continuous spectrum)}. \tag{4}$$

If eqn. (3) is valid, $\overline{\psi}(z)$ has as many poles in the points $z = -s_k$ of the negative real axis as there are terms in the sum. In (4) these poles form a dense sequence of points upon the negative real axis wherever $f(s)$ is not zero, s being the distance to the origin of the complex frequency plane. The resulting linear singularity of $\overline{\psi}(z)$ is a *cut* for this function, which is the *Stieltjes transform* of $f(s)$ ([WIDDER], [WALL], [PERRON]).

The Stieltjes transform of a function, whose indefinite integral is a non-decreasing and bounded function of its upper limit, is an analytic function of z in the entire complex plane cut along the negative real axis.

The fact that the variation of this analytic function on opposite sides of the cut is simply related to the function of which it is the Stieltjes transform leads to an important method of deriving the distribution functions from the experimental data. In Chapter 3 this method and further properties of the Stieltjes transform will be discussed.

The rate of retardation is easily obtained from eqns. (3) and (4). The former equation immediately yields

$$\psi(t) = \sum_k f_k \, e^{-s_k t} \,, \tag{5}$$

which evidently becomes

$$\psi(t) = \int_0^\infty f(s) \, e^{-ts} \, ds \tag{6}$$

in the continuous case. The relation between the rate of creep and the distribution function of retardation frequencies is simply that of a Laplace pair. Since $f(s)$ is a non-negative function, *Bernstein's theorem* [WIDDER] enables us to give a very concise characterization of the rate of retardation and hence of the linear viscoelastic body:

$\psi(t)$ is a completely monotonic function of the time, i.e.,

$$(-1)^n D^n \psi(t) \geqq 0 \,, \quad n = 0, 1, 2, \ldots \tag{7}$$

$$0 < t < \infty \,.$$

In focussing attention upon $\overline{\psi}(z)$ and $\psi(t)$ in this discussion, we missed an interesting aspect of the degeneration to an ideal spring of one Voigt-element in the model of Fig. 1.3.4. According to eqn. (1.3.35), the response, under zero initial conditions, to the unit impulsive stress $\sigma(t) = \delta(t)$ of the system represented by this model is

$$\varepsilon(t) = \sum_1^n \frac{1}{\eta_k} \, e^{-s_k t} \,, \qquad t \geqq 0 \,, \tag{8}$$

where the s_k's of eqn. (1a) have been introduced.

If $\eta_1 \to 0$, the pole of the first term of $S(z)$ of this system moves towards $z = -\infty$; since, subject to the condition Re $z > -s_1$,

$$\frac{1}{E_1 + \eta_1 z} = \frac{1}{\eta_1} \int_0^\infty e^{-s_1 t} e^{-zt} \, dt \, , \tag{9}$$

the Laplace transform of the first term of eqn. (8) approaches $1/E_1$ in this limiting process, whereas the term itself remains noticeably different from zero in an ever decreasing interval of the t-axis. Hence,

$$\lim_{\eta_1 \to 0} \frac{1}{\eta_1} e^{-s_1 t} = \frac{1}{E_1} \delta(t) \, . \tag{10}$$

Note that the function so defined is the asymmetric delta function: the Laplace transform of the symmetric delta function has the value ½ instead of 1 [SNEDDON, 1955].

By integration of eqn. (6), one obtains

$$\Psi(t) = \int_0^t \psi(\theta) \, d\theta = \int_0^\infty \frac{1}{s} f(s) \, (1 - e^{-ts}) \, ds \tag{11}$$

for the creep function. Usually, however, this relation is expressed in terms of another distribution function, the distribution function of retardation *times*, which are the reciprocals of the retardation frequencies:

$$\Psi(t) = \Psi(\infty) \, \{1 - \int_0^\infty F(\tau) \, e^{-t/\tau} \, d\tau\} \, , \tag{12}$$

with

$$\tau = 1/s \, , \qquad ds/s = - d\tau/\tau \, , \tag{13}$$

$$F(\tau) = \{\Psi(\infty)\}^{-1} \, \{\frac{1}{\tau} f(\frac{1}{\tau})\} \, , \tag{14}$$

$$\int_0^\infty F(\tau) \, d\tau = 1 \, . \tag{15}$$

Although, as we saw, the function $f(s)$ leads to simple relations which may be handled by well-known mathematical techniques, the distribution function $F(\tau)$ is universally used instead. The normalization to unity perhaps suggests an analogy to probability distribution functions, but has no other purpose than to bring out that $\Psi(0) = 0$, that is, to avoid another factor in eqn. (12).

The above distribution functions both belong to what was called the retardation family of functions. One may, however, equally well start from the continuous Maxwell-model, i.e., from the generalized mechanical impedance

$$E(z) = E_\infty \, \{1 - \overline{\varphi}(z)\} = E_\infty \, (1 - \int_0^\infty \frac{g(s) \, ds}{s + z}) \, , \tag{16}$$

which defines a distribution function of *relaxation* frequencies $g(s)$. This function is again related to the rate of relaxation by

$$\varphi(t) = \int_0^\infty g(s)\ e^{-ts}\ ds\ , \tag{17}$$

so that $\varphi(t)$ is also a completely monotonic function.

There is also a distribution function of *relaxation* times, $G(\tau)$, defined by

$$\Phi(t) = \Phi(\infty)\ \{1 - \int_0^\infty G(\tau)\ e^{-t/\tau}\ d\tau\} \tag{18}$$

which is again normalized to unity.

The entire discussion about the functions $f(s)$ and $F(\tau)$ may be repeated literally for $g(s)$ and $G(\tau)$. It will be clear, however, from what was said about the parameters of Voigt- and Maxwell-models representing the same viscoelastic system, that both pairs of functions can never be the same.

We shall formulate the relationship between $S(z)$ and $E(z)$ somewhat more precisely for the discrete spectra: the representative models are supposed to be a Voigt-model, consisting of one spring of compliance $S_1 = 1/E_1$ and n-1 Voigt-elements E_k, η_k ($k = 2,3,\ldots,n$), and a Maxwell-model, consisting of one spring with the modulus E_1' and n-1 Maxwell-elements E_k', η_k' ($k = 2,\ldots,n$). From eqns. (37) and (38) of the preceding Section, the generalized compliance and elastic modulus of the viscoelastic system are then found to be

$$S(z) = S_\infty\ (1 + \sum_2^n \frac{F_k^\circ}{1 + \tau_k\ z})\ , \tag{19}$$

$$(S_\infty = 1/E_1,\ F_k^\circ = E_1/E_k,\ \tau_k = \eta_k/E_k)$$

$$E(z) = E_\infty\ (1 - \sum_2^n \frac{G_k^\circ}{1 + \tau_k'\ z})\ , \tag{20}$$

$$(E_\infty = \sum_1^n E_k',\ G_k^\circ = E_k'/E_\infty,\ \tau_k' = \tau_k'/E_k')$$

which are one another's reciprocals.

The normalized distribution functions are obtained from these expressions by the introduction of the normalization constants

$$\beta = \Psi(\infty) = \overline{\psi}(0) = \int_0^\infty \psi(\tau)\ d\tau = \int_0^\infty \frac{f(s)\ ds}{s} = \frac{S_s - S_\infty}{S_\infty} = \frac{E_\infty - E_s}{E_s} \tag{21}$$

and

$$\beta' = \Phi(\infty) = \overline{\varphi}(0) = \int_0^\infty \varphi(\tau)\ d\tau = \int_0^\infty \frac{g(s)\ ds}{s} = \frac{E_\infty - E_s}{E_\infty} = \frac{S_s - S_\infty}{S_s} \tag{22}$$

which are called the retardation strength and the relaxation strength, respectively. Introducing β and β' into (19) and (20) yields:

$$S(z) = S_\infty \left(1 + \beta \sum_2^n \frac{F_k}{1 + \tau_k z}\right) , \qquad F_k = \frac{F_k^\circ}{\beta} , \quad (23)$$

and

$$E(z) = E_\infty \left(1 - \beta' \sum_2^n \frac{G_k}{1 + \tau_k' z}\right) , \qquad G_k = \frac{G_k^\circ}{\beta'} , \quad (24)$$

so that the distribution functions of retardation and relaxation times are

$$F(\tau) = \sum_2^n F_k \, \delta \, (\tau - \tau_k) \quad (25)$$

$$G(\tau) = \sum_2^n G_k \, \delta \, (\tau - \tau_k') . \quad (26)$$

Obviously the poles of $S(z)$ are the zeros of $E(z)$ and, conversely, the zeros of $S(z)$ are the poles of $E(z)$. According to eqns. (19)-(20) and (23)-(24) these poles and zeros are *simple*. If the values of these functions at the origin of the complex plane are compared with the eqns. (21)-(22), the fact that there cannot be other poles and zeros than the n-1 indicated in the foregoing equations leads to

$$S(z) = S_s \frac{(1 + \tau_2' z) \cdot \ldots \cdot (1 + \tau_n' z)}{(1 + \tau_2 z) \ldots (1 + \tau_n z)} = 1/E(z) . \quad (27)$$

An alternative form of this relation is

$$\frac{S(z)}{S_\infty} = \frac{(s_2' + z) \ldots (s_n' + z)}{(s_2 + z) \ldots (s_n + z)} = \frac{E_\infty}{E(z)} . \quad (28)$$

These equations show the nature of the coexistence of the two distribution functions in an entirely new perspective. Consideration of the changes of sign of these quotients along the negative real axis shows that, if

$$\tau_2 < \tau_3 < \ldots < \tau_n ,$$

then

$$\tau_2' < \tau_2 < \tau_3' < \tau_3 < \ldots < \tau_n' < \tau_n . \quad (29)$$

As an illustration of the significance of eqns. (27) – (29), we shall consider the case of the simplest possible viscoelastic body, for which

$$S(z) = S_s \frac{1 + \tau' z}{1 + \tau z} , \quad (30)$$

that is (cf. eqns. (1.3.3) and (1.3.5)),

$$(1 + \tau\, z)\, \bar{\varepsilon}(z) = S_s\, (1 + \tau'\, z)\, \bar{\sigma}(z)\ , \qquad z.i.c., \tag{31}$$

or, according to eqn. (1.3.24),

$$\varepsilon(t) + \tau D\, \varepsilon(t) = S_s\, \{\sigma(t) + \tau' D\, \sigma(t)\}\ . \tag{32}$$

Eqn. (32) is no longér restricted to zero initial conditions: it is the governing *differential equation* of the system and its Voigt- and Maxwell-model (Fig. 1).

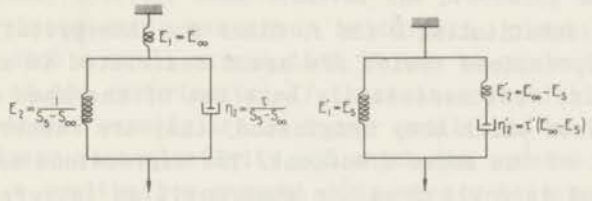

Figure 1.4.1

Since, according to eqns. (19) and (21)

$$S(z) = S_\infty + \frac{S_s - S_\infty}{1 + \tau\, z}\ , \tag{33}$$

we find by means of eqn. (30) that

$$\tau' = \frac{S_\infty}{S_s}\,\tau = \frac{S_s}{E_\infty}\,\tau\ , \tag{34}$$

in agreement with eqn. (29). The differential equation, which is sometimes called the dynamic equation of state, then becomes

$$\varepsilon + \tau\, \dot{\varepsilon} = S_s\, \sigma + S_\infty\, \dot{\sigma}\ . \tag{35}$$

Some introductions to the phenomenological theory of viscoelastic processes start from differential equations of the present type. In a sense this practice is objectionable since differential equations are non-typical for the theory: the frequent use of integral transforms and integral equations is a characteristic feature of the theory of linear relaxation processes necessitated just because of our fundamental ignorance of the governing differential equations [GROSS, 1953].

Eqns. (27) and (28) enable us to give an explicit expression for the compliance and elastic modulus operators introduced at the start of the preceding Section:

$$S_{op} = S_s\, \frac{(1 + \tau_2' D)\ (1 + \tau_3' D)\ \ldots\ (1 + \tau_n' D)}{(1 + \tau_2 D)\ (1 + \tau_3 D)\ \ldots\ (1 + \tau_n D)} = 1/E_{op}\ . \tag{36}$$

It is clear, however, that (36) is restricted to discrete spectra and that it cannot be easily generalized to continuous spectra.

Although their introduction offers no new points of view, we can, in the case of both discrete and continuous distribution functions, give other explicit expressions for the operators. These expressions are obtained from the relations (2) and (16), or the continuous analogues of (23) and (24):

$$S(z) = S_\infty \left(1 + \beta \int_0^\infty \frac{F(\tau)\ d\tau}{1 + z\ \tau}\right) , \tag{37}$$

$$E(z) = E_\infty \left(1 - \beta' \int_0^\infty \frac{G(\tau)\ d\tau}{1 + z\ \tau}\right) , \tag{38}$$

by simply substituting D for z. Since the interpretation of these formal expressions (which are again restricted to zero initial conditions) must necessarily make use of the same operational methods from which they originated, they are rather trivial in the light of the above treatment. The expressions may, however, be derived directly from the superposition integrals and then provide an alternative approach to the viscoelastic operators. As an example, we take the equation (1.1.11)

$$\varepsilon(t) = S_\infty \{\sigma(t) + \int_0^\infty \sigma(t-\tau)\ \psi(\tau)\ d\tau\}$$

and introduce the formal series expansion [HIRSCHMAN-WIDDER]

$$e^{-\tau D} = 1 - (\tau D) + \frac{1}{2!}\ (\tau D)^2 - \frac{1}{3!}\ (\tau D)^3 + \ldots , \quad D = \frac{d}{dt} , \tag{39}$$

into the Taylor series

$$\sigma(t-\tau) = \{1 - (\tau D) + \frac{1}{2!}\ (\tau D)^2 - \ldots\}\ \sigma(t) . \tag{40}$$

The superposition integral then becomes

$$\begin{aligned} \varepsilon(t) &= S_\infty \{\sigma(t) + \int_0^\infty e^{-\tau D}\ \sigma(t)\ \psi(\tau)\ d\tau\} \\ &= S_\infty \{1 + \int_0^\infty e^{-\tau D}\ \psi(\tau)\ d\tau\}\ \sigma(t) \\ &= S_\infty \{1 + \Psi(D)\}\ \sigma(t) \\ &= S_\infty \{1 + \int_0^\infty \frac{f(s)\ ds}{s + D}\}\ \sigma(t) , \quad \text{z.i.c.,} \end{aligned} \tag{41}$$

The subsequent treatment of these formal expressions proceeds by means of the operational methods of Sect. 1.3.

Until now we completely ignored an effect, the phenomenon of

plastic flow, which, to some extent, always accompanies viscoelastic behaviour. Plastic flow causes the strain under constant stress of a viscoelastic body to increase indefinitely; the stress under constant strain decreases to a final value that is *zero*. For linear systems, plastic flow is accounted for by connecting a single dashpot in series with the entire Voigt-model, or with the single spring in the Maxwell-model [ALFREY, 1948]; this amounts to adding a simple pole in the origin to $S(z)$, or a simple zero in the origin to $E(z)$.

It is found, however, that whenever the preceding description of linear viscoelastic behaviour is correct, plastic flow is present to such a small extent that it can be neglected in the time scale of the experiments. If there is appreciable plastic flow, the strains usually are no longer small, and we have to do with non-linear viscoelasticity, of which the present theory at most gives a qualitative account ([STAVERMAN-SCHWARZL, 1956], [ALFREY, 1948]).

The preceding discussion of viscoelastic behaviour was intended to be an introduction to a class of phenomena usually designated by the generic term relaxation phenomena. In this termimology viscoelastic behaviour is synonymous with mechanical relaxation. In the present Chapter this usage was avoided to prevent confusion with the word relaxation in its restricted sense.

The treatment did not aim at completeness: important topics, such as the relations between the dynamic modulus and compliance, and the determination of the distribution functions from the experimental data, are still to be discussed.

Clearly, a multitude of characteristic functions, constants, models and operators may be – and are actually – used to represent the behaviour of a given linear viscoelastic system quantitatively. In the present Chapter we have met the following sets of characteristic quantities, each of which suffices for the complete specification of the system in question:

1. Either E_s or E_∞ and one of the functions $\Psi(t)$, $\Phi(t)$, $\psi(t)$, or $\varphi(t)$, for $0 < t < \infty$.
2. $S(i\omega)$ or $E(i\omega)$, or either of their real or imaginary parts, or argument or modulus, for $0 < \omega < \infty$.
3. S_{op} or E_{op}.
4. $S(z)$ or $E(z)$.
5. The governing Voigt- or Maxwell-model.
6. The governing differential equation.
7. E_s or E_∞ and one of the four distribution functions $F(\tau)$, $G(\tau)$, $f(s)$ or $g(s)$.

8. The poles and zeros of $S(z)$ and $E(z)$ and the value of these functions in one point of the complex frequency plane, if the spectra are discrete.

Chapter 2

LINEAR DIELECTRIC RELAXATION

2.1. The complex permittivity ([BÖTTCHER], [VON HIPPEL], [FRÖHLICH])

The capacitance of a plane parallel plate condensor in vacuum, when edge effects are excluded, is given by

$$C = \frac{\varepsilon_o A}{d} \tag{1}$$

in the rationalized MKSQ-system of units ([SOMMERFELD III], [STRATTON], [VON HIPPEL], [CORNELIUS and HAMAKER]). In this equation ε_o is the absolute permittivity of empty space ($\simeq 8.86\times10^{-12}$ farad.m^{-1}), A is the area of the plates, and d is their distance. When filled with a non-conductor, the condensor increases its capacitance by a numerical factor ε_r, the relative permittivity of the inserted material. If the dielectric is homogeneous and isotropic, the electric field within the condensor is uniform, and of the magnitude

$$E = V/d \ , \tag{2}$$

V being the potential difference between the plates. The dielectric displacement is also uniform and equal to the charge density on the plates,

$$D = Q/A \ , \tag{3}$$

When we use the definition of the capacitance,

$$C = Q/V \ , \tag{4}$$

it is observed that eqns. (1) – (3) make the relation

$$D = \varepsilon_o \, \varepsilon_r \, E = \varepsilon \, E \tag{5}$$

accessible to measurement; in this equation, of course, ε, the absolute permittivity of the dielectric, is a more fundamental quantity than its experimental definition

$$\varepsilon = \varepsilon_o \, C/C_o$$

suggests *). As a rule, ε is independent of E up to quite high field strengths; hence, the denotations permittivity and dielectric constant are used interchangeably.

The electric energy

$$\tfrac{1}{2} Q V^2 \tag{6}$$

stored in the capacitor is equivalent to an amount of energy

$$\tfrac{1}{2} \varepsilon E^2 \tag{7}$$

stored in unit volume of the dielectric.

If the condensor is connected to a source of sinusoidal voltage

$$V(i\omega t) = V_o \, e^{i\omega t} \tag{8}$$

its charge is

$$Q(i\omega t) = C \, V_o \, e^{i\omega t} \, , \tag{9}$$

since the equations (1) – (5) are "instantaneous" relations.

Differentiation of eqn. (9) yields

$$I(i\omega t) = i\omega C \, V_o \, e^{i\omega t} \tag{10}$$

for the current drawn from the voltage generator, so that the steady state admittance is

$$Y(i\omega) = i\omega C = i\omega \, \varepsilon_r \, C_o \, . \tag{11}$$

According to the last two equations the current leads the voltage by a temporal phase angle $\tfrac{1}{2}\pi$. Actually, it is almost universally observed that if ω is varied through the experimentally accessible non-optical part of the electromagnetic spectrum, liquid and solid dielectrics show a more complicated behaviour than indicated by the foregoing equations.

The fact that different experimental techniques must be used to define ε_r for, roughly speaking, $\omega > 10^9$ sec^{-1}, is discussed by von Hippel. This limit is set by the wave length becoming commensurable with the dimensions of the apparatus. Our picture can be theoretically, not actually, saved by decreasing the dimensions of the capacitor and attendant apparatus.

The filled condensor is found to behave not as a pure capacitance but as the parallel combination of a frequency dependent capacitance and a frequency dependent conductance, even if the static conductance of the material is negligible. This phenomenon

*) In the following, the adjective "absolute" will usually be omitted.

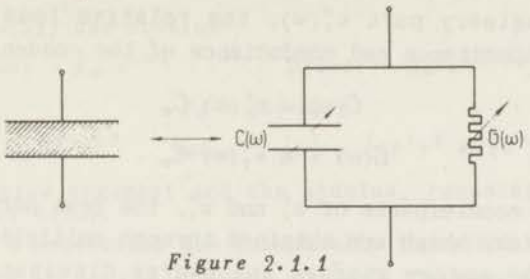

Figure 2.1.1

is called dielectric loss or dielectric relaxation. The function $C(\omega)$ in Fig. 1 is always found to be a monotonically decreasing function between the finite limits $C(0)$ and $C(\infty)$; $G(\omega)$ is monotonically increasing from $G(0)$, which is zero if there is no d.c. conductance, to an upper limit $G(\infty)$. If the system is linear, there is a very general relationship between these functions, which will be discussed in the next Chapter. Provisionally, linearity is defined as the absence of harmonics in the response of the dielectric to a monochromatic oscillatory stimulus, and proportionality of the amplitudes of stimulus and response. Nonlinearity is a rare phenomenon in dielectrics at all but the highest realizable field strengths.

Fig. 1 shows that for the filled condensor,

$$Y(i\omega) = G(\omega) + i\omega C(\omega) \ , \tag{12}$$

and that it is now both a sink and a reservoir for electrical energy. The average amount of energy dissipated per second within the space between its plates is given by

$$\tfrac{1}{2}\, G(\omega)\, V_o^2 \ , \tag{13}$$

the amount of energy alternately delivered and stored there during succeeding quarter cycles is

$$\tfrac{1}{2}\, C(\omega)\, V_o^2 \ . \tag{14}$$

Comparison of eqns. (11) and (12) shows why the dielectric itself is formally described by a complex relative permittivity:

$$\begin{aligned} Y(i\omega) &= i\omega \left\{ \varepsilon_r'(\omega) - i\varepsilon_r''(\omega) \right\} C_o \\ &= i\omega\, \varepsilon_r(i\omega)\, C_o \ . \end{aligned} \tag{15}$$

Its real part $\varepsilon_r'(\omega)$, the real relative permittivity, and its negative imaginary part $\varepsilon_r''(\omega)$, the relative loss factor, are related to capacitance and conductance of the condensor by

$$C(\omega) = \varepsilon_r'(\omega)\, C_o \tag{16}$$

and

$$G(\omega) = \omega\, \varepsilon_r''(\omega)\, C_o\ . \tag{17}$$

The absolute counterparts of ε_r' and ε_r'', the real permittivity and the loss factor, which are obtained through multiplication by ε_o, determine the energy storage and energy dissipation per unit volume of the dielectric within the condensor: the amount of energy stored or delivered by a unit volume during one quarter cycle is

$$\tfrac{1}{2}\, \varepsilon_o\, \varepsilon_r'\, E_o^2 = \tfrac{1}{2}\, \varepsilon'\, E_o^2 \tag{18}$$

if

$$E(i\omega t) = E_o\, e^{i\omega t}\ . \tag{19}$$

During one second, a unit volume of the dielectric converts an average amount of energy

$$\tfrac{1}{2}\, \omega\, \varepsilon_o\, \varepsilon_r''\, E_o^2 = \tfrac{1}{2}\, \omega\, \varepsilon''\, E_o^2 \tag{20}$$

into heat; during one complete cycle ($2\pi/\omega$ seconds), the average energy dissipation is

$$\pi\, \varepsilon''\, E_o^2\ . \tag{21}$$

The dielectric displacement is related to the time dependent field strength (19) by a factor $\varepsilon(i\omega)$, the complex permittivity, thus,

$$D(i\omega t) = \varepsilon(i\omega)\, E_o\, e^{i\omega t} = \{\varepsilon'(\omega) - i\varepsilon''(\omega)\}\, E(i\omega t)\ . \tag{22}$$

According to equations (17) and (20), dielectric loss may equally well be characterized by attributing a specific conductivity

$$\sigma(\omega) = \omega\, \varepsilon'' \tag{23}$$

to the material. If often happens that $\sigma(0)$ is appreciably different from zero, i.e., that ε'' has a pole at $\omega = 0$. Then, the comparative magnitudes of $\sigma(0)$ and $\sigma(\omega) - \sigma(0)$ determine whether the effect is described as dielectric loss with superposed d.c. conductivity or as a dispersion of the conductivity. Another quantity frequently used to describe dielectric loss is the tangent of the loss angle δ, that is, the phase angle by which the steady state voltage over the capacitor leads the charge, or by which $E(i\omega t)$ leads $D(i\omega t)$:

$$\tan \delta = \varepsilon''/\varepsilon' = G/\omega C \qquad (24)$$

From eqn. (22) one obtains

$$E(i\omega t) = E_o\, e^{i\omega t} \qquad D(i\omega t) = D_o\, e^{i(\omega t-\delta)}\,, \qquad (25)$$

where $D_o = |\varepsilon|\, E_o$;

$$\tan \delta = \varepsilon''/\varepsilon' \quad \text{and} \quad |\varepsilon| = \{(\varepsilon')^2 + (\varepsilon'')^2\}^{1/2}\,.$$

are the negative argument and the modulus, respectively, of the complex number $\varepsilon(i\omega)$.

Since tan δ determines the technically important ratio of energy dissipated to energy stored, of both the condensor and the dielectric, it is a figure of merit rather than a measure for the energy dissipation. Occasionally the loss cotangent, the quality factor Q of the dielectric, is used to the same purpose.

Fig. 2 shows the general appearance of experimentally obtained $\varepsilon'(\omega)$- and $\varepsilon''(\omega)$-curves.

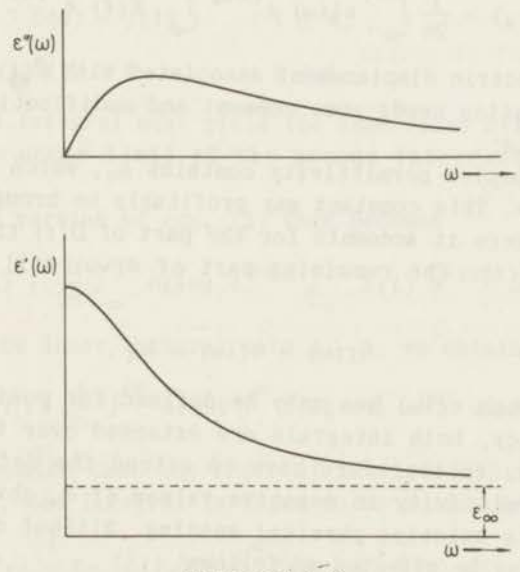

Figure 2.1.2

The maximum of ε'' occurs approximately at a value of ω for which the rate of change of ε' is also maximal. It frequently happens that the ε''-curve has more than one maximum and that the ε'-curve has corresponding "dips". Always, however,

1) $\varepsilon'(\omega)$ is a monotonically decreasing function of ω,
2) $\varepsilon'(\omega)$ has constant limiting values ε_s and ε_∞ for $\omega \to 0$ and $\omega \to \infty$, respectively,

3) the corresponding limiting values of $\varepsilon''(\omega)$ are zero in the absence of d.c. conductivity.

2.2. The dielectric displacement for arbitrary time dependent field strengths

By Fourier's integral theorem, any physically realizable time dependent electric field strength may be expressed as a superposition of sinusoids of all possible frequencies:

$$E(t_o) = \frac{1}{2\pi}\int_{-\infty}^{+\infty} e^{i\omega t_o} \int_{-\infty}^{+\infty} E(t)\, e^{-i\omega t}\, dt\, d\omega\,. \qquad (1)$$

If we extend the validity of the provisional definition of linearity in the foregoing Section to the components of a composite stimulus, we obtain from eqn. (2.1.22) that

$$D(t_o) = \frac{1}{2\pi}\int_{-\infty}^{+\infty} \varepsilon(i\omega)\, e^{i\omega t_o} \int_{-\infty}^{+\infty} E(t)\, e^{-i\omega t}\, dt\, d\omega \qquad (2)$$

is the dielectric displacement associated with $E(t)$.

This equation needs some comment and modification on the following points:

1) The complex permittivity contains ε_∞, which is independent of frequency. This constant may profitably be brought outside the integral, where it accounts for the part of $D(t)$ that is synchronous with $E(t)$. The remaining part of $\varepsilon(i\omega)$ will be denoted by $h(i\omega)$:

$$h(i\omega) = \varepsilon(i\omega) - \varepsilon_\infty\,. \qquad (3)$$

2) Although $\varepsilon(i\omega)$ has only be defined for positive values of the frequency, both integrals are extended over the entire frequency axis. We therefore have to extend the definition of the complex permittivity to negative values of ω, obviously without changing its existing physical meaning. Without difficulty this extension may be effected as follows:

It is well-known that the pair of equations

$$E(i\omega t) = E_o\, e^{i\omega t}\,, \qquad D(i\omega t) = \varepsilon(i\omega)\, E_o\, e^{i\omega t}$$

may be pictorially represented by a pointer diagram, in which the former quantity corresponds to a pointer, of length E_o, rotating counter-clockwise with a radian velocity ω sec^{-1}, and the latter quantity to a pointer, of length D_o, lagging behind the other one by an angle δ (cf. eqn. (2.1.25)). In this picture, a

negative frequency corresponds to a *clockwise* rotation of the two pointers. The ratio of their magnitudes remains unchanged, but the phase angle has the opposite sign, since the D-pointer still lags behind the E-pointer. Hence, the real and imaginary parts of the complex permittivity must be even and odd functions of the frequency, respectively:

$$\varepsilon'(\omega) = \varepsilon'(-\omega) \tag{4}$$

$$\varepsilon''(\omega) = -\varepsilon''(-\omega) \ . \tag{5}$$

The same conclusion is reached by observing that a real function $E(t)$ in eqn. (2) should give a real function $D(t)$ [HIEDEMANN-SPENCE].

3) Eqn. (2) implies a dependence of $D(t_o)$ on future values of $E(t)$, which is contrary to all physical experience. Substitution of

$$E(t) = f(t) \ , \qquad -\infty < t < +\infty \ ,$$

or

$$E(t) = f(t) \ , \qquad t \leqq t_o \ ,$$

$$E(t) = 0 \ , \qquad t > t_o \ ,$$

into the second integral must yield the same value $D(t_o)$. We conclude that the upper limit of the second integration must be changed into t_o.

The improved version of eqn. (2) then becomes

$$D(t_o) = \varepsilon_\infty E(t_o) + \frac{1}{2\pi} \int_{-\infty}^{+\infty} h(i\omega)\, e^{i\omega t_o} \int_{-\infty}^{t_o} E(t)\, e^{-i\omega t}\, dt\, d\omega \ . \tag{2a}$$

Changing t in the inner integral into $t_o - \tau$, we obtain

$$D(t_o) = \varepsilon_\infty E(t_o) + \frac{1}{2\pi} \int_{-\infty}^{+\infty} h(i\omega) \int_{o}^{\infty} E(t_o - \tau)\, e^{i\omega\tau}\, d\tau\, d\omega \ . \tag{6}$$

Under the assumption that the order of the two integrations may be interchanged, the integral is found to be equivalent to

$$D(t_o) = \varepsilon_\infty \{E(t_o) + \int_{o}^{\infty} E(t_o - \tau)\ \psi(\tau)\ d\tau\} \tag{7}$$

with

$$\psi(\tau) = (1/2\pi\varepsilon_\infty) \int_{-\infty}^{\infty} h(i\omega)\, e^{i\omega\tau}\, d\omega \ . \tag{8}$$

In eqn. (7) we recognize the superposition integral (1.1.11), although the resemblance may be formal since, as yet, nothing is known about the present function $\psi(t)$.

Subject to conditions on $\psi(t)$ and $h(i\omega)$, eqn. (8), rewritten

as $$\psi(\tau) = \frac{1}{2\pi i} \int_{-i\infty}^{+i\infty} \bar{\psi}(i\omega)\ e^{i\omega\tau}\ \mathrm{d}(i\omega)\ , \tag{9}$$

in which $$\bar{\psi}(i\omega) = \frac{\varepsilon(i\omega) - \varepsilon_\infty}{\varepsilon_\infty}\ , \tag{10}$$

is observed to be a special instance of the inversion formula (1.3.19) of the Laplace transform. The more general form of eqn. (9) obtained by introducing the analytic continuations of $\bar{\psi}(i\omega)$ and $\varepsilon(i\omega)$ in the complex frequency plane shows the function $\psi(t)$ in its proper perspective:

$$\psi(t) = \frac{1}{2\pi i} \int_{c-i\infty}^{c+i\infty} \frac{\varepsilon(z) - \varepsilon_\infty}{\varepsilon_\infty}\ e^{iz t}\ \mathrm{d}z = \frac{1}{2\pi i} \int_{c-i\infty}^{c+i\infty} \bar{\psi}(z)\ e^{iz t}\ \mathrm{d}z \tag{12}$$

$$\bar{\psi}(z) = \frac{\varepsilon(z) - \varepsilon_\infty}{\varepsilon_\infty} = \int_0^\infty \psi(t)\ e^{zt}\ \mathrm{d}t\ . \tag{13}$$

[HIEDEMANN-SPENCE].

In our treatment of the phenomenological theory of dielectric relaxation we have now reached a stage which may be compared with the beginning of Sect. 1.3 in the theory of viscoelasticity. The present derivation of the superposition integral illustrates once again the first method, mentioned in that Section, of analyzing a linear operator relation. For lossy dielectrics, this operator relation is

$$D(t) = \varepsilon_{op}\, E(t)\ . \tag{14}$$

There is no need to elaborate the inverse equation

$$E(t) = \varepsilon_{op}^{-1}\, D(t) \tag{15}$$

since dielectric loss is exclusively described in terms of the retardation (or admittance) family of functions: the electric field strength should be compared with the stress, the dielectric displacement with the strain of elastic systems. Provisionally, this correspondence will be justified by the fact that the first pair are intensive quantities, the second pair extensive quantities. The comparison of different kinds of relaxation processes will be more fully discussed in Sect. 3.1.

With eqns. (7) and (14) as a starting-point, we may transcribe all the results, obtained in Chapter 1 for the linear viscoelastic body, into formulae for linear lossy dielectrics. For example, eqns. (1.1.1 - 2) and (1.1.12) correspond to the following relations for the transient behaviour of the dielectric at rest:

if $E(t) = E_o\, S_1(t)$, $D(t) = \varepsilon_\infty \{1 + \Psi(t)\} E_o\, S_1(t)$; (16)

if $E(t) = E_o\, \delta(t)$, $D(t) = \varepsilon_\infty \{1 + \psi(t)\} E_o\, S_1(t)$. (17)

In the former equation,

$$\Psi(t) = \int_o^t \psi(\tau)\, d\tau \ . \tag{18}$$

By analogy with the functions $\Psi(t)$ and $\psi(t)$ of the first Chapter, the present functions will be called the dielectric retardation function and the dielectric rate of retardation, respectively.

If an arbitrary time dependent field strength $E(t)$ is applied to a dielectric under zero initial conditions at $t = 0$, the Laplace transform of the resulting dielectric displacement is found from

$$\bar{D}(z) = \varepsilon(z)\, \bar{E}(z) \ , \quad \text{z.i.c.,} \tag{19}$$

the analogue of eqn. (1.3.3). The analytic function $\varepsilon(z)$ also occurs in the response of the dielectric upon application of the exponentially increasing or decreasing oscillatory field strength

$$E_o\, e^{zt} \ , \quad t > -\infty \ , \tag{20}$$

which produces a dielectric displacement

$$D(t) = \varepsilon(z)\, E_o\, e^{zt} = \varepsilon_\infty \{1 + \bar{\Psi}(z)\} E_o\, e^{zt} \ . \tag{21}$$

Eqns. (20) and (21) are the counterpart of eqns. (17) and (18) of Sect. 1.3. The properties of the permittivity operator of lossy dielectrics are again completely determined by the behaviour of the generalized permittivity $\varepsilon(z)$ in the complex frequency plane. We conclude from the discussion of the preceding Cbapter that the singularities of $\varepsilon(z)$ must be located in the left half of the complex plane. Eqns. (4) and (5) may be combined to yield

$$\varepsilon(z^*) = \varepsilon^*(z) \ . \tag{22}$$

The generalized compliance and modulus of the first Chapter have the same property. It might perhaps be thought that this property is a consequence of the fact that the singularities of the complex functions are located on the negative real axis, but this is a sufficient rather than a necessary condition: even if the singularities are located elsewhere, equation (22) holds for the generalized quantities. Its significance is that singularities may only occur pairwise, the real axis being an axis of symmetry.

The most distinctive feature of dielectric relaxation, apart from linearity, is again that the singularities of $\varepsilon(z)$ lie on or

close to the negative real axis of the complex frequency plane. In the next Section we will discuss a method of presentation of the experimental data resulting from dynamical measurements which gives better support for this contention than we were able to give in Chapter 1.

2.3. The semi-circular Cole-Cole diagram

In 1941, Cole and Cole proposed – in analogy to the Nyquist-diagram of electric network theory – expression of the frequency dependence of both ε_r' and ε_r'' in one single diagram, by plotting the latter as a function of the former, ω being a parameter (COLE-COLE).

In 1940, F.K.du Pré used an identical diagram for magnetic relaxation [DU PRÉ].

Although Cole and Cole called the resulting diagram the complex plane locus of the complex dielectric constant, the name Cole-Cole diagram is commonly used. It is remarkable that, for many dielectrics, the Cole-Cole diagram is found to be a semi-circle within the limits of experimental accuracy.

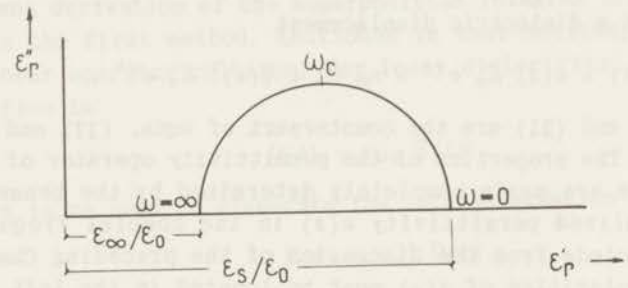

Figure 2.3.1

The frequency at which the relative loss factor attains its maximum value is called the critical frequency ω_c.

The question arises why the semi-circle is so common a diagram for dielectrics. An answer is easily found by regarding the absolute analogue of the Cole-Cole plot, obtained through multiplication by ε_o, as one particular curve in a more general diagram, the conformal representation of the complex frequency plane upon the $\varepsilon(z)$-plane. Any Cole-Cole diagram is the map of the positive imaginary axis of the z-plane upon the generalized permittivity plane, according to this interpretation. An additional detail is that, because of the convention to define the negative imaginary part of $\varepsilon(i\omega)$ as the loss factor, the actual map is reflected in

the real axis to give the Cole-Cole plot in its usual upright position.

As eqn. (2.2.10) shows, the corresponding map of the z-plane upon the $\Psi(z)$ plane is obtained from the present one by a displacement ε_∞ to the left and a change of scale $\varepsilon_\infty : 1$; the shape of the figures is thereby retained.

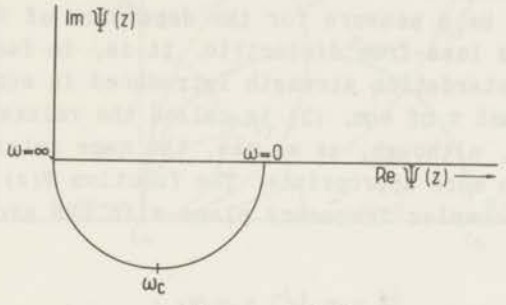

Figure 2.3.2

From eqn. (2.2.22) we gather that the map of the complete ω-axis ($-\infty \leqq \omega \leqq +\infty$) is a full circle of which Fig. 2 shows the lower half only. Then, however, the transformation by the function $\Psi(z)$ cannot be anything else than a *Möbius-* or *bilinear* transformation [PHILLIPS] and this function must have the form

$$\Psi(z) = \frac{a\ z + b}{c\ z + d} . \tag{1}$$

Fig. 2 shows that $z = \infty$ is mapped on $\Psi(z) = 0$, whence $a = 0$. Furthermore, no generality is lost by assuming $c = 1$. It remains, then, so to determine the constants in

$$\Psi(z) = \frac{b}{z + d} \tag{2}$$

as to obtain agreement with the Figure. Clearly

$$\Psi(0) = b/d = \frac{\varepsilon_s - \varepsilon_\infty}{\varepsilon_\infty}$$

and $$\Psi(i\omega_c) = \frac{\varepsilon_s - \varepsilon_\infty}{\varepsilon_\infty} \left(\frac{1 - i}{2}\right) = \frac{b}{i\omega_c + d} .$$

The final result is therefore

$$\Psi(z) = \frac{\varepsilon_s - \varepsilon_\infty}{\varepsilon_\infty} \frac{\omega_c}{\omega_c + z} = \frac{\beta}{1 + z\,\tau} \tag{3}$$

where

$$\beta = \frac{\varepsilon_s - \varepsilon_\infty}{\varepsilon_\infty} \tag{4}$$

and $$\tau = 1/\omega_c \, . \tag{5}$$

From Fig. 1, the dimensionless constant β is observed to be the ratio of the diameter of the semi-circle to its lower intercept, and as such to be a measure for the departure of the material from the simple loss-free dielectric. It is, in fact, the analogue of the retardation strength introduced in eqn. (1.4.21). The time constant τ of eqn. (3) is called the relaxation time of the dielectric, although, as we saw, the name retardation time would have been more appropriate. The function $\overline{\psi}(z)$ is analytic in the entire complex frequency plane with the exception of a single pole in

$$z = -1/\tau = -\omega_c \, .$$

For such a function all the formulae of Sect. 2.2 are correct and one easily obtains

$$\psi(t) = (\beta/\tau)\, e^{-t/\tau} \, , \tag{6}$$

$$\Psi(t) = \beta\,(1 - e^{-t/\tau}) \, , \tag{7}$$

$$\varepsilon(i\omega) = \varepsilon_\infty + \frac{\varepsilon_s - \varepsilon_\infty}{1 + i\omega\tau} \, , \tag{8}$$

whence

$$\varepsilon'(\omega) = \varepsilon_\infty + \frac{\varepsilon_s - \varepsilon_\infty}{1 + \omega^2 \tau^2} \tag{9}$$

$$\varepsilon''(\omega) = \frac{(\varepsilon_s - \varepsilon_\infty)\, \omega \tau}{1 + \omega^2 \tau^2} \tag{10}$$

The last two equations are the well-known Debye equations (cf. Chapt. 5). Rewriting (9) and (10) as

$$\varepsilon'(\omega) = \tfrac{1}{2}\,(\varepsilon_s - \varepsilon_\infty) + \tfrac{1}{2}\,(\varepsilon_s - \varepsilon_\infty)\cos\alpha$$

$$\varepsilon''(\omega) = \tfrac{1}{2}\,(\varepsilon_s - \varepsilon_\infty)\sin\alpha$$

with $$\sin\alpha = \frac{2\omega\tau}{1 + \omega^2 \tau^2} \, ; \qquad \cos\alpha = \frac{1 - \omega^2 \tau^2}{1 + \omega^2 \tau^2}$$

readily shows them to be a common parameter representation of the circle.

The construction of the distribution of frequencies along the semi-circular arc is illustrated in Fig. 3, actually part of the map of the z-plane upon the $\varepsilon(z)$-plane.

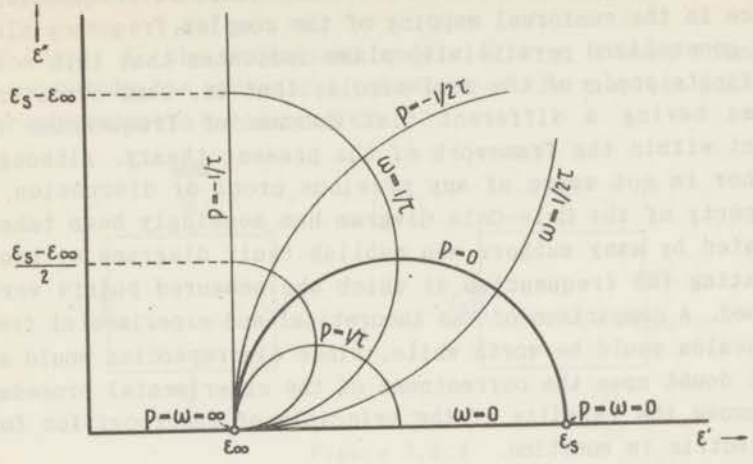

Figure 2.3.3

Eqn. (3) yields

$$\varepsilon(z) = \varepsilon_\infty + \frac{\varepsilon_s - \varepsilon_\infty}{1 + z\tau} = \varepsilon_\infty + \frac{\varepsilon_s - \varepsilon_\infty}{1 + (p + i\omega)\tau}, \qquad (11)$$

so that straight lines in the z-plane parallel to the real axis

$$\omega\tau = c_1, \qquad p \text{ variable},$$

are mapped on the circles

$$(\varepsilon' - \varepsilon_\infty)^2 + (\varepsilon'' - \frac{\varepsilon_s - \varepsilon_\infty}{2c_1})^2 = (\frac{\varepsilon_s - \varepsilon_\infty}{2c_1})^2 \qquad (12)$$

in the $\varepsilon(z)$-plane. These circles are tangential to the ε'-axis and their centres are located upon the straight line $\varepsilon' = \varepsilon_\infty$. Straight lines in the z-plane

$$p\tau = c_2, \qquad \omega \text{ variable},$$

become circles

$$\{\varepsilon' - (\varepsilon_\infty + \frac{\varepsilon_s - \varepsilon_\infty}{2(1 + c_2)})\}^2 + \varepsilon''^2 = \{\frac{\varepsilon_s - \varepsilon_\infty}{2(1 + c_2)}\}^2 \qquad (13)$$

tangential to the line $\varepsilon' = \varepsilon_\infty$ and having their centres upon the ε'-axis. The Cole-Cole diagram is one of these circles, viz. the one for which $c_2 = 0$.

From the second Debye equation, in the slightly different form

$$\varepsilon''(\omega) = \frac{\varepsilon_s - \varepsilon_\infty}{\omega\tau + 1/\omega\tau}, \qquad (14)$$

it is at once apparent that there is a symmetric distribution of frequencies along the semi-circular Cole-Cole diagram.

It follows from the previous discussion that the semi-circular

plot is incomplete without an attached scale of frequencies. Its place in the conformal mapping of the complex frequency plane on the generalized permittivity plane indicates that this scale is an innate scale of the semi-circle, that is, semi-circular diagrams having a different distribution of frequencies cannot exist within the framework of the present theory. Although the author is not aware of any previous proof or discussion, this property of the Cole-Cole diagram has seemingly been taken for granted by many authors who publish their diagrams without indicating the frequencies at which the measured points were obtained. A comparison of the theoretical and experimental frequency scales would be worth while, since discrepancies would either cast doubt upon the correctness of the experimental procedure or disprove the validity of the principle of superposition for the dielectric in question.

An alternative check upon the agreement of the theoretical and experimental frequency scales for the semi-circular diagram is provided by the relation ([Cole, 1955], [von Hippel])

$$\varepsilon'(\omega) = \varepsilon_s - \omega\tau\,\varepsilon''(\omega)\ , \tag{15}$$

which is a consequence of the Debye equations. According to this formula, a plot of ε' vs. $\omega\varepsilon''$, the specific conductivity of eqn. (2.1.23), should be a straight line of slope $-\tau$ intersecting the ε'-axis in ε_s.

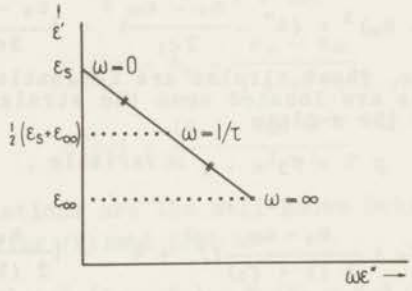

Figure 2.3.4

Eqns. (2.1.16) and (2.1.17) show that this plot is similar to a plot of $C(\omega)$ against $G(\omega)$ of the measuring cell. Two advantages of the diagram are that it allows a more accurate estimation of τ than the semi-circle does and that ε_∞ needs not be known for this purpose. Other useful properties of the diagram are given in [Cole, 1955]. Its utility, however, is restricted to the simple dielectrics of this Section.

2.4. Macroscopic models for dielectric relaxation

In Chapt. 1, the mechanical models of Fig. 1 were found to copy accurately the mechanical behaviour of the simplest possible linear viscoelastic substances.

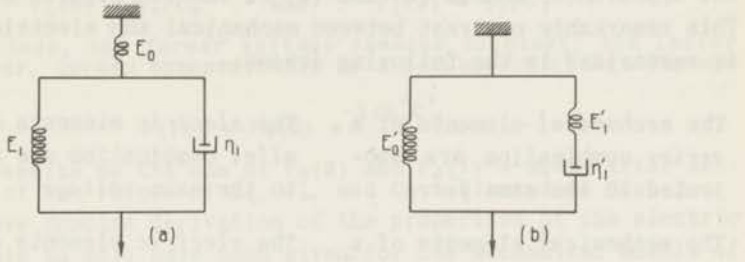

Figure 2.4.1

Model (a) proved to be more suitable for a description in terms of the retardation family of functions, model (b) in terms of the relaxation family of functions. Similarly, the following two simple electric networks faithfully represent the behaviour of a unit cube of the dielectrics of the preceding Section, if contained in an ideal condensor (VON HIPPEL).

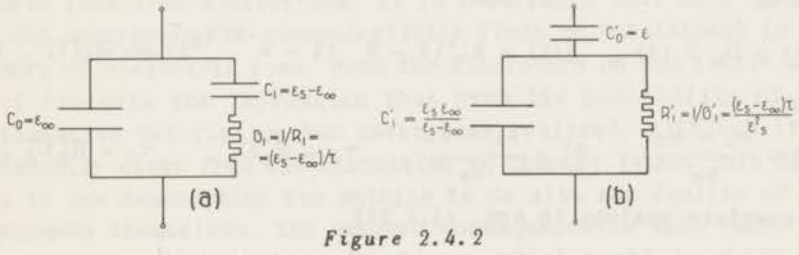

Figure 2.4.2

The known rules of electric network theory yield for the steady-state admittance of model (a)

$$Y(i\omega) = i\omega C_0 + \frac{1}{1/i\omega C_1 + R_1}$$

$$= i\omega\,(\varepsilon_\infty + \frac{\varepsilon_s - \varepsilon_\infty}{1 + i\omega\tau}) \,. \qquad (1)$$

The steady-state impedance of model (b) is found to be

$$Z(i\omega) = 1/i\omega C_o' + 1/(i\omega C_1' + G_1')$$

$$= (1/i\omega)\ \left(\frac{1 + i\omega\tau}{\varepsilon_s - \varepsilon_\infty\ i\omega\tau}\right)\ , \qquad (2)$$

which is indeed the reciprocal of (1). In spite of their different appearance, models (a) and (b) of the two Figures correspond. This remarkable contrast between mechanical and electric networks is summarized in the following scheme:

The *mechanical* elements of a *series* combination are subjected to the same *force*.	The *electric* elements of a *parallel* combination are subjected to the same *voltage*.
The *mechanical* elements of a *parallel* combination have the same rate of *deformation*.	The *electric* elements of a *series* combination are traversed by the same *current*.

In many respects, the electric models provide the most elegant and illustrative approach to the behaviour of the simplest lossy dielectrics. Almost without calculation, e.g., inspection of the models of Fig. 2 shows that, if

$$E(t) = E_o\ S_1(t)\ ,\quad D(t) = \varepsilon_\infty \{1 + \beta\ (1 - e^{-t/\tau_1})\}\ E_o\ S_1(t)\ , \qquad (3)$$

and if

$$D(t) = D_o\ S_1(t)\ ,\quad E(t) = \varepsilon_\infty^{-1}\{1 - \beta'\ (1 - e^{-t/\tau_2})\}\ D_o\ S_1(t)\ , \qquad (4)$$

with

$$\beta = \frac{\varepsilon_s - \varepsilon_\infty}{\varepsilon_\infty}\ ,\quad \beta' = \frac{\varepsilon_s - \varepsilon_\infty}{\varepsilon_s}\ ,\quad \tau_1 = R_1 C_1\ ,\quad \tau_2 = R_2' C_2'\ .$$

In complete analogy to eqn. (1.4.34)

$$\tau_1 = \frac{\varepsilon_\infty}{\varepsilon_s}\,\tau_2\ . \qquad (5)$$

For, if model (a) is initially free of charge, a voltage $V_o S_1(t)$ instantaneously charges C_o with

$$Q_i = C_o\ V_o\ S_1(t)\ .$$

The retarded charge leaking into C_1 through R_1 is given by the well-known law

$$Q_r = C_1\ V_o\ (1 - e^{-t/R_1C_1})\ .$$

The sum of these two charges is identical with eqn. (3) when the proper substitutions are made.

Eqn. (4) is most easily found by considering what happens when a charge $Q_o S_1(t)$ is applied to model (b), also initially free of

charge. Then, at $t = 0+$, the model behaves as if R_1' were infinite; i.e., its instantaneous capacitance is given by

$$1/C_\infty' = 1/C_o' + 1/C_1' \ ,$$

the charge of each capacitance is Q_o and their voltages are

$$V_o(0) = Q_o/C_o' \qquad \text{and} \qquad V_1(0) = Q_o/C_1' \ .$$

At later times, the former voltage remains constant; the latter one, however, decays exponentially by a leakage of charge through R_1':

$$V_1(t) = V_o(0)\ e^{-t/R_1'C_1'} \ .$$

Eqn. (4) results as the sum of $V_o(0)$ and $V_1(t)$ – again after substitution of the values of R_1', C_o' and C_1' indicated in Fig. 2.

The above concise derivation of the properties of the electric models could as well have been given for the mechanical models of Fig. 1.4.1. It was postponed till here because the properties of electric networks are better known.

After eqn. (2.2.15), it was stated that dielectric loss is exclusively described in terms of the retardation family of functions. Clearly, model (a) of Fig. 2 is more suitable for this purpose than model (b), which readily led to eqn. (4), the electric analogue of eqns. (1.1.13-14). This one-sided aspect of the phenomenological theory of dielectric loss has no other reason than that one is wont to write $D = \varepsilon E$ and not $E = \varepsilon^{-1} D$ for isotropic loss-free dielectrics. It is remarkable that this duality in the description of viscoelasticity finds no counterpart in the theory of dielectric loss. From the literature on the latter subject one gets the impression that even the possibility of the alternative description has never been realized. Although it is abundantly clear from the discussion in Chapter 1 that this duality in the description has nothing to do with any duality of the phenomena themselves, the awkward consequence is that there are two possible distribution functions, which ought to shake the general belief that these are the quantities of the phenomenological theory that have a direct bearing upon the underlying molecular processes. The difference between these two functions is usually quite appreciable: for the dielectric represented by the two models (a) and (b), the "retardation" time τ_1 and the "relaxation" time τ_2 differ by a factor $\varepsilon_s/\varepsilon_\infty$ which may be as large as 16 (for water [BROT et al.]) *).

It is possible to introduce distribution functions of retarda-

*) Recently it has been suggested that the Cole-Cole diagram of water is not a semi-circle but a circular arc. Since the characteristic parameter α of the circular arc is only 0.02 (cf. eqn. (3.3.14)) the difference is very slight [GRANT-BUCHANAN-COOK].

tion and relaxation times or frequencies in complete analogy to those of Chapter 1; it is also necessary: for, many dielectrics have non-semi-circular Cole-Cole diagrams. The models for these dielectrics, then, cannot be those of Fig. 2; as yet, however, no linear dielectrics are known whose behaviour, in the regions of frequency accessible to measurement, cannot be represented by the more complicated models of Fig. 3 and their continuous generalizations.

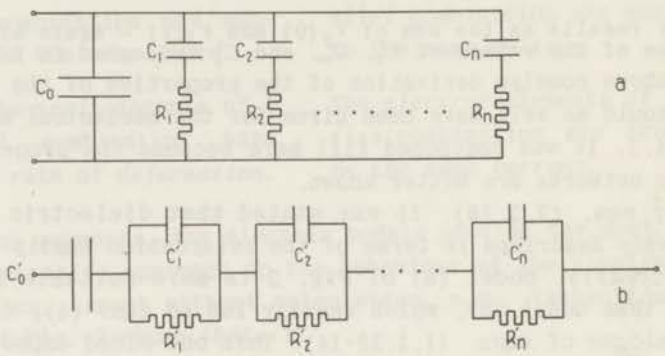

Figure 2.4.3

Model (a) should be compared with the Voigt-model, model (b) with the Maxwell-model of a viscoelastic substance. The steady state admittance of model (a) is

$$Y(i\omega) = i\omega C_o + \sum_k \frac{i\omega C_k}{1 + i\omega\tau_k} \tag{6}$$

with $$\tau_k = R_k C_k \ . \tag{6a}$$

The steady state impedance of model (b) is

$$Z(i\omega) = 1/i\omega C'_o + \sum_k \frac{R'_k}{1 + i\omega\tau'_k} \tag{7}$$

with $$\tau'_k = R'_k C'_k \ . \tag{7a}$$

The former equation leads to a complex permittivity

$$\varepsilon(i\omega) = \varepsilon_\infty + \sum_k \frac{F^o_k}{1 + i\omega\tau_k}, \tag{8}$$

where $$\sum_k F^o_k = \varepsilon_s - \varepsilon_\infty \ , \tag{8a}$$

or, in the continuous case ([Böttcher], [von Hippel])

$$\varepsilon(i\omega) = \varepsilon_\infty + (\varepsilon_s - \varepsilon_\infty) \int_0^\infty \frac{F(\tau)\ d\tau}{1 + i\omega\tau} \tag{9}$$

with $$\int_0^\infty F(\tau)\ d\tau = 1\ . \tag{10}$$

$F(\tau)$ should be called the distribution function of retardation times, but is invariably called the distribution function of relaxation times. Eqn. (7), after slight modification, yields

$$1/\varepsilon(i\omega) = 1/\varepsilon_\infty - \left(\frac{1}{\varepsilon_\infty} - \frac{1}{\varepsilon_s}\right) \int_0^\infty \frac{G(\tau)\ d\tau}{1 + i\omega\tau} \tag{11}$$

as the defining equation for the (true) distribution function of relaxation times in the continuous case, which is again normalized to unity. Of course, the discrete case is again included in the equations (9) and (11) if the distribution functions are also allowed to be sums of delta functions.

The discussion of Sect. 1.4 and its results may be applied unchanged to the present dielectric distribution functions. For instance, the general equations for the dielectric retardation function $\Psi(t)$ and the dielectric relaxation function $\Phi(t)$ become

$$\Psi(t) = \frac{\varepsilon_s - \varepsilon_\infty}{\varepsilon_\infty} \{1 - \int_0^\infty F(\tau)\ e^{-t/\tau}\ d\tau\} \tag{12}$$

$$\Phi(t) = \frac{\varepsilon_s - \varepsilon_\infty}{\varepsilon_s} \{1 - \int_0^\infty G(\tau)\ e^{-t/\tau}\ d\tau\}\ . \tag{13}$$

As before, it is more elegant to introduce the frequency distribution functions (cf. eqns. (2), (14) and (16) of Sect. 1.4). In analogy to eqns. (6) and (17) of that Section, the dielectric rate of retardation is the Laplace transform of $f(s)$:

$$\psi(t) = \int_0^\infty f(s)\ e^{-ts}\ ds \tag{14}$$

and the dielectric rate of relaxation the Laplace transform of $g(s)$:

$$\varphi(t) = \int_0^\infty g(s)\ e^{-ts}\ ds\ . \tag{15}$$

The Laplace transforms $\psi(z)$ and $\varphi(z)$ of these functions are the Stieltjes transforms of the frequency distribution functions:

$$\overline{\psi}(z) = \int_0^\infty \frac{f(s)\ ds}{s + z} \tag{16}$$

$$\overline{\varphi}(z) = \int_0^\infty \frac{g(s)\ ds}{s + z}\ . \tag{17}$$

To conclude the present Chapter, we state some properties of the Cole-Cole diagram which follow from the properties of the distribution functions and vice versa. As yet, only the semi-circular diagram, for dielectrics whose distribution functions are simple delta functions, was discussed. According to eqns. (16) and (2.2.10), the Cole-Cole plot of dielectrics having a discrete spectrum with two or more retardation times or frequencies is found by *vector* addition of the circles in Fig. 2.3.2 resulting from each term in the sum

$$\frac{\varepsilon(i\omega) - \varepsilon_\infty}{\varepsilon_\infty} = \Psi(i\omega) = \sum_k \frac{f_k}{s_k + i\omega}. \qquad (18)$$

Since the vectors of all these circles have in common that they are purely imaginary in $\omega = \infty$ and purely real in $\omega = 0$, we infer that the Cole-Cole diagrams of dielectrics characterized by discrete spectra are perpendicular to the ε'-axis in their extremities $\omega = \infty$ and $\omega' = 0$, provided that the summation in eqn. (18) contains a finite number of terms. Another proof of this property will be given in Chapter 4. There are, however, some important exceptions to the above rule:

1. It often happens that dielectrics have appreciable d.c. conductivity. According to eqn. (2.1.23), this means that the product $\omega\varepsilon''$ remains finite if $\omega \to 0$. Static conductivity in dielectrics is the counterpart of plastic flow in viscoelastic substances: if a fixed amount of charge is brought onto a condensor containing such a dielectric, the electric field ultimately breaks down completely. In mechanical systems plastic flow causes the stress under constant strain to decay to a final value zero. Just as plastic flow in viscoelastic systems was accounted for by connecting a dashpot in *series* with the Voigt- or Maxwell-models, static conductivity in dielectrics may be represented by connecting a resistance in *parallel* with the models of Fig. 3.

Plastic flow added a simple pole at the origin to the analytic function $S(z)$; here it adds a simple pole at the origin to $\varepsilon(z)$. In contrast with viscoelastic systems exhibiting plastic flow, dielectrics with static conductivity usually are linear systems. The foregoing phenomenological theory may be applied to these dielectrics by simply subtracting σ_o/ω from the loss factor ε'', if σ_o is the specific d.c. conductivity. If this correction is omitted, the Cole-Cole diagram never reaches the ε'-axis at its low frequency end, but instead has a pole there.

2. Apart from the semi-circular Cole-Cole diagram, there are two other kinds, the *circular* arc plot and the *skewed* arc plot,

that have a remarkably wide-spread occurrence. Detailed discussion of these diagrams will be postponed to Chapters 3 and 4; here it suffices to mention that both of them do not conform with the above rule. It will be shown that diagrams of this kind necessarily lead to continuous distribution functions, and that these distribution functions show anomalous behaviour at the ends of the retardation frequency and time axes.

3. It will also be shown in Sect. 4.3 that *resonance relaxation* leads to *grazing* instead of normal incidence of the diagram at its high frequency end.

Chapter 3

EXTENDED SCOPE OF THE THEORY

3.1. Application to other relaxation processes

The discussion of linear viscoelasticity and dielectric loss in the first two Chapters was deliberately kept to the minimum necessary to demonstrate the fundamental identity of the phenomenological theories of mechanical and dielectric relaxation. There are other relaxation processes that conform to the same mathematical pattern and that share with the former systems the physical property of storing as well as dissipating various kinds of energy. Instead of subjecting each of these processes to a separate treatment, we prefer to formulate the theory in a general way so that description of these processes involves a simple substitution of the relevant physical quantities in the mathematical relations.

All linear relaxation phenomena may be regarded as a perturbation of the simplest possible mathematical relationship in physics, the proportionality of two parameters X and Y:

$$X = a\,Y \tag{1}$$

or

$$Y = b\,X\,. \tag{2}$$

It is essential for the processes under consideration that the product of these quantities has the dimension of an energy or an energy density, i.e., that they are thermodynamically conjugate quantities. We suppose the element of work done by the surroundings upon the system or unit volume of the system to be

$$\mathrm{d}W = X\,\mathrm{d}Y\,. \tag{3}$$

In adopting this form for $\mathrm{d}W$, we automatically made a classification of X and Y. We hesitate to state that X and Y are intensive and extensive parameters, respectively, since, according to some authors ([Sommerfeld III], [Guggenheim]), the magnetic quantities H and B are a notable exception to this rule. If the relations (1) and (2) remain valid irrespective of the rate of change of X

	X	name	dimension	Y	name	dimension	dW	a	b	name
1.	σ	stress	F/A	ε	strain	–	$\sigma\, d\varepsilon$	E		elastic modulus
2.	F	force	F	Δl	deformation	l	$F\, d\Delta l$	E		force constant
3.	σ_γ	shear stress	F/A	γ	angle of shear	–	$\sigma_\gamma\, d\gamma$	G		shear modulus
4.	p_e	excess pressure	F/A	ρ_e/ρ_o	relative excess density	–	$p_e d(\rho_e/\rho_o)$	K_s		bulk modulus
5.	E	electric field strength	F/Q	D	dielectric displacement	Q/A	$E\, dD$		ε	permittivity
6.	V	potential difference (voltage)	W/Q	Q	charge	Q	$V\, dQ$		C	capacitance
7.	H	magnetic field strength	I/l	B	magnetic induction	$V\times t/A$	$H\, dB$		μ	permeability
8.	I	current	Q/t	Φ	voltage pulse ($\int V\, dt$)	$V\times t$	$I\, d\Phi$		L	inductance

and Y, we infer that the system or its unit volume have stored an amount of energy

$$W = \tfrac{1}{2}\, a\, Y^2 = \tfrac{1}{2}\, X\, Y = \tfrac{1}{2}\, b\, X^2 \qquad (4)$$

which can be completely recovered at any time after its insertion. The quantities of the Table, when substituted into the above equations, lead to relations that apply to many well-known physical systems. Other sets of quantities, governed by eqns. (1) to (4), for which this is true, were deliberately not included in the Table, since it represents a list of parameters of the better-known relaxational systems, i.e., it is restricted to systems to which the theory of the preceding Chapters may, at least in some cases, be applied.

There are, of course, deviations of the systems of the Table from eqns. (1), (2), and (4) that are easily detectable and of a different nature. These are the non-linear effects, such as mechanical failure or permanent deformation of the mechanical systems under excessive stress, magnetic hysteresis, breakdown of the dielectrics, etc. Also, the systems may be governed by non-linear equations that do not necessarily lead to dissipative behaviour. The present discussion will, however, be limited to relaxational behaviour of the kind considered in the preceding Chapters.

The first three systems of the list, have already been discussed in Chapter 1; example 2., e.g., refers to the mechanical models of Sect. 1.3 or to a spring constructed from a linear viscoelastic material. It was stated in Sect. 1.1 that the behaviour of these materials in shear is completely analogous to that in one-dimensional deformation. The same is true for these substances in isotropic compression ([Staverman-Schwarzl, 1956], [Alfrey, 1948]). The fourth example was, however, mainly intended to be an illustration of ultrasonic losses in matter [Markham *et al.*], which, to some extent, may be accounted for by the present theory. Examples 5. and 6. were treated in Chapter 2. The last two examples refer to, e.g., paramagnetic relaxation ([Gorter], [van der Marel]) *).

In all these examples of relaxation systems, the linear theory may be expected to be primarily valid for small values of the parameters X and Y [Meixner, 1953]. How small these need be dif-

* It should be added that this presentation of paramagnetic relaxation is somewhat misleading. The small variations ΔH and ΔB of relatively large field quantities H and B are usually found to be the parameters fitting into the present theory.

fers widely between the various kinds of system: in dielectrics, e.g., linearity persists up to quite high values of D and E, on a laboratory scale, but these values are very small compared with the inter-molecular field strengths [BÖTTCHER]. On the other hand, it is easy to realize magnetic fields that cause non-linear behaviour in ferro-magnetics.

In terms of the general quantities X and Y, the linear relaxational systems differ from those governed by eqns. (1), (2) and (4) in being described by the operator relations

$$X(t) = (a_\infty + a_{op})\ Y(t)\ , \tag{5}$$

$$Y(t) = (b_\infty + b_{op})\ X(t)\ . \tag{6}$$

The analysis of this kind of linear operator equation has been so exhaustively treated in the first two Chapters that we may confine the discussion to a short summary. First, however, it is important to determine which of these operators leads to quantities of the retardation family of functions and which to quantities of the relaxation family of functions. We do this by investigating whether the functions in the responses of the systems at rest upon application of unit step stimuli:

$$X(t) = a_\infty \{1 - \Phi(t)\}\ Y_o\ S_1(t) \qquad \text{if} \qquad Y(t) = Y_o\ S_1(t)\ , \tag{7}$$

$$Y(t) = b_\infty \{1 + \Psi(t)\}\ X_o\ S_1(t) \qquad \text{if} \qquad X(t) = X_o\ S_1(t)\ , \tag{8}$$

are positive functions of the time. Clearly, it suffices to establish this property for one of the functions. Inspection of eqns. (3) and (7) shows that all the XY-energy is inserted into the system at $t = 0$; by definition, the amount of energy that can be extracted at later times is always less than this. Hence, $X(t)$ is inevitably smaller than $X(0)$, and $\Phi(t)$ must be a positive function.

We conclude that the position of the parameters X and Y in the fundamental relation (3) is what determines the dualism of relaxation family of functions and retardation family of functions in the phenomenological theory of relaxation processes. We may also state that a and a_{op} are of impedance type, b and b_{op} of admittance type, but we should then realize that this classification is in conflict with the accepted nomenclature of electric network theory (example 9. in the Table).

As before, the operators of eqns. (5) and (6) are implicitly given by the *superposition* integrals

$$X(t) = a_\infty \{1 - \int_0^\infty Y(t-\tau)\ \varphi(\tau)\ d\tau\}\ , \qquad (9)$$

$$Y(t) = b_\infty \{1 + \int_0^\infty X(t-\tau)\ \psi(\tau)\ d\tau\}\ ,$$

where the *completely monotonic* functions $\varphi(t)$ and $\psi(t)$ are again the time derivatives of the functions $\Phi(t)$ and $\Psi(t)$ of the relations (7) and (8). The considerations of Sect. 1.3 then lead to the formulae

$$\overline{X}(z) = a_\infty \{1 - \overline{\varphi}(z)\}\ \overline{Y}(z)\ , \qquad \text{z.i.c.}, \qquad (10)$$

$$\overline{Y}(z) = b_\infty \{1 + \overline{\psi}(z)\}\ \overline{X}(z)\ , \qquad \text{z.i.c.}, \qquad (11)$$

relating the complex Laplace transforms of the functions $X(t)$ and $Y(t)$. Once again, the complex functions

$$a(z) = a_\infty \{1 - \overline{\varphi}(z)\} = 1/b(z) \qquad (12)$$

and

$$b(z) = b_\infty \{1 + \overline{\psi}(z)\} = 1/a(z) \qquad (13)$$

in these relations play a multiple role in the phenomenological theory.

The following list recapitulates the properties of $a(z)$ and $b(z)$ obtained for the special cases $a(z) = E(z)$ and $b(z) = S(z)$ in Chapter 1, and $b(z) = \varepsilon(z)$ in Chapter 2.

1) $a(z)$ and $b(z)$ are the Laplace transforms of the $X(t)$ and $Y(t)$ resulting from application of

$$Y(t) = \delta(t) \qquad \text{and} \qquad X(t) = \delta(t),$$

respectively, to the system at rest.

2) $a(z)$ and $b(z)$ are the characteristic functions in the response of the systems to exponentially increasing or decreasing sinusoids (from $t = -\infty$ onwards):

$$X(t) = a(z)\ Y(t) \qquad \text{if} \qquad Y(t) = Y_o\ e^{zt}\ , \qquad (14)$$

$$Y(t) = b(z)\ X(t) \qquad \text{if} \qquad X(t) = X_o\ e^{zt}\ . \qquad (15)$$

3) In the special case where $z = i\omega$, $a(i\omega)$ and $b(i\omega)$ are functions governing the steady state dynamical behaviour of the system:

$$X(i\omega t) = a_\infty \{1 - \overline{\varphi}(i\omega)\}\ Y(i\omega t) \quad \text{if} \quad Y(i\omega t) = Y_o\ e^{i\omega t}\ , \qquad (16)$$

$$Y(i\omega t) = b_\infty \{1 + \overline{\psi}(i\omega)\}\ X(i\omega t) \quad \text{if} \quad X(i\omega t) = X_o\ e^{i\omega t}\ . \qquad (17)$$

4) The numerical evaluation of the functions of one family, if those of the other family are experimentally known, involves $a(z)$ and $b(z)$ (cf. (1.1.22) and (1.2.7)).

5) $a(z)$ and $b(z)$ are analytic functions whose singularities, on – or near – the negative real axis of the complex frequency plane, are generally believed to convey the most revealing macroscopic information about relaxational systems.
This latter point, of course, refers to the distribution functions, defined by

$$\overline{\Psi}(z) = \int_0^\infty \frac{f(s)\,ds}{s+z}\,, \tag{18}$$

$$\overline{\varphi}(z) = \int_0^\infty \frac{g(s)\,ds}{s+z}\,, \tag{19}$$

$$\psi(t) = \int_0^\infty f(s)\,e^{-ts}\,ds\,, \tag{20}$$

$$\varphi(t) = \int_0^\infty g(s)\,e^{-ts}\,ds\,, \tag{21}$$

$$\Psi(t) = \Psi(\infty)\,\{1 - \int_0^\infty F(\tau)\,e^{-t/\tau}\,d\tau\}\,, \tag{22}$$

$$\Phi(t) = \Phi(\infty)\,\{1 - \int_0^\infty G(\tau)\,e^{-t/\tau}\,d\tau\}\,, \tag{23}$$

with $$\int_0^\infty F(\tau)\,d\tau = \int_0^\infty G(\tau)\,d\tau = 1\,, \qquad \tau = 1/s\,. \tag{24}$$

All these equations imply that the singular behaviour of $a(z)$ and $b(z)$ – a cut for continuous spectra and a finite number of simple poles for discrete spectra – is located exactly upon the negative real axis of the z-plane, i.e., that the distribution functions are real and positive and that the functions $\psi(t)$ and $\varphi(t)$ are completely monotonic.

At this point, the essential analogies between various kinds of linear *XY*-relaxation have either been given or may be obtained simply by substituting the appropriate parameters into the relations of the first two Chapters or in specific equations still to be given. As far as the author is aware, only one type of effect, plastic flow in viscoelastic systems and static conductance in dielectrics, finds no counterpart in the numbers 4. and 7. of the Table.

As a final illustration of the generalized phenomenological theory, the *models* of *Voigt*-type for mechanical, electric, and magnetic systems, characterized by a single time constant, will be compared. The eqns. (2) for non-relaxational systems of this type are, respectively,

$$\varepsilon = S\,\sigma\,, \qquad D = \varepsilon\,E\,, \qquad \text{and} \qquad B = \mu\,H$$

The allowable elements (cf. the discussion in Sect. 1.3) in the representative linear networks are governed by the relations

$$\Delta l = S\,F \quad , \quad Q = C\,V \quad , \quad \int V\,dt = L\,I \quad ,$$

$$\Delta l = \frac{1}{\eta}\int F\,dt \quad , \quad Q = \frac{1}{R}\int V\,dt \quad , \quad \int V\,dt = R\int I\,dt \quad ,$$

$$\Delta l = \frac{1}{m}\iint F(dt)^2 \quad , \quad Q = \frac{1}{L}\iint V(dt)^2 \quad , \quad \int V\,dt = \frac{1}{C}\iint I(dt)^2 \quad ,$$

which are, of course, merely the equations for ideal mechanical and electric network elements in a somewhat different form. The transient responses of the respective relaxational systems:

$$\varepsilon(t) = \{S_\infty + (S_s - S_\infty)\,(1 - e^{-t/\tau})\}\,\sigma_o\,S_1(t) \quad ,$$

$$D(t) = \{\varepsilon_\infty + (\varepsilon_s - \varepsilon_\infty)\,(1 - e^{-t/\tau})\}\,E_o\,S_1(t) \quad ,$$

$$B(t) = \{\mu_\infty + (\mu_s - \mu_\infty)\,(1 - e^{-t/\tau})\}\,H_o\,S_1(t) \quad .$$

are easily found to be those of the corresponding quantities in the representative models, if the elements have the indicated values (Figure 1).

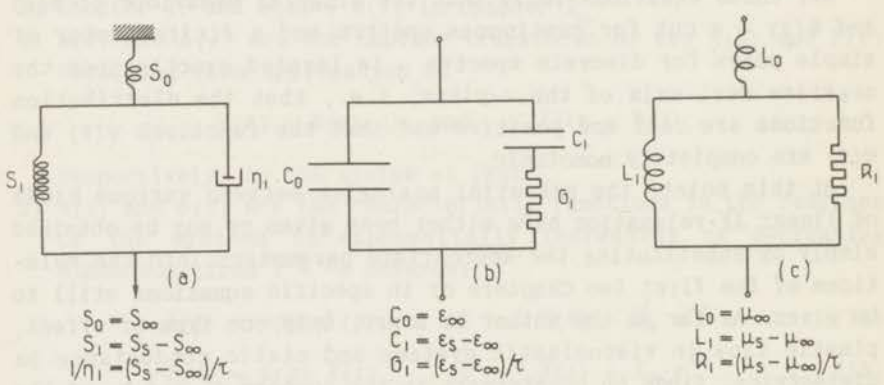

Figure 3.1.1

The perhaps somewhat confusing dimensions of the parameters in this Figure are clarified by considering the relations between the field quantities on the right sides and the instrumental quantities on the left sides of these equations. Ideal "measuring cells", in which the respective field vectors are uniform and

parallel – the materials inside the cells are homogeneous and isotropic – provide a basis for this comparison. These structures are:

1. The long fiber of uniform small cross-section, governed by Hooke's law, for which

$$\varepsilon = \Delta l / l_o \,, \qquad \sigma = F/A \,, \qquad \Delta l = S_f \, F \,,$$

$$\varepsilon = S \, \sigma \,, \qquad S_f = S l_o / A \,, \tag{25}$$

where A = area of cross-section of the fiber,
l_o = initial length.

2. The ideal condensor, for which

$$D = Q/A \,, \qquad E = V/d \,, \qquad Q = C \, V \,,$$

$$D = \varepsilon \, E \,, \qquad C = \varepsilon \, A/d \,, \tag{26}$$

where A = area of the plates,
d = distance of the plates.

3. The ideal one-turn coil, for which

$$B = (\int V \, \mathrm{d}t)/A \,, \qquad H = I/l \,, \qquad \int V \, \mathrm{d}t = L \, I \,,$$

$$B = \mu \, H \,, \qquad L = \mu \, A/l \,, \tag{27}$$

where A = area of cross-section of the coil,
l = length of the coil.

Note that in the actual approximation of these systems the ratios l/A for fiber and coil have to be large but that the ratio d/A for the condensor must be small. The dimensions of the relevant parameters are found to be:

$$[S_f] = \frac{\text{length}}{\text{force}} \,, \qquad [S] = \frac{\text{area}}{\text{force}} \,,$$

$$[C] = \frac{\text{charge}}{\text{voltage}} \,, \qquad [\varepsilon] = \frac{\text{charge}}{\text{voltage} \times \text{length}} \,,$$

$$[L] = \frac{\text{voltage} \times \text{time}}{\text{current}} \,, \qquad [\mu] = \frac{\text{voltage} \times \text{time}}{\text{current} \times \text{length}} \,.$$

We conclude that the relations of Fig. 1 are to be interpreted as *numerical* equations, and that the models have to refer to a unit cube of the materials in the "cell".

3.2. The Kronig-Kramers relations

In the present Section we will discuss the relationship existing between energy storage and loss factors for dynamical steady state processes in linear relaxational systems. According to the analyses of Sects. 1.2 and 2.1, these quantities are the real and imaginary parts of the functions $a(i\omega)$ and $b(i\omega)$ in eqns. (3.1.16 -17). That such an interdependence exists is an immediate consequence of the fact that the functions $a(z)$ and $b(z)$ are analytic functions of z along the imaginary axis of the complex frequency plane (cf. [EISENLOHR]). Accordingly, the subsequent formulae will be derived by means of a function theoretical discussion. We start from eqns. (3.1.12-13):

$$a(z) = a_\infty \{1 - \overline{\varphi}(z)\} ,$$

$$b(z) = b_\infty \{1 + \overline{\psi}(z)\} ,$$

and investigate the properties of the complex Laplace transforms in these relations. It is essential for the following argument that the singularities of these functions are confined to the finite part of the left half of the complex plane, and in particular, that they are regular in every point of the imaginary axis.

When we denote either of the functions $\overline{\varphi}$ or $\overline{\psi}$ by $\overline{y}$, the following relations are valid under the conditions stated:

$$\overline{y}(z) = \int_0^\infty y(t)\, e^{-zt}\, dt , \qquad \mathrm{Re}\ z > c , \tag{1}$$

where the negative real number c defines the abscissa of convergence. The inversion formula will be used in the form (cf. eqn. 2.2.8))

$$y(t) = \frac{1}{2\pi} \int_{-\infty}^{+\infty} \overline{y}(i\omega)\, e^{i\omega t}\, d\omega . \tag{2}$$

These equations, when combined, yield

$$\overline{y}(z_o) = \frac{1}{2\pi} \int_{-\infty}^{+\infty} \frac{\overline{y}(i\omega)\, d\omega}{z_o - i\omega} , \qquad \mathrm{Re}\ z_o > 0 , \tag{3}$$

which is an extension of Cauchy's well-known integral formula [CHURCHILL], written in a somewhat unusual form. This equation ceases to be valid when z_o is located *upon* instead of to the right of the imaginary axis. Eqn. (3) is based upon integration – in a clock-wise sense – around a contour consisting of the entire Im-axis and an infinite semi-circle about the origin in the right half of the complex plane, of which only the first part

contributes to the integral. The simple pole of the integrand lies inside this contour. If, however, $z_o = i\omega_o$, the straight part of the path should be indented by an infinitely small semicircle to the right of the pole upon the Im-axis so as to *exclude* it from the contour. Then ([PHILLIPS], [BODE], [HIEDEMANN-SPENCE])

$$\bar{y}(z_o) = \frac{1}{\pi} P \int_{-\infty}^{+\infty} \frac{\bar{y}(i\omega)\ d\omega}{z_o - i\omega}, \qquad \text{Re } z_o = 0 . \tag{3a}$$

i.e., twice the value we found in the preceding formula. The P in this equation stands for *Cauchy principal* value, meaning that the integral on the right side should be read as

$$\lim_{\rho \to 0} \int_{-\infty}^{\omega_o - \rho} + \int_{\omega_o + \rho}^{+\infty} ,$$

ρ being the radius of the indentation. Although this P will be omitted in the following equations, it should be thought to be present before all integrals where the path of integration apparently crosses a pole of the integrand. From eqn. (1) it follows that the real and imaginary parts of $\bar{y}(i\omega)$ are even and odd functions of ω, respectively.

When we introduce the real and imaginary parts of $\bar{y}(i\omega)$, as follows:

$$\bar{y}(i\omega) = \bar{y}'(\omega) + i\ \bar{y}''(\omega) , \tag{4}$$

the integrals of eqns. (3) and (3a) may be written as

$$2 \int_o^\infty \frac{z_o\ \bar{y}'(\omega) - \omega\ \bar{y}''(\omega)}{z_o^2 + \omega^2}\, d\omega , \tag{5}$$

since the odd parts of the integrand cancel in the integration, and the even parts yield the same result along the positive and negative imaginary axis. Introducing eqn. (5) into eqn. (3a), substituting $z_o = i\omega_o$, and equating real and imaginary parts, one obtains:

$$\bar{y}''(\omega_o) = \frac{2}{\pi} \int_o^\infty \frac{\omega_o\ \bar{y}'(\omega)\ d\omega}{\omega^2 - \omega_o^2} \tag{6}$$

and

$$\bar{y}'(\omega_o) = \frac{2}{\pi} \int_o^\infty \frac{\omega\ \bar{y}''(\omega)\ d\omega}{\omega_o^2 - \omega^2} , \tag{7}$$

which are a form of the well-known Kronig-Kramers relations ([KRONIG], [KRAMERS, 1927]). If the corresponding relations for the real and imaginary parts of $a(i\omega)$ and $b(i\omega)$ are wanted, it

should be noted that the decomposition of these quantities is usually taken to be

$$a(i\omega) = a'(\omega) + i\, a''(\omega) \tag{8}$$

and

$$b(i\omega) = b'(\omega) - i\, b''(\omega)\ , \tag{9}$$

which has the advantage that positive functions of frequency are obtained. As an example, the Kronig-Kramers relations for the complex permittivity, which is decomposed as indicated in eqn. (9), are

$$\varepsilon''(\omega_o) = \frac{2}{\pi}\int_o^\infty \frac{\omega_o\, \varepsilon'(\omega)\, d\omega}{\omega_o^2 - \omega^2} \tag{10}$$

and

$$\varepsilon'(\omega_o) = \varepsilon_\infty + \frac{2}{\pi}\int_o^\infty \frac{\omega\, \varepsilon''(\omega)\, d\omega}{\omega_o^2 - \omega^2}\ . \tag{11}$$

A consequence of the latter relation is obtained by putting $\omega_o = 0$:

$$\tfrac{1}{2}\,\pi\,(\varepsilon_s - \varepsilon_\infty) = \int_o^\infty \varepsilon''(\omega)\,\frac{d\omega}{\omega} = \int_{-\infty}^{+\infty} \varepsilon''(\omega)\, d \log \omega\ , \tag{12}$$

which shows that the area under the plot of the loss factor in a logarithmic frequency scale is proportional to the difference of the static and instantaneous permittivity, whatever the distribution function for the dielectric may be. In fact, it is not even necessary for the validity of the foregoing relations that a distribution function exists.

The qualitative meaning of eqn. (10) may be illustrated by the following analysis [Bode]:

Since

$$\frac{d}{d\omega} \log \left|\frac{\omega + \omega_o}{\omega - \omega_o}\right| = \frac{2\omega_o}{\omega_o^2 - \omega^2}\ ,$$

$$\varepsilon''(\omega_o) = \frac{1}{\pi}\int_o^\infty \varepsilon'(\omega)\, d \log \left|\frac{\omega + \omega_o}{\omega - \omega_o}\right|\ ,$$

which, by partial integration, yields

$$\varepsilon''(\omega_o) = -\frac{1}{\pi}\int_o^\infty (d\varepsilon'/d\omega) \log \left|\frac{\omega + \omega_o}{\omega - \omega_o}\right| d\omega\ .$$

When we go over to a logarithmic frequency scale, by introducing $u = \log \omega$ and $u_o = \log \omega_o$, this becomes

$$-\varepsilon''(e^{u_o}) = \frac{1}{\pi}\int_o^{+\infty} \frac{d\varepsilon'(e^u)}{du} \log\coth\frac{|u-u_o|}{2}\,du\,. \qquad (13)$$

The function $\log\coth \frac{1}{2}|u|$ is even, positive, singular at the origin, and rapidly goes to zero for increasing $|u|$. Of the total area $\frac{1}{2}\pi^2$ under the curve, a fraction .66 is found between the points $|u| = .88$. Hence, as a rough approximation, we may put

$$\log\coth \tfrac{1}{2}|u-u_o| \approx \tfrac{1}{2}\pi^2\,\delta\,(u-u_o)\,,$$

whence
$$\varepsilon''(e^{u_o}) \approx -\tfrac{1}{2}\pi\left[\frac{d}{du}\varepsilon'(e^u)\right]_{u=u_o}\,. \qquad (14)$$

The above argument shows that the negative slope of the graph of ε' against the logarithm of frequency is roughly proportional to ε'', and also that exact proportionality is impossible.

According to the Konig-Kramers relations, dissipative behaviour of a linear – not necessarily relaxational – system inevitably implies a frequency dependence – i.e., a *dispersion* – of the energy storage factor, and vice versa, provided that processes such as plastic flow and static conductance, if present, are separately accounted for.

Eqns. (6)-(14) solve the problem of finding the real or imaginary part of either $a(i\omega)$ or $b(i\omega)$ for any value of the frequency if the imaginary or real parts of these quantities are known for all values of ω.

Related expressions connecting $a(z)$ and $b(z)$ in the right half of the complex frequency plane with $a'(\omega)$ or $a''(\omega)$, and $b'(\omega)$ or $b''(\omega)$, respectively, follow from eqns. (3) and (5). According to these equations

$$\bar{y}(z_o) = \frac{1}{\pi}\int_o^{\infty} \frac{z_o\,\bar{y}'(\omega)\,d\omega}{z_o^2+\omega^2} - \frac{1}{\pi}\int_o^{\infty} \frac{\omega\,\bar{y}''(\omega)\,d\omega}{z_o^2+\omega^2}\,, \qquad \mathrm{Re}\ z_o > 0\,. \qquad (15)$$

The latter relation has the remarkable property that the absolute values of the two terms on the right side are equal, whence

$$\bar{y}(z_o) = \frac{2}{\pi}\int_o^{\infty} \frac{z_o\,\bar{y}'(\omega)\,d\omega}{z_o^2+\omega^2} = -\frac{2}{\pi}\int_o^{\infty} \frac{\omega\,\bar{y}''(\omega)\,d\omega}{z_o^2+\omega^2}\,. \qquad (16)$$

This property is an immediate consequence of

$$0 = \frac{1}{2\pi}\int_{-\infty}^{+\infty} \frac{\bar{y}(i\omega)\,d\omega}{z_o - i\omega}\,. \qquad \mathrm{Re}\ z_o < 0\,, \qquad (3b)$$

the third alternative of eqn. (3), which follows from the fact that the integrand has no longer a pole inside or upon the contour. Because of (3b),

$$\int_{-\infty}^{+\infty} \frac{\bar{y}^*(i\omega)\ d\omega}{z_o - i\omega} = \int_{-\infty}^{+\infty} \frac{\bar{y}(-i\omega)\ d\omega}{z_o - i\omega} = -\int_{-\infty}^{+\infty} \frac{\bar{y}(i\omega)\ d\omega}{-z_o - i\omega} = 0\ , \qquad (17)$$

$$\text{Re}\ z_o > 0\ ,$$

but then the analogue of eqn. (5), with a plus instead of a minus sign, also vanishes, which proves the above contention. Eqns. (3) show that one has to exercise caution when substituting different variables in integral expressions of this kind [Goursat].

The relations in eqn. (16) were previously given in [Gross, 1948] for purely real values of z_o. Gross uses a different derivation, however, which does not show the special nature of eqns. (3), (3a), and (3b).

3.3. Elucidation of the complex functions; the Fuoss-Kirkwood method

The present Section will be devoted to a closer examination of the behaviour of the analytic functions $\bar{\psi}(z)$ and $\bar{\varphi}(z)$ in the complex frequency plane. An intuitive approach to the properties of these functions will be made by means of two physical analogies. The first of these is based on the fact that large parts of the theory of analytic functions may be identified with the theory of two-dimensional potentials ([Sommerfeld II], [Bateman]). The notation $\bar{y}(z)$ of the preceding Section for either $\bar{\psi}(z)$ or $\bar{\varphi}(z)$ will again be used; it is assumed that $\bar{y}(z)$ is the Stieltjes transform of a positive real function $f(s)$:

$$\bar{y}(z) = \int_o^\infty \frac{f(s)\ ds}{s + z}\ . \qquad (2)$$

Then, $\bar{y}(z)$ is an analytic function of z in the entire complex frequency plane, with the exception of the negative real axis (Sect. 1.4). This means that the derivative of the real part of $\bar{y}(z)$ in a direction s, and the derivative of its imaginary part in a direction n, which is obtained from s by positive rotation over a right angle, are equal:

$$(\partial/\partial s)\ \bar{y}'(p,\omega) = (\partial/\partial n)\ \bar{y}''(p,\omega)\ . \qquad (2)$$

Here,

$$z = p + i\omega \qquad (3)$$

and

$$\bar{y}(z) = \bar{y}'(p,\omega) + i\bar{y}''(p,\omega)\ . \qquad (4)$$

Equation (2) is a well-known generalized form of the Cauchy-Riemann equations. The functions $\bar{y}'$ and $\bar{y}''$ of the preceding Sec-

tion clearly are special examples of the real functions on the right side of eqn. (4). According to eqn. (2), the families of curves

$$\bar{y}'(p,\omega) = \text{const} \tag{5a}$$

and

$$\bar{y}''(p,\omega) = \text{const} \tag{5b}$$

in the p,ω-plane are orthogonal. Moreover, it can easily be shown that each of these functions is a solution of the two-dimensional Laplace equation:

$$\nabla^2 \bar{y}'(p,\omega) = \nabla^2 \bar{y}''(p,\omega) = 0 . \tag{6}$$

All these properties apply to regions of the complex frequency plane containing no points of the negative real axis.

As yet, only one *Stieltjes pair* was explicitly mentioned:

$$f(s) = c\,\delta(s - s_0) ; \qquad \bar{y}(z) = c/(s_0 + z) .$$

Another example of a Stieltjes pair, which will lead to the potential interpretation, is readily obtained from the distribution function

$$\begin{aligned} &= 0 , && s < a , \\ f(s) &= P , && a \leqq s \leqq b , \\ &= 0 , && s > b , \end{aligned} \tag{7}$$

P being a positive real constant.

The Stieltjes transform of this function is

$$\bar{y}(z) = P \int_a^b \frac{ds}{s + z} = P \log \frac{z + b}{z + a} , \tag{8}$$

where the principal value of the logarithm is meant, i.e., $\bar{y}(z)$ is real for real values of z. The curves of constant $\bar{y}'$ and $\bar{y}''$ in the complex frequency plane are most easily found by introducing new, so-called bipolar, coordinates, as follows:

$$z + a = r_1 e^{i\varphi_1}$$

$$z + b = r_2 e^{i\varphi_2}$$

$$\rho = \log (r_2/r_1)$$

$$\varphi = \varphi_1 - \varphi_2$$

Then

$$\bar{y}(z) = P \log \frac{r_2}{r_1} e^{-i\varphi} = P\,(\rho - i\varphi) = \bar{y}' + i\bar{y}'' . \tag{9}$$

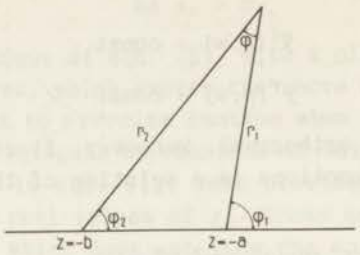

Figure 3.3.1
Bipolar coordinates

Therefore, the loci of eqns. (5) form a net of orthogonal circles ρ = const and φ = const; the latter of these pass through the points $z = -a$ and $z = -b$ and the centres of the former are located on the negative and positive real axis of the complex plane (Fig. 2).

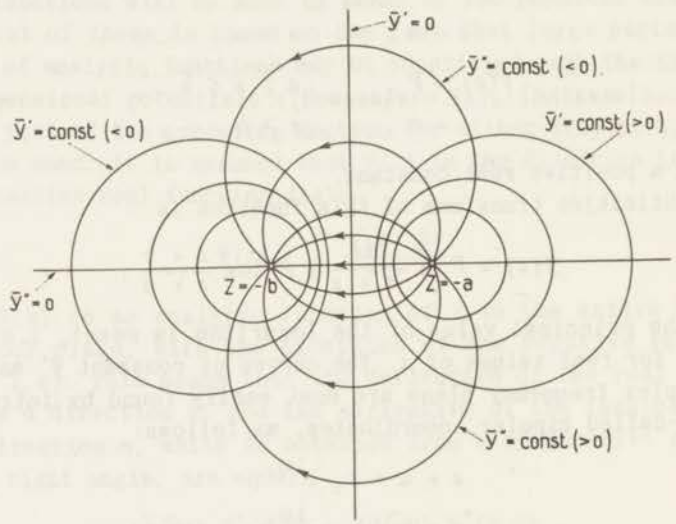

Figure 3.3.2

This picture is identical with the well-known map of the equipotential and stream lines of a two-dimensional hydrodynamic dipole [SOMMERFELD II]. In this map the circles $\bar{y}' = const$ are loci of constant velocity potential and the circles $\bar{y}'' = const$ are

streamlines; a source and sink, of strength $+P$ and $-P$, are located in the points $z = -a$ and $z = -b$ of the real axis, respectively.

When these physical interpretations of the two families of circles in Fig. 2 are interchanged, the map represents the potential flow caused by two vortices in $-a$ and $-b$; obviously there are many other two-dimensional physical situations to which the Figure applies.

Eqn. (1) is a linear relation between the functions $f(s)$ and $\bar{y}(z)$: if $f(s)$ is a linear combination of functions $\bar{y}(z)$ is the same linear combination of the Stieltjes transforms of these functions. Subdivision of the area under the graph of any continuous distribution function $f(s)$ into a large number of narrow strips then shows that the following physical interpretation may be given to Stieltjes's integral equation (1):

The function $\bar{y}(z)$ is the *complex potential* describing the potential flow resulting from the presence of a linear distribution of sources and sinks upon the negative real axis of the z-plane. At a distance s from the origin, the density of a continuous distribution is df/ds; positive or negative values of this derivative indicate that sources or sinks, respectively, are present. Finite discontinuities of $f(s)$ are accounted for by the presence of single point-sources and -sinks.

Finally, discrete behaviour of the distribution function is represented by the presence of infinitesimal, ideal, hydrodynamic dipoles in the appropriate points of the negative real axis (Fig. 3).

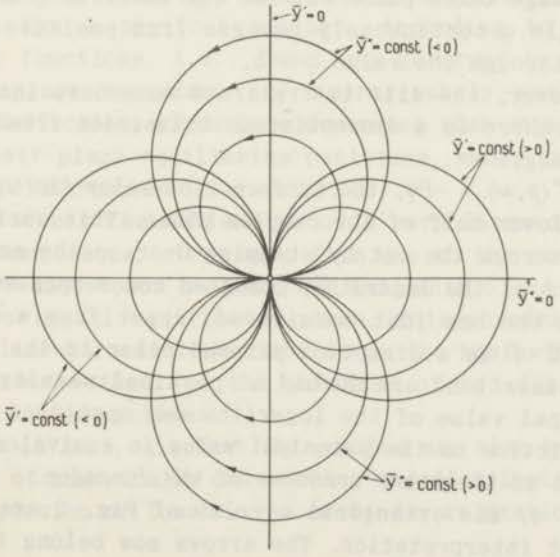

Figure 3.3.3

It is clear from this interpretation of eqn. (1) that the determination of the distribution function from measured data is a potential problem of an unusual, and difficult, type. The earliest method suggested for this purpose [FUOSS-KIRKWOOD] is essentially the known inversion formula for Stieltjes's integral equation ([WIDDER], [WALL], [PERRON]).

To derive this inversion formula, we first note that Fig. 2, if regarded as a map of the equipotential and streamlines of a dipole, does not show the essential fact that the points where the source and sink are located are *branch points* of the function $\bar{y}(z)$ of eqn. (8), and that the segment of the real axis between these points is a *cut* for this function. What this means is most clearly illustrated by regarding the Figure as a relief map of a surface whose height above a datum plane, the z-plane, is given by $\bar{y}''(p,\omega)$.

When looked upon in this way, the circles through $z = -a$ and $z = -b$ are contour lines and the circles, perpendicular to the real axis, are lines of steepest descent. (It should be realized that the slopes of these latter curves are, in general, not constant.) According to eqn. (9), the height of the points of this surface over the complex plane is proportional to the angle at which the segment ab is seen from projections of the points in this plane. Evidently, there are two distinct possibilities when the real axis is crossed along some path leading from the upper to the lower half plane:

1. The passage takes place outside the interval $(-a \ldots -b)$. Then, the angle φ continuously changes from positive to negative values through the value $\varphi = 0$.
2. If, however, the axis is traversed somewhere inside this interval, there is a discontinuous transition from the angle $+\pi$ to the angle $-\pi$.

Since $\bar{y}''(p,\omega) = -P\varphi$, the surface lies below the upper half and above the lower half of the complex plane. This surface might be continued across the cut by stepping over on the next higher or lower branch of the logarithm; one then comes upon surfaces identical with the one just considered, apart from a displacement $+2\pi P$ or $-2\pi P$ in a direction perpendicular to the datum plane. These continuations are devoid of physical meaning; therefore, the principal value of the logarithm was specified in eqn. (8). This restriction to the principal value is equivalent to barring transitions to the other branches of the function.

In fig. 4, the orthogonal circles of Fig. 2 are repeated in the present interpretation. The arrows now belong to the gradi-

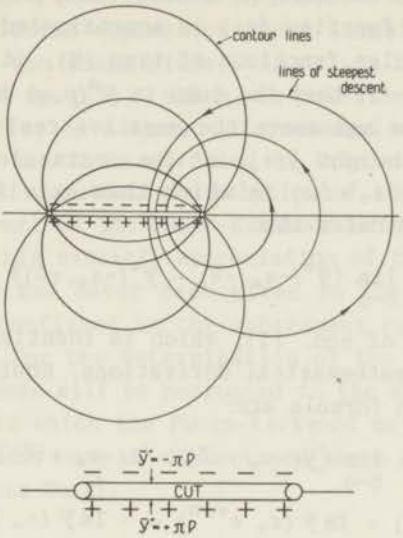

Figure 3.3.4

ents $\bar{y}'$ = const of the surface and point in the direction of decreasing values of $\bar{y}''$. Evidently, these lines of steepest descent no longer are closed circles, as they were in the former Figure.

It is interesting to observe that this geometrical picture of $\bar{y}''$ once again has a physical analogy. According to Prandtl, plane-harmonic functions, i.e., functions governed by the two-dimensional Laplace equation, are approximately realized in nature as the deflections of certain membranes (for example, soap films) from their plane equilibrium positions, under the influence of static disturbances [SOUTHWELL].

Fig. 4 reproduces the deflection of a very large idealized (weightless, homogeneous, etc.) soap film due to the presence of a rectangular "window", of height $2\pi P$ and width $b-a$, at right angles to its original equilibrium plane. This physical interpretation of plane-harmonic functions forms the basis for *Southwell's relaxation method* for the solution of two-dimensional potential and related problems.

We will show in Sect. 4.4 that this method may also be applied to the problem of numerically calculating the distribution functions from dispersion or loss curves of linear relaxational systems.

The classical inversion formula for the Stieltjes equation at

once follows from the foregoing description of the changes in $\bar{y}''(p,\omega)$ when the real axis is crossed. For, if an actual continuous distribution function $f(s)$ is approximated by a large number of rectangular pulse functions of type (7), it is clear from the linearity of eqn. (1) that the jump in $\bar{y}''(p,\omega)$ between two points, immediately below and above the negative real axis, is only determined by the height $f(s_o)$ of the rectangle belonging to the interval $(s_o \ldots s_o + \Delta s)$ in which this axis is crossed. Hence, this argument indicates that

$$2\pi f(s_o) = \lim_{\delta \to o} \{\bar{y}''(-s_o,-\delta) - \bar{y}''(-s_o,+\delta)\} , \quad \delta > o , \qquad (10)$$

is the inversion of eqn. (1), which is identical with the result of more refined mathematical derivations. Equivalent expressions for the inversion formula are:

$$2\pi i f(s_o) = \lim_{\delta \to o} \{\bar{y}(-s_o - i\delta) - \bar{y}(-s_o + i\delta)\} , \quad \delta > o , \qquad (11)$$

or

$$\pi f(s_o) = \mathrm{Im}\,\bar{y}\,(s_o\, e^{-i\pi}) = -\,\mathrm{Im}\,\bar{y}\,(s_o\, e^{i\pi}) . \qquad (12)$$

Since Fuoss and Kirkwood used a logarithmic frequency scale, they formulated the problem of obtaining the retardation time spectrum from an experimentally known dielectric loss *vs.* frequency curve in somewhat different terms. The essence of their method, however, is

(a) to represent the loss data by a suitable analytic function,

(b) to insert this function in an equation closely related to (11).

On closer inspection, this simple prescription turns out to be a practically useless solution of the problem of deriving the spectra from the measured data. The reason for this is to be found in the first step. fitting a suitable analytic function to the loss curve. Only in a few exceptionally simple cases, e.g., when the Cole-Cole diagram is a semi-circle or a circular arc, it is at once apparent what this function should be. In general, however, it is evident from the preceding discussion that a suitable analytic function must necessarily be of the form

$$\bar{y}(i\omega) = \int_o^\infty \frac{f(s)\,ds}{s + i\omega} \qquad (13)$$

to account for the total measured loss curve. For, the second part of the Fuoss-Kirkwood prescription involves *analytic continuation* of the function fitting the loss data towards its sin-

gularities, which are presupposed to lie on the negative real axis. Thus, fitting a power series in positive integral powers of z to the data yields an expression whose singularities are certainly located in the wrong place, viz. $z = \infty$. Representing the measured loss curve by (13) – which, in practice, would come down to approximating $f(s)$ by a number of rectangular and delta functions – obviously has to be effected by trial-and-error methods and would in itself constitute a solution of the Stieltjes equation; the second part of the Fuoss-Kirkwood method is then superfluous. Although this explicit appreciation of the Fuoss-Kirkwood method apparently has never been given in the literature, its shortcomings are confirmed by the subsequent publication of alternative methods for the determination of the spectra. Discussion of these methods will be postponed to the next Chapter.

As an example in which the Fuoss-Kirkwood method does work we discuss the important case of dielectrics whose Cole-Cole plot is a circular arc [Cole-Cole].

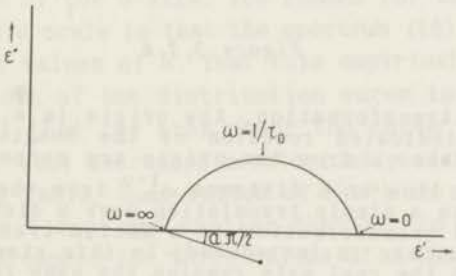

Figure 3.3.5
Circular arc plot

Cole and Cole first drew attention to the fact that a surprising number of dielectrics are characterized by this diagram, i.e., by a complex permittivity

$$\varepsilon(i\omega) = \varepsilon_\infty + \frac{\varepsilon_s - \varepsilon_\infty}{1 + (i\omega\tau_0)^{1-\alpha}}, \qquad (0 \leqq \alpha < 1) . \qquad (14)$$

That this expression corresponds to the diagram of Fig. 5 readily follows from the interpretation of the Cole-Cole plot as the map of the positive imaginary axis of the complex frequency plane in its conformal representation upon the $\varepsilon(z)$-plane. To show this, we notice that $\varepsilon(z)$ is of the form

$$a + b/(c + w) \qquad \text{with} \qquad w = z^{1-\alpha} .$$

The four steps by which the $+\omega$-axis of the z-plane is transformed are sketched in Fig. 6.

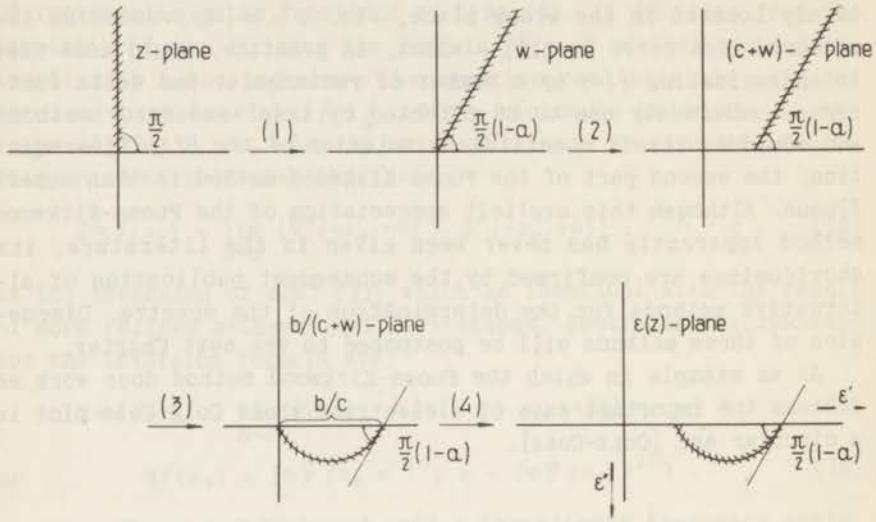

Figure 3.3.6

In the first transformation, the origin is a branch point; apart from the indicated rotation of the imaginary axis, its points at a distance ω from the origin are mapped into points upon the sloping line at a distance $\omega^{1-\alpha}$ from the point $w = o$. The second step is a simple translation over a distance c to the right. The third transformation is a Möbius-transformation by which the circular arc is introduced; in this step the angle of intersection with the real axis remains the same in both planes. Finally, the fourth step yields the circular arc plot in its up-side down representation.

It follows from eqn. (14) that

$$\overline{\Psi}(z) = \overline{\Psi}(o)/\{1 + (z\tau_o)^{1-\alpha}\} , \qquad (15)$$

which, on substitution into (11), gives

$$2\pi i f(s_o) =$$

$$= \overline{\Psi}(o) \lim_{\delta \to o} \left[\frac{1}{1 + \{\tau_o (-s_o - i\delta)\}^{1-\alpha}} - \frac{1}{1 + \{\tau_o (-s_o + i\delta)\}^{1-\alpha}} \right] .$$

When we put

$$-s_o \pm i\delta = s_o \, e^{\pm i(\pi - \nu)}$$

and let ν approach zero, application of some algebra leads to

$$f(s_o) = \frac{\overline{\Psi}(o)}{\pi} \frac{\sin \pi (1 - \alpha)}{(s_o \tau_o)^{\alpha-1} + (s_o \tau_o)^{1-\alpha} + 2 \cos \pi (1 - \alpha)},$$

whence

$$F(\tau) = \frac{1}{\pi\tau} \frac{\sin \pi (1 - \alpha)}{(\tau/\tau_o)^{1-\alpha} + (\tau_o/\tau)^{1-\alpha} + 2 \cos \pi (1 - \alpha)}. \qquad (16)$$

In the literature, this distribution function of retardation times is more usually given in terms of the logarithmic variable $u = \log \tau/\tau_o$, $du = d\tau/\tau$. Then

$$F(\tau)\, d\tau = \frac{1}{2\pi} \frac{\sin \pi (1 - \alpha)}{\cosh u (1 - \alpha) + \cos \pi (1 - \alpha)} du, \qquad (17)$$

an expression which is normalized to unity, as it should be.

Clearly, the logarithmic distribution function (17) is an even function of u; it attains its maximum value

$$(1/2\pi) \tan \tfrac{1}{2} \pi (1 - \alpha) = F(\tau_o) \qquad (18)$$

in the origin of the u-axis. The reason for the introduction of the logarithmic scale is that the spectrum (16) is very broad for not too small values of α. That this empirical parameter determines the width of the distribution curve is at once apparent from the fact that the area under the curve is unity and that $F(\tau_o)$ in eqn. (18) decreases monotonically with increasing α. In the following Table, some ratios of $F(e^u)$ in $u = \pm 1$, where τ is $e \approx 2.7$ times larger and smaller than τ_o, to its maximum value $F(\tau_o)$ are reproduced for three values of α that are of the order required to fit many experimental data:

α	$F(e^1)/F(e^o)$
.1	.061
.2	.279
.3	.655

The geometrical significance of α (Fig. 5) shows that, when it is zero, the circular arc plot is the semi-circular diagram of Section 2.3; accordingly, the normalized distribution function degenerates to a delta function.

Chapter 4

THE DISTRIBUTION FUNCTIONS

4.1. Introduction

We have now reached a stage in the macroscopic theory of linear relaxation phenomena where the fundamental mathematical structure of the theory and the physical systems to which it applies have been rather completely defined. The present Chapter will be concerned with some topics that have a bearing on the question of the microscopic significance of the distribution functions. Other subjects to be treated are the properties of the Cole-Cole diagram, resonance relaxation, and methods for the numerical evaluation of the spectra from experimental data.

4.2. Discrete and continuous distribution functions

Clearly, a conclusive answer to the question of whether the distribution functions are continuous or discrete can not be given from experimental evidence alone, since the limited precision of all measurements always leaves room for an interpretation in terms of either a discrete or a continuous spectrum. The following numerical example, e.g., shows that a system normally thought to be characterized by a single retardation time may as well be described by means of a continuous distribution function. The example is based on a published Cole-Cole diagram (of n-heptanol, [OPPENHEIM]) which was found to be a perfect semi-circle within the experimental limits of error.

The observed parameters for this semi-circle are:

$$\varepsilon_s = 13.7,$$
$$\varepsilon_\infty = 3.3,$$
$$\omega_c = 2.67 \cdot 10^8 \text{ sec}^{-1},$$

(the "critical wavelength" was stated to be 7.1 m).

In the following table some calculated values of relative per-

mittivities and loss factors belonging to the retardation frequency distribution functions

a) the delta function (cf. eqns. (2.3.9-10)),

b) the function (3.3.7) between $s = 2.60.10^8$ and $s = 2.74.10^8$,

c) ibid., between $s = 2.50.10^8$ and $s = 2.84.10^8$,

d) ibid., between $s = 2.225.10^8$ and $s = 3.204.10^8$,

are reproduced for various values of ω. In functions b) and c) the arithmetic mean and in d) the more correct geometric mean of the indicated values of s was made to coincide with the critical frequency. In each case the height of the functions was chosen so as to fix the ends of the Cole-Cole plot in $\varepsilon' = 3.3$ and $\varepsilon' = 13.7$.

	a)		b)		c)		d)	
$\omega.10^8$	ε'	ε''	ε'	ε''	ε'	ε''	ε'	ε''
0.20	13.64	0.775	13.64	0.774	13.64	0.776	13.64	0.779
0.50	13.35	1.882	13.35	1.881	13.35	1.884	13.34	1.889
1.00	12.42	3.42	12.41	3.42	12.41	3.42	12.40	3.42
2.00	9.96	4.99	9.96	4.99	9.95	4.99	9.95	4.97
2.60	8.64	5.20	8.63	5.20	8.64	5.20	8.64	5.17
3.00	7.90	5.17	7.90	5.16	7.86	5.17	7.90	5.14
4.00	6.51	4.80	6.51	4.80	6.50	4.80	6.53	4.78
10.00	3.99	2.59	3.95	2.59	3.99	2.59	4.01	2.60

Measurements with an accuracy of a few tenths of a percent in this frequency range are considered quite good; hence, if the results of the last column had been obtained experimentally, one would certainly fit a semi-circle to the values and proclaim the dielectric in question to be one characterized by a single retardation time! Of course, no physical meaning should be attached to the choice of the rectangular distribution function as an approximation to the delta function. Any other narrow distribution function would have yielded similar results, as may be inferred from the potential analogy of Sect. 3.3 (cf. also [MÜLLER, 1953]); the present function was chosen because it leads to a relatively simple numerical evaluation of the permittivity and loss curves. Evidently, the energy storage and loss curves of relaxational systems are remarkably insensitive to changes in the distribution functions.

Whereas the above result might be interpreted as an argument against the occurrence of delta functions in the spectra, another property of the distribution functions leads to the conclusion that delta functions must necessarily be present in the spectra.

For, if a continuous retardation frequency distribution function is characterized by

$$f(s) = 0 , \qquad s < a , \; s > b ,$$
$$f(s) > 0 , \qquad a < s < b ,$$

the corresponding relaxation frequency spectrum $g(s)$ has the same properties, but in addition consists of an isolated delta function outside $(a \ldots b)$ [MEIXNER, 1953]. To show this we need the following equations ((1.1.22), (3.1.18-19), and (3.3.10)):

$$\{1 - \overline{\varphi}(z)\} \{1 + \overline{\psi}(z)\} = 1 , \tag{1}$$

$$\overline{\psi}(z) = \int_0^\infty \frac{f(s)\, ds}{s + z} , \tag{2}$$

$$\overline{\varphi}(z) = \int_0^\infty \frac{g(s)\, ds}{s + z} , \tag{3}$$

$$2\pi f(s_0) = \lim_{\delta \to 0} \{\bar{y}''(-s_0, -\delta) - \bar{y}''(-s_0, +\delta)\} . \tag{4}$$

The first equation leads to the following expression for the imaginary part of $\overline{\varphi}(z)$ in terms of the real and imaginary parts of $\overline{\psi}(z)$:

$$\overline{\varphi}'' = \frac{\overline{\psi}''}{(1 + \overline{\psi}')^2 + (\overline{\psi}'')^2} . \tag{5}$$

We found in Sect. 3.3 that if $\bar{y}''$ continuously changes through the value zero when the negative real axis is crossed along a path intersecting this axis in $z = -s_0$, the frequency distribution function vanishes for the value s_0 of its argument. Accordingly, $g(s_0)$ is zero when the right side of eqn. (5) is zero, that is, when the numerator of that expression vanishes and its denominator is finite. This is almost always true when $f(s) = 0$, but, evidently, the case $\overline{\psi}' = -1$ should be more closely inspected, since then both the numerator and the denominator vanish. When $f(s)$ is again a rectangular function, the analysis is not difficult: if we use the bipolar coordinates of Fig. 3.3.1, the relation (5) for this function (cf. eqn. (3.3.7)) becomes

$$\overline{\varphi}''(p, \omega) = -\frac{P\varphi}{(1 + P\rho)^2 + P^2 \varphi^2} \tag{6}$$

with

$$\rho = \tfrac{1}{2} \log \frac{(b + p)^2 + \omega^2}{(a + p)^2 + \omega^2} \tag{6a}$$

and $$\varphi = \tan^{-1} \frac{\omega\,(b-a)}{(a+p)\,(b+p)+\omega^2}\,. \qquad (6b)$$

The equations (4) and (6) readily yield

$$g(s_o) = P/\{(1 + P \log \frac{b - s_o}{s_o - a})^2 + P^2\,\pi^2\} \quad \text{for} \quad a < s_o < b. \qquad (7)$$

This shows that $g(s)$ no longer has the hypothetical shape of the rectangular function $f(s)$: the equation represents a continuously variable function in $(a \ldots b)$ with a single maximum in

$$s_o = a + (b - a)/(1 + e^{-1/P})\,,$$

i.e., to the right of the middle of this interval, where the first term of the denominator of (7) is zero. Outside $(a \ldots b)$, the first term of the denominator of (6) is zero in

$$z' = -\{b + (b - a)/(e^{1/P} - 1)\}\,. \qquad (8)$$

The effect of this upon $g(s)$ is found by inspection of the behaviour of $\overline{\psi}(z)$ in the immediate neighbourhood of z'. Introducing

$$\zeta = z - z' \qquad (o < |\zeta| < \delta) \qquad (9)$$

one obtains

$$\overline{\psi}(z) = P \log \frac{b + z}{a + z} =$$

$$= P \log \frac{\zeta - (b - a)/(e^{1/P} - 1)}{\zeta - (b - a)/(1 - e^{-1/P})} \approx$$

$$\approx -1 - \{2\,P\,\zeta \cosh\,(1/P)\}/(b - a) \quad \text{for} \quad \delta \to o\,. \qquad (10)$$

Application of eqn. (1) yields

$$\overline{\varphi}(z) \approx \frac{b - a}{2\,P\,\zeta \cosh\,(1/P)} \qquad (\delta \to o)\,, \qquad (11)$$

which confirms the contention that $g(s)$ contains a delta function. Unfortunately, a general proof for other frequency distribution functions cannot be based upon a decomposition of $f(s)$ into a number of rectangular functions, since eqn. (1) represents a non-linear relationship between $f(s)$ and $g(s)$. However, according to the illustrations for the behaviour of the complex functions given in Sect. 3.3, it is plausible that, where the equipotential line $\overline{\psi}' = -1$ (if it exists) intersects the negative real axis to the left of the cut $(-a \ldots -b)$, the behaviour of $\overline{\varphi}(z)$ is

qualitatively the same for any $f(s)$ of the type under consideration.

Inspection of the equation

$$\Psi'' = \frac{\Phi''}{(1 - \Phi')^2 + (\Phi'')^2}$$

shows that, if a continuous $g(s)$ is different from zero in the interval $(a \ldots b)$ of the s-axis and nowhere else, the associated $f(s)$ has the same property but in addition consists of a delta function in $o < s < a$. That the isolated delta function is found at higher frequencies in $g(s)$ and at lower frequencies in $f(s)$ is in accordance with eqn. (1.4.29). One may formulate the present findings by saying that if a discrete retardation frequency spectrum is "compressed" so as to change it into a continuous one, the "lines" of the corresponding relaxation frequency distribution which, according to Sect. 1.4, are located between each pair of lines of the former spectrum, also change into a continuous distribution. One line of the latter spectrum, however, does not separate a pair of lines of the retardation distribution; this line apparently stays behind and gives rise to the isolated delta function at the high frequency end [MEIXNER, 1953].

In the theory of relaxation phenomena, the terms "spectrum" and "distribution function" are applied indiscriminately, although, because of its connotations, the former name is somewhat deceptive. In dielectric relaxation, e.g., the dielectric loss *vs.* frequency curve is more properly entitled to this denotation, since it is essentially the extension of the optical absorption spectrum. When calling the distribution functions spectra, one is inclined to expect their characteristics to be largely those of optical spectra. It is then not surprising that the distribution functions have been proposed to correspond with a similar distribution of molecular mechanisms responsible for the macroscopic phenomena [KAUZMANN]. The existence of two fundamentally different distribution functions, and in particular, the fact that one of these may contain an isolated delta function, makes this interpretation hard to accept.

Another peculiarity, not readily associated with the term "spectrum", was encountered in the distribution functions of the circular arc plot: these functions are different from zero for all finite values of their arguments. Accordingly, isolated delta functions do not appear in the corresponding relaxation distribution functions, which are, in fact, very similar to the retardation spectra already given in Sect. 3.3.

The sloping incidence of the circular arc upon the ε'-axis is brought about by singular behaviour of the derivative of the retardation frequency spectrum in $s=0$ and $s=\infty$. Since the Cole-Cole plot is the map of the imaginary axis of the z-plane, and the ε'-axis the map of the real axis of that plane, one would ordinarily expect their perpendicularity to be preserved in the conformal representation. This was indeed found to be true for discrete distribution functions (cf. Sect. 2.4). The argument used in that Section also leads to normal incidence of the Cole-Cole diagrams associated with frequency distribution functions built up from a finite number of rectangular functions. (It is easily proved that one single rectangular function gives rise to such a plot.) For the circular arc plot, however, the points $z=0$ and $z=\infty$ are *critical* points of the transformation [PHILLIPS], in which the conformal property does not hold. These points are the branch points of the $\bar{\psi}(z)$ of eqn. (3.3.15), caused by the presence of a fractional power of z (cf. Fig. 3.3.6). In the potential analogy of the preceding Chapter, the singular behaviour of $f'(s)$ indicates the presence of an infinitesimal source and sink in these points.

We infer from the above considerations that, if a distribution function is only different from zero in a finite interval $(a..b)$, the corresponding Cole-Cole plot is perpendicular to the ε'-axis, and conversely. It should be noted that the properties of the distribution functions of the circular arc plot are hard to reconcile with a molecular interpretation of the spectra. On the other hand, it is experimentally very difficult to verify whether the complex permittivity of a given system fits this plot at its extremities.

4.3. Restrictions on Cole-Cole plot and loss curve. Resonance relaxation

Apart from the restrictions upon the behaviour of the Cole-Cole diagram at its extremities discussed at the end of the preceding Section there are some other limitations that will be treated here.

First of all, it will be clear that the diagram is always continuous, however discontinuous the distributions functions may be. Evidently, the same is true for the energy storage and loss factors as functions of the frequency. In spite of this, the latter function bears an approximate resemblance to the correspond-

ing frequency distribution function: its width is roughly proportional to that of the spectrum and the positions of the maxima approximately – sometimes exactly – coincide. The proof of this property is not easily given from the Stieltjes equation itself or from its potential analogy. We infer from this analogy, however, that any conformal transformation of the z-plane that brings the positive imaginary and negative real axes closer together should provide more information about the relationship between frequency spectrum and loss curve. A convenient transformation is to map the z-plane upon the w-plane by means of

$$w = \log z = \log re^{i\theta} = \log r + i\theta \,. \qquad (1)$$

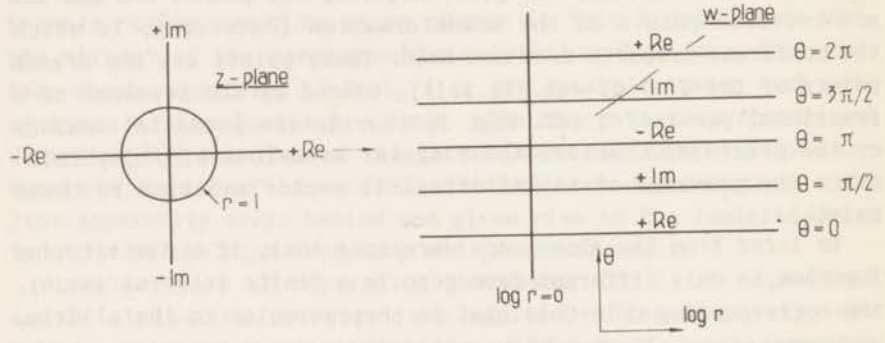

Figure 4.3.1

Then, the four semi-axes of the z-plane are mapped upon a periodical repetition of four straight lines in the w-plane, five of which are reproduced in Fig. 1. The circles r = const in the z-plane yield straight lines perpendicular to these maps of the semi-axes. The origin of the z-plane corresponds to $w = -\infty$.

The potential analogy for $\bar{y}(z)$ consisted of a system of equipotential and stream lines in the z-plane originating in a distribution of sources and sinks upon the negative real axis. The transformation (1) of this system of curves and the source-sink distribution yields the potential analogy for $\bar{y}(e^{w})$ in the w-plane. The sources and sinks characteristic for this function are evidently periodically repeated upon the lines $\theta = \pm\pi$, $\pm 3\pi$, $\pm 5\pi$, ... Since the stream lines in the z-plane do not intersect its positive real axis, each strip between two successive maps of this axis in the w-plane contains an identical complete map of the picture in the z-plane. Analytically, the transformation (1) yields:

$$-\bar{y}''(\omega) = \int_0^\infty \frac{\omega f(s)\,ds}{s^2+\omega^2} \quad \rightarrow \quad -\bar{y}_1''(v) = \tfrac{1}{2}\int_{-\infty}^{+\infty} f_1(u)\ \mathrm{sech}\ (u-v)\,du\ , \tag{2}$$

with $u = \log\,(s/s_0)$, $v = \log\,(\omega/s_0)$,

where the suffix 1 indicates loss and distribution functions on a logarithmic scale. The constant s_0 determines a change of scale in the z-plane, i.e., a shift of the source-sink distribution and its associated field in the w-plane to the right or left, serving to locate the maximum of either loss curve or spectrum in a convenient place. The relation (2) between logarithmic loss curve and logarithmic frequency spectrum is a convolution equation in which the distribution function is "scanned" by the *kernel* sech x [HIRSCHMAN-WIDDER]. This kernel is again an approximation to π times the delta function (cf. eqn. (3.2.13)), which analytically explains the qualitative analogy between the two curves. Since the hyperbolic secant is an even function of its argument, symmetry of the logarithmic loss curve necessarily entails symmetry of the logarithmic frequency spectrum, and conversely. If, in this case, the curves have a single maximum, the frequencies at which these maxima occur coincide; then, the obvious choice for s_0 is to equate it to this frequency, which makes the functions in equation (2) even functions of u and v. All these properties of the functions $\bar{y}_1''(v)$ and $f_1(u)$ are confirmed by an inspection of the potential analogy in the w-plane.

The three distribution functions specifically mentioned so far, viz. those of the semi-circular and the circular arc Cole-Cole plots, and the rectangular function, happen to be symmetric in a logarithmic frequency scale: each of these functions (defined by eqns. (2.3.14), (3.3.16) and (3.3.7), respectively) assumes equal values for frequencies f times and $1/f$ times the frequency at which the maximum in the loss curve occurs.

The counterpart of eqn. (2) is

$$\bar{y}'(\omega) = \int_0^\infty \frac{sf(s)ds}{s^2+\omega^2} \quad \rightarrow \quad \bar{y}_1'(v) = \int_{-\infty}^{+\infty} \{\tfrac{1}{2} + \tfrac{1}{2}\tanh\,(u-v)\}\, f_1(u)\,du\ . \tag{3}$$

Subtraction of the constant term $\frac{1}{2}\,\bar{y}(0)$ from both sides of this equation yields another convolution equation with the *odd* kernel $\tanh x$. If the logarithmic spectrum is symmetrical, an odd function of v results when s_0 is properly chosen. As a consequence the Cole-Cole diagram corresponding to a symmetrical logarithmic spectrum is also symmetrical. Moreover, equal values of the loss

factor are found at frequencies whose geometric mean is equal to the frequency at which the top of the diagram is located.

A representative asymmetrical Cole-Cole plot is the so-called "skewed arc" plot, which is observed to describe the dielectric behaviour of polyhydric alcohols ([DAVIDSON-COLE], [COLE, 1955]). The equation for the skewed arc plot is

$$\varepsilon(i\omega) = \varepsilon_\infty + (\varepsilon_s - \varepsilon_\infty)/(1 + i\omega\tau_o)^\beta , \qquad o < \beta < 1 .$$

The logarithmic retardation time distribution function, defined by

$$\varepsilon(i\omega) = \varepsilon_\infty + (\varepsilon_s - \varepsilon_\infty) \int_{-\infty}^{+\infty} \frac{F(\tau)\ \mathrm{d}\ \log\ \tau}{1 + i\omega\tau} ,$$

is found to be

$$F(\tau/\tau_o) = \frac{\sin\ \beta\ \pi}{\beta} \left(\frac{\tau}{\tau_o - \tau}\right)^\beta S_1\ (\tau_o - \tau) ,$$

S_1 being the unit-step function. Recently it was found that alkyl-halides at low temperatures show the same behaviour [COLE, private communication].

An important limitation on both the loss curve and the Cole-Cole diagram is obtained from eqn. (2) and the second Kronig-Kramers relation (3.2.7): We saw in eqn. (3.2.10) that the integral over the logarithmic loss curve is proportional to the difference of the extreme values of the storage factor; also, according to eqn. (2), the width of the loss curve increases with that of the distribution function. Hence, when the ends of a Cole-Cole diagram are kept fixed and the distribution function is varied, the delta function yields the highest possible maximum in the loss curve. In other words, the top of no Cole-Cole plot may lie outside the semi-circle through its ends.

All the above results presuppose the existence of real distribution functions, i.e., singular behaviour of $\bar{y}(z)$ on the negative real axis of the complex frequency plane and nowhere else. Hitherto, we repeatedly used this restriction to distinguish relaxation in the usual sense of the word from resonance relaxation. We will now consider the latter kind of process in some detail; among other things, it will be found that the original definition must be slightly changed.

The most convenient approach to resonance relaxation starts from the first model of Fig. 2.4.2 for the simplest possible lossy dielectric:

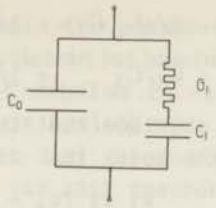

Figure 4.3.2

Although many known dielectrics are accurately described by this model in the experimentally accessible frequency range ($\nu = \omega/2\pi \approx 10^{-1} \ldots 10^{11}$ sec^{-1}), the description certainly ceases to be correct at still higher frequencies. For, it is evident that the energy dissipation per second (2.1.20), not only for this dielectric, but for all dielectrics characterized by analogous more complicated models, approaches a constant limiting value at high enough frequencies *. This would lead to appreciable energy absorption for all lossy dielectrics in the optical frequency range, which evidently is not true. An obvious correction to this paradoxical behaviour of the models is to introduce a small inductance in series with each resistance. The implications for the behaviour of the dielectrics will be investigated for the modified model of Fig. 3. The generalized admittance of this model is found to be

$$Y(z) = C_0\, z + \left(\frac{1}{G_1} + \frac{1}{C_1\, z} + L_1\, z\right)^{-1} . \qquad (4)$$

The relation between the Laplace transforms of the time dependent charge and voltage of the model, under zero initial conditions, is governed by

$$Y(z)/z = C_0 + \{L_1\, (z^2 + s_1\, z + s_1\, s_2)\}^{-1} , \qquad (5)$$

where *two* characteristic frequencies (reciprocal time constants)

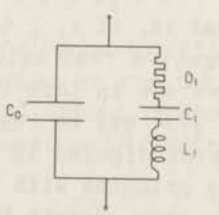

Figure 4.3.3

*) The entire voltage drop in the models occurs over the resistances, since the capacitors are short circuits at these frequencies (cf. also eqn. (2)).

$$s_1 = 1/(L_1 G_1) = 1/\tau_1 \tag{6}$$

and

$$s_2 = G_1/C_1 \quad = 1/\tau_2 \tag{7}$$

have been introduced. We conclude that the generalized dielectric constant represented by the model is

$$\varepsilon(z) = \varepsilon_\infty + \frac{s_1 s_2 (\varepsilon_s - \varepsilon_\infty)}{z^2 + s_1 z + s_1 s_2}$$

$$= \varepsilon_\infty + \frac{\varepsilon_s - \varepsilon_\infty}{1 + \tau_2 z + \tau_1 \tau_2 z^2} . \tag{8}$$

Accordingly, the Laplace transform of the rate of retardation is

$$\overline{\Psi}(z) = \frac{s_1 s_2 (\varepsilon_s - \varepsilon_\infty)}{\varepsilon_\infty} \cdot \frac{1}{z^2 + s_1 z + s_1 s_2} . \tag{9}$$

Now, there are two distinct possibilities, according as the denominator of eqns. (8) and (9) has a pair of real or complex conjugate roots. Again, the potential analogy in the complex frequency plane and the interpretation of the Cole-Cole plot as the conformal map of the imaginary axis of this plane considerably clarify the analysis of the physical behaviour of model and dielectric in the various cases. Explicit introduction of the negative roots

$$z_{12} = \tfrac{1}{2} s_1 (1 \mp \sqrt{\Delta}) , \qquad \Delta = 1 - (4 s_2/s_1) \tag{10}$$

$$= 1 - (4 L_1 G_1^2/C_1)$$

into eqn. (9) yields (cf. eqn. (2.4.3) for β)

$$\overline{\Psi}(z) = \frac{\beta s_1 s_2}{(z + z_1)(z + z_2)} =$$

$$= \frac{\beta s_2}{\sqrt{\Delta}} \left(\frac{1}{z + z_1} - \frac{1}{z + z_2} \right) . \tag{12}$$

If Δ is non-negative, that is, if $s_1 \geqq 4 s_2$, the poles of $\overline{\Psi}(z)$ are still located on the negative real axis of the z-plane. We observe, however, a new feature in this function: the pole in $-z_2$ has a negative residue; $\overline{\Psi}(z)$ may be regarded as the complex potential of two equal point dipoles in $-z_1$ and $-z_2$. The dipole closest to the origin is oriented with its source towards $z = 0$, the other dipole, farther away, points in the opposite direction. Clearly, this anomalous behaviour can also be described by means of a distribution function that is still real, but partly negative [Gross, 1954]. As soon as $\Delta < 0$, the poles of $\overline{\Psi}(z)$ move away

from the negative real axis, to occupy symmetrical positions on both sides of it *). The potential analogy again consists of two equal and opposite point dipoles in $-z_1$ and $-z_2$, but now they have made a quarter turn in a clock-wise sense: the one originally closest to the origin has moved to the lower half of the z-plane, and points with its sink towards the negative real axis; the other one is its reflection in this axis. In the special case that $\Delta = 0$, there is a hydrodynamic point *quadrupole* in $z = -2s_2$, that is, $\overline{\psi}(z)$ has a pole of order two there. The physical consequences of this behaviour of the roots are best illustrated by the changes in $\psi(t)$ and in the Cole-Cole diagram.

In Chapter 2 we saw that, apart from a factor, $\psi(t)$ is the retarded part of the response $D(t)$ resulting from the application of $E(t) = \delta(t)$ to the dielectric at rest. If $\Delta \neq 0$, the inversion of (12) is

$$\psi(t) = \frac{\beta\, s_2}{\sqrt{\Delta}} \left(e^{-z_1 t} - e^{-z_2 t}\right) . \qquad (13)$$

When the roots are real, the most important change in $\psi(t)$, compared to its former description in Chapters 1 and 2, is that $\psi(0) = 0$, and that it has obtained a maximum for $t > 0$. If $-z_2$ is much larger than $-z_1$ (L_1 small), these changes are confined to the immediate vicinity of $t = 0$: the behaviour for $t >> -1/z_2$ remains practically unchanged.

When the roots are complex, however, the behaviour of the model or dielectric is completely different: since $\psi(t)$ is of the form

$$\gamma\, e^{-pt} \sin \omega t , \qquad (14)$$

the system performs an exponentially damped sinusoidal oscillation.

Finally, when $\Delta = 0$, inversion of (11) yields

$$\psi(t) = 4\, \beta\, s_2^2\, t\, e^{-2 s_2 t} , \qquad (15)$$

which is qualitatively analogous to (13). These three different types of behaviour are known as supercritically, subcritically and critically damped oscillations, respectively.

To obtain the corresponding Cole-Cole diagrams, we must analyze

*) It is easily shown that the locus of the poles, if s_2 is kept constant and s_1 varied, is a circle of radius s_2, tangent to the imaginary axis.

$$\bar{\psi}(i\omega) = \frac{\beta\, s_1\, s_2}{(s_1\, s_2 - \omega^2) + i\omega s_1}. \qquad (16)$$

Dividing numerator and denominator by $s_1 s_2$, ignoring the factor β and introducing the new variable $\bar{\omega} = \omega/s_2$ yields the considerably simpler expression

$$u(i\bar{\omega}) = \frac{1}{(1 - \bar{\omega}^2/a) + i\bar{\omega}} = 1/v(i\bar{\omega}) \quad \text{with} \quad a = s_1/s_2\,. \qquad (17)$$

The map of the Im-axis of the $\bar{z}$-plane in its conformal representation on the $u(\bar{z})$-plane has the same shape as the wanted Cole-Cole plots. Its map in the $v(\bar{z})$-plane is at once recognized as a parabola:

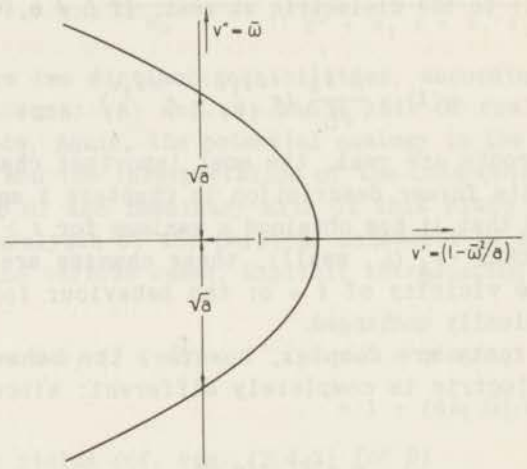

Figure 4.3.4

If the parabola is inverted with respect to the unit circle about the origin $v = 0$ [PHILLIPS], which is equivalent – for our purposes – to the transformation $u = 1/v$, one obtains a curve whose shape is identical with that of the Cole-Cole plot determined by the parameter a, i.e., by the ratio of s_1 to s_2 (cf. Figs. 4 and 5).

If the inductance in the model of Fig. 3 is absent, $a = \infty$, and the parabola degenerates to the straight line $v' = 1$ in the v-plane. Its inversion is a circle of radius ½, tangent to both the line itself and the inside of the unit circle. (We identify the v-plane with the u^*-plane.) Since, evidently, the upper half of this smaller circle is the usual semi-circular Cole-Cole plot,

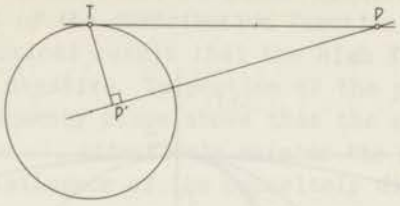

Figure 4.3.5
Geometrical inversion. P' is the inversion of P with respect to the circle, and conversely.

we may reintroduce the original scale by attaching the values ε_∞ and ε_s to its ends (Fig. 6).

As long as $a \geqq 2$ $(s_1 \geqq 2s_2)$, the parabolas lie between the straight line and the larger circle (Fig. 6B). Hence, their inversions with respect to this circle – which are fourth degree curves – are found in the area between the two circles. We notice that the low frequency ends of these Cole-Cole plots show normal incidence, the other ends *grazing* incidence to the axis. The latter property is a consequence of the fact that the tangents in $v = \infty$ to the parabolas are parallel lines and of the isogonality of the transformation.

If $a < 2$, the parabolas in the v-plane intersect the unit circle, so that their low frequency parts lie in its interior (Fig. 6A). Accordingly, upon inversion, the resulting fourth degree curves initially lie outside the larger circle. The points of intersection of parabola and unit circle are invariant under the transformation, and the high frequency parts are again confined to the region between the inner and outer circle. Just as in the former case, there is normal and grazing incidence at the low and high frequency ends, respectively.

It should be noted that the limiting cases, $a = 2$ for the steady state and $a = 4$ for the transient behaviour, do not coincide (cf. [COURANT-HILBERT I]).

The curves of Fig. 6 show that, for finite values of the parameter a, the $\varepsilon'(\omega)$-curve, at high frequencies, descends below its final value ε_∞. The low frequency part of this curve rises above its static value ε_s if $a < 2$. The more important changes in the loss curve are the increased value of its maximum, as compared with the Debye curve, and its different high frequency behaviour: the faster descent of the loss curve, as shown by the grazing incidence of the Cole-Cole plot, explains why the energy loss per second in the dielectric disappears before the optical frequency range has been reached. Note that, in spite of the similarity

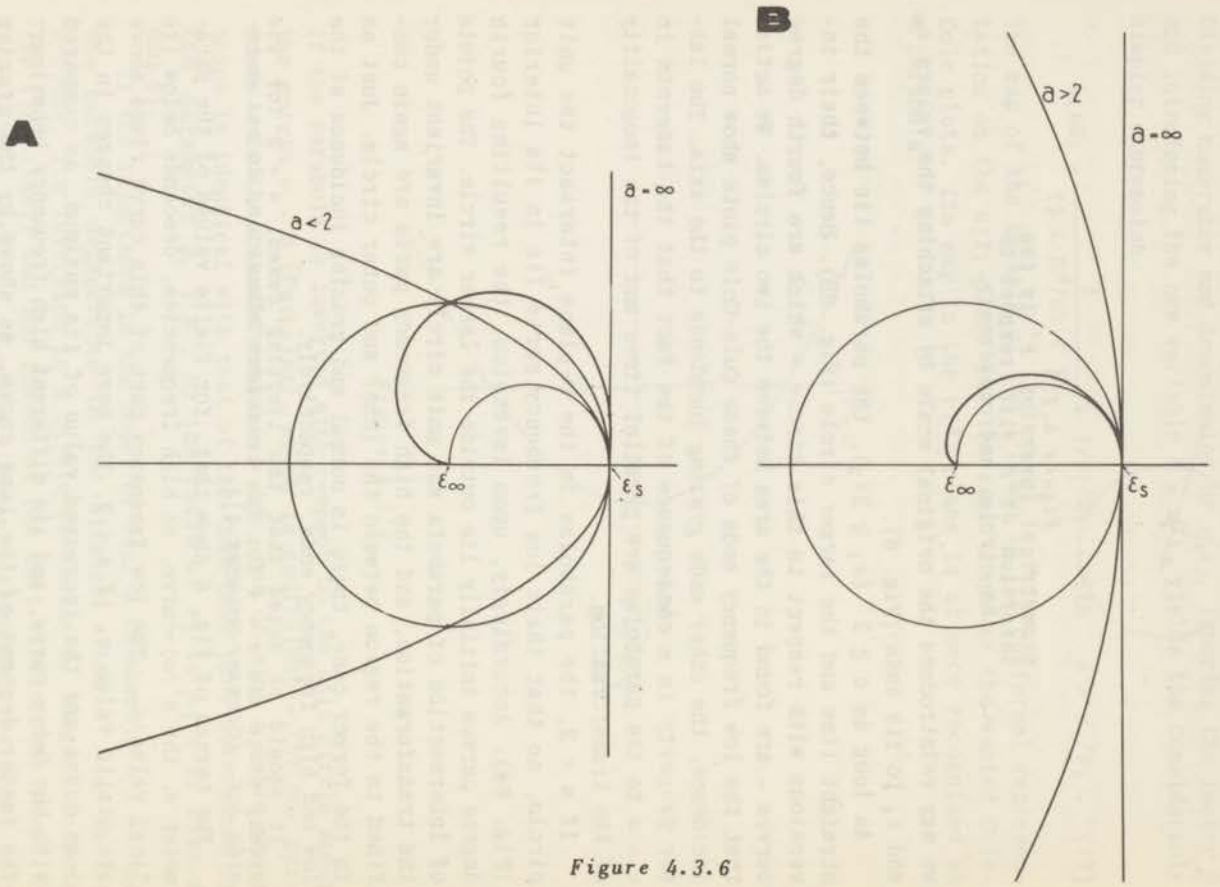

Figure 4.3.6

between the loss curve and the frequency spectrum, the existence of a negative part of the distribution function ($a > 4$) does not lead to the paradoxical result that the high frequency part of the loss curve is negative. Inspection of the potential analogy in the complex frequency plane shows that the normally oriented point dipole in $z = -z_1$ effectively shields the positive imaginary axis from the influence of the oppositely directed dipole in $z = -z_2$ (eqn. (12)).

At present, no direct evidence of the presence of resonance absorption in dielectrics (and viscoelastic or ultrasonic systems) is available. Resonance absorption has been found, however, in the non-linear magnetic behaviour of ferrites [VON HIPPEL]. The indirect evidence for resonance relaxation, viz. the correction of the high-frequency losses in dielectrics, shows that the parameter a must be very large, i.e., $s_2 \ll s_1$. Then (cf. eqns. (6), (7) and (10))

$$z_1 \approx s_2 \qquad \text{and} \qquad z_2 \approx s_1 ,$$

and there is no appreciable change in the Cole-Cole diagram. The failure of the present experimental techniques to detect resonance relaxation places s_1 somewhere in the infrared frequency region.

4.4. Methods for determining the distribution functions

Returning to relaxation phenomena characterized by positive real spectra, we shall now review various procedures that have been suggested as alternatives to the usually unsatisfactory Fuoss-Kirkwood method.

Schwarzl's method ([SCHWARZL, 1951, 1954], [SCHWARZL-STAVERMAN, 1952]), originally proposed for obtaining approximate expressions for the distribution functions from transient measurements on viscoelastic systems, but applicable to the transient responses in other relaxation phenomena, is based on Post's inversion formula for the Laplace transformation ([WIDDER], [HIRSCHMAN-WIDDER]):

If

$$\psi(t) = \int_0^\infty e^{-ts} f(s)\, ds , \tag{1}$$

then

$$f(s) = \lim_{n\to\infty} \frac{(-1)^n}{n!} (n/s)^{n+1} (d/ds)^n \psi(n/s) . \tag{2}$$

Schwarzl uses the approximate expressions resulting from (2) for $n = 1, 2, \ldots$; in addition, he introduces another, similar, approximation for $n = 0$, for which value Post's formula yields zero:

$$ {}_0f(s) \approx (1/s)\ \psi(1/s)\ , \tag{3} $$

$$ {}_1f(s) \approx -\ (1/s^2)\ \psi'(1/s)\ , \tag{3a} $$

$$ {}_2f(s) \approx (4/s^3)\ \psi''(2/s)\ , \tag{3b} $$

etc.

A general estimation of the inherent errors of these expressions cannot be given. They are, however, equivalent to substitution of

$$ {}_0K(st) = (1/st^2)\ \delta(s - 1/t) \tag{4} $$

$$ \begin{aligned} {}_1K(st) &= 1\ , \qquad 0 < s < 1/t\ , \\ &= 0\ , \qquad 1/t < s < \infty\ , \end{aligned} \tag{4a} $$

$$ \begin{aligned} {}_2K(st) &= 1 - st/2\ , \quad 0 < s < 2/t\ , \\ &= 0 \qquad\quad , \quad 2/t < s < \infty\ , \end{aligned} \tag{4b} $$

as crude approximations to the kernel

$$ K(st) = e^{-st} $$

of the Laplace transformation into eqn. (1). Earlier methods for approximately deriving the spectra, based on this artifice, were shown by Schwarzl to be equivalent to Post's formula for low values of n. Schwarzl has also given a number of approximate expressions connecting the spectra with the dynamic loss and storage curves. The first order approximation to the spectrum from the loss curve is contained in our formula (4.3.2); higher order approximations involve higher order derivatives. All these methods have in common that the objectionable analytic continuation of the Fuoss-Kirkwood method, which they are intended to avoid, is replaced by the hardly less objectionable higher order derivations of experimental curves, which increasingly magnifies the experimental errors in the measured data. The objection sometimes raised against the present type of inversion formulae can not be sustained, namely that they imply a one-to-one correspondence of the points of the spectra with the points of the experimental curves, whereas the true relationships connect one value of the latter functions with all the values of the distribution functions. For, the obvious procedure for obtaining the derivatives from the measured curves is numerical differentiation by means of

finite difference operators, which should make use of all the datum points ([HARTREE], [SOUTHWELL]). If one compares this method of numerical differentiation with numerical analytic continuation by means of the finite difference approximation (eqn. (29)) to Laplace's equation, one is struck by the great similarity between the two methods; in particular, one finds that both procedures fail because of excessive errors after about the same number of steps have been made.

Recently, Roesler and Pearson published a method free from the inherent shortcomings of the Fuoss-Kirkwood and Schwarzl procedures for calculating the distribution functions [ROESLER-PEARSON]. The principle of this method will be exemplified by the formulae for obtaining the logarithmic frequency spectrum from the logarithmic loss curve. (Actually, Roesler and Pearson's method is more versatile than suggested by this illustration.) In eqn. (4.3.2) we found the following relationship between these two functions:

$$-\bar{y}_1''(v) = \tfrac{1}{2}\int_{-\infty}^{+\infty} f_1(u)\ \operatorname{sech}\ (u - v)\ du\ . \tag{5}$$

It is shown in the theory of Fourier integrals ([TITCHMARSH], [SNEDDON, 1955]) that if

$$h_1(x) = \int_{-\infty}^{+\infty} h_2(x - y)\ h_3(y)\ dy\ , \tag{6}$$

then

$$H_1(\xi) = \sqrt{2\pi}\ H_2(\xi)\ H_3(\xi)\ , \tag{7}$$

with

$$H(\xi) = (1/\sqrt{2\pi}) \int_{-\infty}^{+\infty} h(x)\ e^{ix\xi}\ dx$$

$$\downarrow\uparrow$$

$$h(x) = (1/\sqrt{2\pi}) \int_{-\infty}^{+\infty} H(\xi)\ e^{-ix\xi}\ d\xi \tag{8}$$

(subject to conditions on the functions in the convolution integral (6) that are fulfilled in the present case). Hence, there exists the following relation between the Fourier transforms of the functions in eqn. (5):

$$-\bar{Y}_1''(\xi) = \sqrt{\pi/2}\ F_1(\xi)\ S(\xi)\ , \tag{9}$$

where

$$S(\xi) = (1/\sqrt{2\pi}) \int_{-\infty}^{+\infty} \operatorname{sech}\ x\ .\ e^{ix\xi}\ dx = \sqrt{\pi/2}\ \operatorname{sech}\ \tfrac{1}{2}\pi\xi\ . \tag{10}$$

(The hyperbolic secant is self-reciprocal with respect to Fourier transformation.) Accordingly,

$$-F_1(\xi) = \left(\frac{2}{\pi}\cosh\frac{\pi}{2}\xi\right)\bar{Y}_1''(\xi)\ , \tag{11}$$

which, upon inversion (cf. (8)), yields:

$$\text{if}\qquad \bar{y}_1''(v) = (1/\sqrt{2\pi})\int_{-\infty}^{+\infty}\bar{Y}_1''(\xi)\,e^{-iv\xi}\,d\xi \tag{12}$$

$$\text{then}\quad f_1(u) = -(1/\sqrt{2\pi})\int_{-\infty}^{+\infty}\left(\frac{2}{\pi}\cosh\frac{\pi}{2}\xi\right)\bar{Y}_1''(\xi)\,e^{-iu\xi}\,d\xi\ . \tag{12'}$$

This pair of equations forms the basis of the Roesler-Pearson method. For the numerical evaluation the complex Fourier integrals are replaced by real Fourier sine series; this implies that the loss and distribution function are replaced by odd periodic functions. The period of these functions is taken at least twice as large as the interval of the v-axis over which the loss-curve is significantly different from zero. If a length L of the v-axis is deemed sufficiently large, it is linearly mapped upon an x-axis such that it corresponds to $(o..x..\pi)$. The coefficients a_k of $\sin k\,x$ in the Fourier sine series for $-\bar{y}_1''(x)$ yield the corresponding coefficients b_k of the Fourier series of $f_1(x)$ by the equation

$$b_k = a_k\frac{2}{\pi}\cosh\,(k\pi^2/2L)\ . \tag{13}$$

According to Roesler and Pearson, the artificial periodicity of the functions does not influence the final results. The odd continuation of the functions is used as a matter of mathematical expedience and also has no physical consequences. These statements seem plausible when one compares the relative insignificance of a sufficiently distant negative replica of the frequency spectrum in the underdamped case of resonance relaxation in the preceding Section.

The author devised yet another procedure for the numerical evaluation of the frequency distribution function from loss measurements which has some points in common with both the Fuoss-Kirkwood and Roesler-Pearson methods. The first step, in this method, consists of conformally mapping the entire complex frequency plane, cut along the negative real axis, upon a finite domain. A suitable function to effect this transformation is

$$w = \frac{1 - \sqrt{z}}{1 + \sqrt{z}} \tag{14}$$

It is easily obtained by mapping the cut z-plane upon the right half of the $\sqrt{z}$-plane, followed by a bilinear transformation of this half-plane upon the unit circle of the w-plane.

The four semi-axes of the complex frequency plane are transformed as indicated in Fig. 1. In general, circles $|z| = r$ and radii $\arg z = \theta$ in the z-plane are mapped upon circular arcs defined by, respectively,

$$(\sigma - \frac{1 + r}{1 - r})^2 + \tau^2 = (\frac{2\sqrt{r}}{1 - r})^2 , \tag{15}$$

and

$$\sigma^2 + (\tau - \operatorname{cotan} \tfrac{1}{2}\theta)^2 = \operatorname{cosec}^2 \tfrac{1}{2}\theta , \tag{16}$$

with

$$w = \sigma + i\tau , \tag{17}$$

inside the unit circle $|w| = 1$.

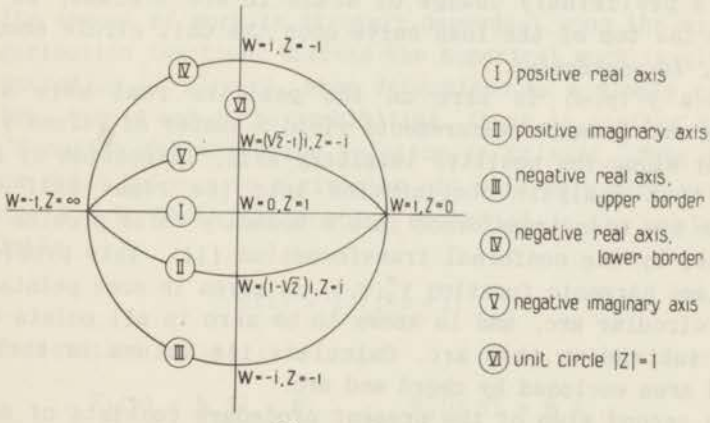

Figure 4.4.1
Semi-axes and unit-circle of z-plane in w-plane.

Interpretations similar to those of Sect. 3.3 may be given to

$$\bar{y}_2(w) = \bar{y}\left\{(\frac{1 - w}{1 + w})^2\right\} \tag{18}$$

in the w-plane. When, e.g., the frequency spectrum is a rectangular function, that is, if

$$\bar{y}(z) = P \log \frac{b + z}{a + z} , \tag{19}$$

the corresponding $\bar{y}_2(w)$ may be looked upon as the complex potential belonging to a pair of finite hydrodynamic dipoles symmetri-

cally located with respect to the real axis on the circumference of the unit circle of the w-plane.

Note that:

1. Every $\bar{y}(z)$ defined by Stieltjes's equation yields a $\bar{y}_2(w)$ which is regular inside $|w| = 1$.

2. The source-sink distribution upon this circle also gives rise to a potential field *outside* it. Since every z_o that is not a negative real number is transformed into *two* points $\frac{1-\sqrt{z_o}}{1+\sqrt{z_o}}$ and $\frac{1+\sqrt{z_o}}{1-\sqrt{z_o}}$ inside and outside the unit circle of the w-plane, respectively, the exterior potential is a repetition of the interior potential; only the latter one is used for the present purpose.

3. The symmetry and anti-symmetry of $\bar{y}'(p,\omega)$ and $\bar{y}''(p,\omega)$ in ω causes $\bar{y}_2'(\sigma,\tau)$ and $\bar{y}_2''(\sigma,\tau)$ to have the same properties in τ.

4. A preliminary change of scale in the z-plane, so as to locate the top of the loss curve upon the unit circle about the origin, is convenient.

Since $\bar{y}''(p,\omega)$ is zero on the positive real axis of the z-plane and dynamic measurements yield a number of values $\bar{y}''(o,\omega) = \bar{y}''(\omega)$ along the positive imaginary axis, inspection of Fig. 1 shows that analytic continuation into the right half of the z-plane has been transformed into a boundary value problem in the w-plane, by the conformal transformation (14). This problem is: The plane harmonic function $\bar{y}_2''(\sigma,\tau)$ is given in some points along a 90° circular arc, and is known to be zero in all points of the chord subtending this arc. Calculate its values in the lens-shaped area enclosed by chord and arc.

The second step of the present procedure consists of solving this boundary value problem. Originally, the author used Southwell's relaxation method for numerically evaluating $y_2''(\sigma,\tau)$ inside the lens [Southwell]. In this method, the Laplace equation is replaced by its finite difference approximation in a square or triangular grid.

It is well-known that the value of a plane harmonic function at a point is the mean of the values it assumes upon an infinitesimal circle surrounding it. In the finite difference equation corresponding to Laplace's equation, this fundamental property of a plane harmonic function is replaced by equality of its value at a point of the square or triangular grid to the average of the values it assumes in four or six symmetrically arranged equidistant points of the grid. Southwell's method essentially consists of assuming arbitrary trial values of the function in question at the nodal points of the grid, calculating the deviations (residuals) of these values from the finite difference equation, and systematically improving the trial values until the residuals

are negligible or zero. Southwell gives an intuitive mechanistic background to the procedure by describing the grid as a tensioned net of springs: the distances from a reference plane of the nodal points of the unloaded net in equilibrium are equal to the values of the function at these points. (Cf. Prandtl's membrane analogue for plane harmonic functions mentioned in Sect. 3.3.) This equilibrium deflection of the net is caused by constraints at its boundary determined by the boundary conditions. The trial values at the start correspond to arbitrary non-equilibrium deflections of the nodal points caused by residual forces (residuals) normal to the reference plane. In the relaxation process, these residual forces are systematically eliminated by mutual neutralization and by transfer to the boundary.

Unfortunately, application of the relaxation method to the present problem is complicated by several factors: the circular arc part of the boundary generally passes between the nodal points of either a square or a triangular net; also, the measured points will not, in general, lie upon the lines of a net, so that a preliminary interpolation is necessary. The author found the actual calculations to be extremely lengthy, but distinctly got the impression that one's speed vastly increases with experience. Also, the amount of work is strongly dependent upon the width of the distribution function. Whereas the numerical work involved in the computation of $\bar{y}_2''(\sigma,\tau)$, when determined by a single relaxation time, turned out to be prohibitive, there is another distribution function for which the solution is trivial. This is the spectrum which belongs to a circular arc Cole-Cole plot having a parameter $\alpha = \frac{1}{2}$. Then, the complex potential in the z-plane is essentially

$$\bar{y}(z) = 1/(1 + \sqrt{z}) \tag{20}$$

and (cf. equation (18))

$$\bar{y}_2(w) = \tfrac{1}{2}\,(1 + w)\,, \qquad \bar{y}_2''(\sigma,\tau) = \tfrac{1}{2}\,\tau\,. \tag{21}$$

Clearly, the distribution function yields a source-sink distribution upon the unit circle in the w-plane causing a homogeneous flow field inside the circle (Fig. 2).

The exterior field is derived from the complex potential $\frac{1}{2}(1+w^{-1})$: the potential outside the circle behaves as if a point dipole were present at the origin. Compare the analogous situation in three dimensions ([BÖTTCHER], [SCHOLTE]).

We conclude that, if $\alpha \approx \frac{1}{2}$, the relaxation procedure for obtaining $\bar{y}_2''(\sigma,\tau)$ inside the lens must also be very simple and that this remains true for distribution functions which qualitatively resemble the functions for these circular arc plots.

The second step of the present method can also be carried out by means of a Fourier sine series development. To do this we need another transformation of the z-plane analogous to (14):

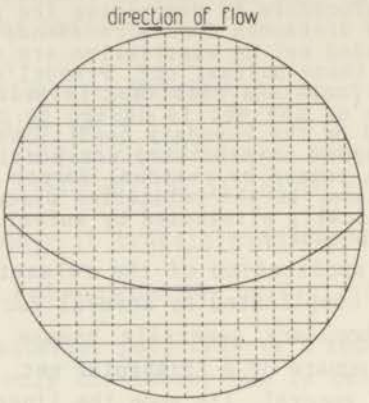

Figure 4.4.2

$$W = \frac{1 - z}{1 + z} = \xi + i\eta = R\, e^{i\alpha} , \tag{22}$$

$$\bar{y}\ (\frac{1 - W}{1 + W}) = \bar{y}_3(W) = \bar{y}_3'(\xi,\eta) + i\bar{y}_3''(\xi,\eta) . \tag{23}$$

We infer from the discussion of eqn. (14) that the imaginary axis of the z-plane maps into the circle $|W| = 1$ and that the interior of this circle is the map of the right half of the z-plane. Analytically, the computation of $\bar{y}_3''(\xi,\eta)$ inside the circle from its given values on the circumference is a much simpler problem than the corresponding calculation of $\bar{y}_2''(\sigma,\tau)$ inside the lens of Fig. 1. For, $\bar{y}_3(W)$ is regular for $|W| \leq 1$, which is a necessary and sufficient condition for

$$\begin{aligned} \bar{y}_3(W) &= \sum_0^\infty a_n\, W^n \\ &= \sum_0^\infty (a_n\, R^n \cos n\alpha + i\ a_n\, R^n \sin n\alpha) . \end{aligned} \tag{24}$$

Hence,
$$\bar{y}_3'' = \sum_0^\infty a_n\, R^n \sin n\alpha \tag{25}$$

inside and on the unit circle about the origin of the W-plane. Some of its values are known for $R = 1$; by smoothing and interpolation, and, if necessary, extrapolation, one is then able to compute the coefficients a_n numerically, for instance, by the method of Danielson and Lanczos, which is also used by Roesler and Pearson in their calculations [DANIELSON-LANCZOS]. When the a_n's are known, it is simply a matter of substituting the appro-

priate values of R (< 1) to obtain (approximately) all the values of $\bar{y}_3''(\xi,\eta)$ inside the circle, and, therefore, of $\bar{y}_2''(\sigma,\tau)$ inside the lens and of $\bar{y}''(p,\omega)$ in the right half of the complex frequency plane.

It may be readily shown that

$$W = e^{-i\alpha} \qquad \text{corresponds to} \qquad \omega/\bar{\omega} = -\tan \tfrac{1}{2}\alpha \,.$$

The frequency scale along the circle $|W| = 1$ is identical with the scale of the semi-circular Cole-Cole diagram (cf. Fig. 2.3.3).

Having obtained $\bar{y}_2''(\sigma,\tau)$ inside the lens by either the relaxation or Fourier series method, we now come to the third step: its values upon the circle $|w| = \sqrt{2} - 1$ are once again developed in a Fourier sine series. Just as for $\bar{y}_3(W)$, we have

$$\bar{y}_2(w) = \sum_0^\infty b_n \rho^n (\cos n\varphi + i \sin n\varphi) \,, \qquad (26)$$

if $\qquad w = \rho e^{i\varphi} \qquad$ and $\qquad \rho < 1 \,.$

Fourier development of $\bar{y}_2''$ upon the smaller circle will yield coefficients

$$c_n = b_n (\sqrt{2} - 1)^n$$

from which the b_n's in eqn. (26) can be obtained immediately (except b_0, whose determination is given below). When the b_n's are known, the analytic continuation of $\bar{y}_2''$ into the area of the unit circle outside the lens and, therefore, of $\bar{y}''$ in the left half of the complex frequency plane is known, so that the classical inversion formula (3.3.12) can be applied:

The counterpart of the frequency distribution function in the w-plane is found to be

$$-(1/\pi) \sum_1^\infty b_n \sin n\varphi \,. \qquad (27)$$

The function $f(s)$ itself is obtained by means of eqn. (14): When

$$z = s_0 e^{\pm i\pi} \,, \qquad w = \frac{1 - s_0}{1 + s_0} \mp i \frac{2\sqrt{s_0}}{1 + s_0} = \cos\varphi \mp i \sin\varphi \,. \qquad (28)$$

It is again supposed that a preliminary change of scale of the z-plane nas placed the maximum of $f(s)$ at or near $s = 1$.

The above method is, of course, also applicable to the calculation of the frequency distribution function from dynamic measurements of the energy storage factor. If the Fourier series procedure is used throughout, one should take cosine instead of sine series. If the relaxation method is used for the second step, the appropriate region into which analytic continuation should be

effected is the one bounded by the *two* 90° circular arcs, i.e., two times the lens of the foregoing description.

The usefulness of the Fourier series method is not restricted to the computation of $f(s)$ from the measured values of loss or storage factor. The second step alone, e.g., adapts the Kronig-Kramers relations to numerical evaluation:

If $\bar{y}_3'(\xi,\eta)$ is known along $|W| = 1$, the coefficients a_n of eqn. (24), and therefore $\bar{y}_3''(\xi,\eta)$, can be calculated.

If, on the other hand, $\bar{y}_3''$ is known for $R = 1$, all the a_n's except a_o can be found; hence, the Fourier cosine series yields $\bar{y}_3'$ apart from this constant. However, the requirement that $\bar{y}_3' = o$ for $R = 1$, $\alpha = \pm\pi$, relates a_o to the other coefficients through

$$a_o = a_1 - a_2 + a_3 - a_4 + \ldots .$$

(This is also the method for obtaining b_o referred to above.)

It is not easy to give an appraisal of the procedures described in the foregoing. The method for the frequency spectrum is certainly at least twice as laborious as the Roesler-Pearson procedure; for, not counting the transformations, it generally involves the calculation of two Fourier series instead of one, or the application of the Southwell method and the calculation of one Fourier series. A point in favour of the present method is that the periodicity in the representation does not come in artificially, which is, however, probably only of academic interest. The main reason for including a description of our method here was that it is a logical consequence and an extension of the potential analogy for Stieltjes' integral equation. Originally, the author tried to obtain a numerical inversion procedure by exclusively using Southwell's relaxation method. This method, however, although it never fails to solve the kind of problem of the second step, viz. the determination of a plane harmonic function *within* from its given values *upon* a closed boundary, can not be used – and is not intended – for the extrapolation of a potential towards its sources. A tentative extrapolation by means of the finite difference approximation to the Laplace equation for a square net:

$$\begin{array}{ccccc} & & \circ\ \bar{y}_2 & & \\ \bar{y}_3 & \circ & \circ\ \bar{y}_o & \circ\ \bar{y}_1 & \\ & & \circ\ \bar{y}_4 & & \end{array} \qquad 4\,\bar{y}_o = \bar{y}_1 + \bar{y}_2 + \bar{y}_3 + \bar{y}_4 \,. \qquad (29)$$

showed an intolerable accumulation of errors after the first few steps outside the boundary had been taken.

Only after Roesler and Pearson's publication came to his attention did the author think of transforming the cut z-plane into the interior of a unit circle, which leads to the third step in the above description. Our method for the calculation of the loss factor from the storage factor, or conversely, is somewhat simpler than a numerically similar, but theoretically different procedure given in [ROESLER].

4.5. Continued fractions as an alternative to the distribution functions

The introduction in Chapters 1 and 2 of the distribution functions into our description of the phenomenological theory was based on the existence of two kinds of mechanical and electric networks that are simply related to the Laplace transforms $\overline{\psi}(z)$ and $\overline{\varphi}(z)$. It was observed that many other linear networks could have been used for the characterization of the operators; the choice that led to the distribution functions was made because of its mathematical simplicity. The discussion of the present Section will mainly be concerned with electric networks and dielectrics; the application to other relaxational systems will by now be obvious.

In Figure 2.4.3, the two macroscopic models that are intimately related to the retardation and relaxation distribution functions were reproduced. We now introduce a third type of electric network, the configuration of which is simply and unambiguously related to a quite different kind of analytical expression for its generalized impedance and admittance (Fig. 1).

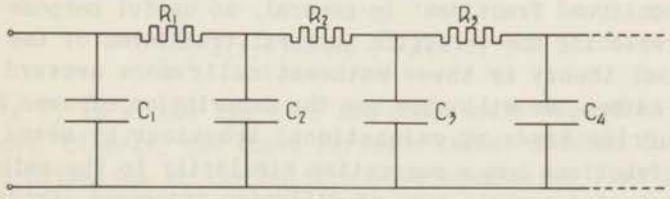

Figure 4.5.1

The generalized impedance of this *ladder* network is found to be the following *continued fraction* (cf. [JAEGER]):

$$Z(z) = \cfrac{1}{C_1 z + \cfrac{1}{R_1 + \cfrac{1}{C_2 z + \cfrac{1}{R_2 + \cfrac{1}{C_3 z + \ddots}}}}} \qquad (1)$$

The generalized admittance clearly is the denominator of this expression, i.e., the sum of $C_1 z$ and a continued fraction with R_1 for its first partial denominator. The expression (1) is known as the *continued fraction of Stieltjes*. (C_n and R_n are required to be positive real numbers, as is obvious when they are capacitances and resistances.) As is to be expected, these continued fractions are intimately connected with Stieltjes's integral equation [STIELTJES].

The continued fraction (1) may be either finite or infinite; a rather trivial example of the former alternative is provided by the Voigt-type model for a dielectric characterized by a single retardation time (Fig. 4.3.2), for which

$$Z(z) = \cfrac{1}{C_1 z + \cfrac{1}{R_1 + \cfrac{1}{C_2 z}}} \qquad (2)$$

It can be shown that the poles of the *approximants* of (1) are all real, simple and have positive residues [WALL]. These poles all lie on the negative half of the real axis.

The $(2n - 1)$-st approximant of (1) is the generalized impedance of the ladder network obtained by omitting the elements to the right of C_n in fig. 1. The even approximants have a mathematical meaning only.

The present Section will not be devoted to a systematic treatment of linear relaxation phenomena based upon the analytic theory of continued fractions: in general, no useful purpose is served by replacing the versatile integral transforms of the phenomenological theory by these mathematically more awkward expressions. Rather, we will show how the description of some frequently occurring kinds of relaxational behaviour by means of continued fractions has a suggestive similarity to the mathematical treatment of a certain type of diffusion processes [GROSS, 1953].

The following example provides a simple illustration:

If the ladder network of Fig. 1 contains an infinite number of elements, the capacitances all having the value C and the resistances the value R, its generalized impedance is given by the *periodic* continued fraction

$$Z(z) = \cfrac{1}{Cz + \cfrac{1}{R + \cfrac{1}{Cz + \ddots}}} \tag{2}$$

Periodic continued fractions of this type are readily evaluated: if the first two elements of the infinite ladder network are omitted, its impedance remains the same. Therefore

$$Z(z) = \cfrac{1}{Cz + \cfrac{1}{R + Z(z)}}$$

and

$$Z(z) = -\tfrac{1}{2} R + \{\tfrac{1}{4} R^2 + (R/Cz)\}^{\frac{1}{2}} . \tag{3}$$

We suppose now that both R and C become infinitesimally small, but that their ratio remains finite. The generalized impedance of the resulting network evidently becomes

$$Z(z) = \sqrt{(R/Cz)} . \tag{4}$$

The electric network obtained from the ladder network by the above limiting process is well-known: it is a semi-infinite uniform *RC-transmission line*; the generalized impedance (4) is its so-called *characteristic* or *surge* impedance ([JAEGER], [MCLACHLAN]).

A technical realization of this kind of network is the "unloaded" submarine cable.

The transmission line is an electric network characterized by distributed instead of *lumped* circuit parameters; the present *RC*-transmission line has a resistance R and a capacitance C *per unit length*. The uniform transmission line is governed by a *partial* differential equation, the well-known *telegrapher's equation*. For the uniform *RC*-line, this equation is

$$\frac{\partial^2}{\partial x^2} X(x,t) = RC \frac{\partial}{\partial t} X(x,t) , \tag{5}$$

where $X(x,t)$ is either the time and coordinate dependent voltage or current. Clearly, the above periodic ladder network is a physical approximation to the uniform *RC*-transmission line in which the distributed resistance and capacitance have been replaced by the lumped elements corresponding to a unit length: its time and coordinate dependent voltage and current are governed by the finite difference approximation to the partial differential equation (5).

Similarly, the two-dimensional Laplace equation governs the

steady state voltages in a homogeneous conductive sheet of material. Its finite difference approximation (4.4.29) describes the voltages in a substitute for the sheet, namely a square grid of identical resistors.

In two respects, the above results are significant for the theory of relaxation processes:

1. According to Cole and Cole, dielectrics characterized by a circular arc plot can be represented by the following equivalent network [COLE-COLE]:

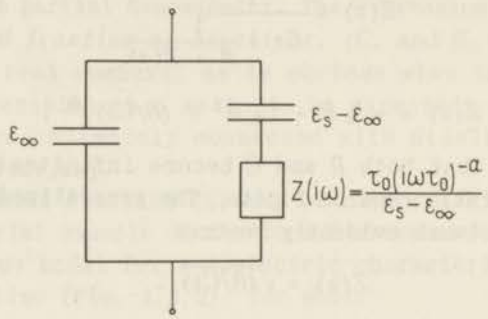

Figure 4.5.2

The component represented by the rectangle has the remarkable property that its loss angle is independent of frequency (cf. Fig. 3.3.6, second picture). The construction of this component from the fundamental network elements was not discussed by Cole and Cole. Here, a physical realization of this component, for the special case that $\alpha = \frac{1}{2}$, has just been found in the uniform semi-infinite *RC*-line.

2. This apparently trivial result becomes more meaningful when we realize that (5) is identical with the one-dimensional *diffusion* equation. This identity is not merely formal: the processes taking place in the *RC*-line, under given initial and boundary conditions, may equally well be interpreted as diffusion of electric charge into a semi-infinite continuum.

Attractive as this approach to a possible interpretation of relaxation phenomena appears, it is somewhat premature to base it solely upon the present example, the more so since apparently no special significance attaches to the value ½ of the parameter α of the circular arc plot. To obviate at least this objection, the author tried to generalize the foregoing interpretation to other values of the parameter. The straightforward method for obtaining the Stieltjes continued fraction expansion of a given function is a difficult task [WALL]. Moreover, although (3) is equivalent to

such an expansion, (4) is obtained by means of a limiting process, and it can be shown that it does not correspond to a Stieltjes fraction proper. It was, however, found to be possible to start from the *continued fraction of Gauss* and to obtain, by means of equivalence transformations, an expression for $z^{-\alpha}$ which is the required limit of a Stieltjes continued fraction.

A special case of the continued fraction of Gauss is

$$(1+z)^{\alpha} = 1 + \cfrac{a_1 z}{1 + \cfrac{a_2 z}{1 + \cfrac{a_3 z}{1 + \cfrac{a_4 z}{1 + \ddots}}}} \tag{6}$$

with $a_1 = \alpha$, $a_2 = \dfrac{1\,(1-\alpha)}{1.2}$,

$a_3 = \dfrac{1\,(1+\alpha)}{2.3}$, $a_4 = \dfrac{2\,(2-\alpha)}{3.4}$,

$a_{2n+1} = \dfrac{n\,(n+\alpha)}{2n\,(2n+1)}$, $a_{2n} = \dfrac{n\,(n-\alpha)}{(2n-1)\,2n}$.

The expansion (6) is valid exterior to the cut along the negative real axis from -1 to $-\infty$ and furnishes the analytic continuation of the Taylor series expansion of the function on the left side outside its circle of convergence $|z| = 1$. It is convenient to throw (6) into another form by means of a so-called *equivalence transformation*. This consists in multiplying numerators and denominators of successive fractions by numbers different from zero. We obtain

$$(1+z)^{\alpha} = 1 + \cfrac{c_1 a_1 z}{c_1 + \cfrac{c_1 c_2 a_2 z}{c_2 + \cfrac{c_2 c_3 a_3 z}{c_3 + \cfrac{c_3 c_4 a_4 z}{c_4 + \ddots}}}} \tag{7}$$

Evidently, the partial numerators of this continued fraction may be made all equal to unity by determining the c_n recurrently from the equations

$$c_1 a_1 z = 1\,, \qquad c_n c_{n+1} a_{n+1} z = 1\,, \qquad n = 1,\ 2,\ 3,\ \ldots$$

In the resulting continued fraction

$$(1 + z)^{\alpha} = 1 + \cfrac{1}{c_1 + \cfrac{1}{c_2 + \cfrac{1}{c_3 + \ddots}}} \tag{8}$$

the c_n's are found to be

$$c_1 = \frac{1}{\alpha z} ,$$

$$c_n = 2\,\frac{(\alpha)_k}{(1 - \alpha)_k} , \qquad n = 2k$$

$$c_n = \frac{2k + 1}{\alpha} \cdot \frac{(1 - \alpha)_k}{(1 + \alpha)_k} \cdot \frac{1}{z} , \qquad n = 2k + 1 .$$

The usual notation

$$(p)_k = p\ (p + 1)\ (p + 2)\ \ldots\ (p + k - 1) = \frac{\Gamma(p + k)}{\Gamma(p)} \tag{8'}$$

has been introduced here [Sneddon, 1956]. Substituting $1/z$ instead of z yields the Stieltjes continued fraction for $(1 + 1/z)^{\alpha} - 1$, provided that $0 < \alpha < 1$; this expansion is valid exterior to the cut from 0 to -1 along the real axis. Next we observe that

$$(h + \frac{1}{z})^{\alpha} = h^{\alpha}\,(1 + \frac{1}{hz})^{\alpha} = h^{\alpha} + \cfrac{h^{\alpha}}{\cfrac{hz}{\alpha} + \cfrac{1}{2\,\cfrac{\alpha}{1 - \alpha} + \cfrac{1}{3\,\cfrac{(1 - \alpha)}{\alpha\,(\alpha + 1)}\,hz + \ddots}}}$$

(9)

where h is a positive real factor and the expression holds outside the cut from $z = 0$ to $z = -1/h$ along the real axis. Another simple equivalence transformation yields

$$(h + \frac{1}{z})^{\alpha} = h^{\alpha} + \cfrac{1}{d_1 + \cfrac{1}{d_2 + \cfrac{1}{d_3 + \ddots}}} , \tag{10}$$

with $d_1 = \dfrac{h^{1-\alpha}\, z}{\alpha}$

$$d_n = 2\,\frac{(\alpha)_k}{(1 - \alpha)_k} \cdot h^{\alpha} , \qquad n = 2k ,$$

$$d_n = \frac{2k+1}{\alpha} \cdot \frac{(1-\alpha)_k}{(1+\alpha)_k} \cdot h^{1-\alpha} \cdot z, \qquad n = 2k+1 .$$

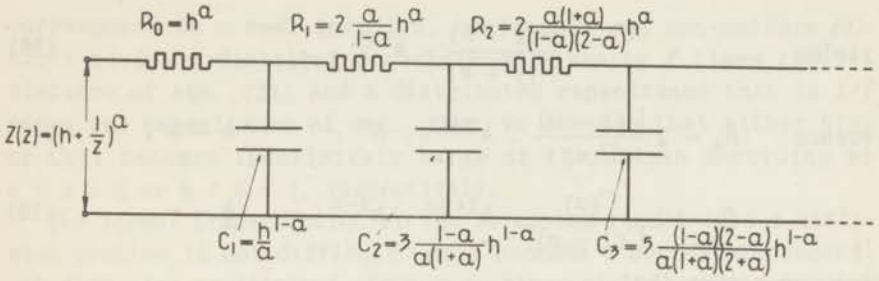

Figure 4.5.3

Figure 3 shows the two-terminal network having the generalized impedance (10). A check upon the correctness of eqn. (10) is provided by the substitution of the special value $\alpha = \frac{1}{2}$; then, $R_o = \sqrt{h}$ and $R_n = C_n = 2\sqrt{h}$, which makes the network of the Figure very similar to the one described by eqn. (2). It is easily shown that the generalized impedance

$$Z(z) = f\,(h + \frac{1}{z})^\alpha \qquad (11)$$

corresponds to a ladder-network in which all the resistances are f times as large and all the capacitances $1/f$ times as large as those of the network of Fig. 3; this is the physical counterpart of a simple equivalence transformation of the right side of eqn. (10), when multiplied by the factor f.

Finally, we have to devise a limiting process which corresponds to the transition from eqn. (3) to eqn. (4). The network of Fig. 3 is again regarded as the discrete approximation to a continuous semi-infinite *RC*-line which now, however, is non-uniform when $\alpha \neq \frac{1}{2}$. From (8') and (10) the k^{th} resistance and capacitance in the discrete network are found to be

$$R_k = 2\frac{\Gamma(1-\alpha)}{\Gamma(\alpha)} \cdot \frac{\Gamma(\alpha+k)}{\Gamma(1-\alpha+k)}\, h^\alpha \qquad (12)$$

and

$$C_k = (2k+1)\frac{\Gamma(\alpha)}{\Gamma(1-\alpha)} \cdot \frac{\Gamma(1-\alpha+k)}{\Gamma(1+\alpha+k)}\, h^{1-\alpha} . \qquad (13)$$

(The latter expression was simplified by means of the fundamental property

$$\Gamma(1+\alpha) = \alpha\,\Gamma(\alpha) \qquad (14)$$

of the gamma function.)

When k is large, Stirling's formula

$$\log \Gamma(x) \approx (x - \tfrac{1}{2}) \log x - x + \log \sqrt{2\pi} \tag{15}$$

yields

$$\frac{\Gamma(x + k)}{\Gamma(y + k)} \approx k^{x-y} , \tag{16}$$

whence

$$R_k \approx 2 \frac{\Gamma(1 - \alpha)}{\Gamma(\alpha)} \cdot k^{2\alpha-1} \cdot h^{\alpha} , \qquad k \to \infty , \tag{17}$$

$$C_k \approx 2 \frac{\Gamma(\alpha)}{\Gamma(1 - \alpha)} \cdot k^{1-2\alpha} \cdot h^{1-\alpha} , \qquad k \to \infty . \tag{18}$$

Now, we assume that

$$k = x N , \qquad \Delta k = 1 \leftrightarrow \Delta x = 1/N , \tag{19}$$

where N is a large integer and x the distance of a point of the continuous semi-infinite cable from its end; furthermore, h be connected with N by

$$h = c/N^2 , \tag{20}$$

where c is an arbitrary positive real constant. Then it follows from (17) that

$$R_k = 2 \frac{\Gamma(1 - \alpha)}{\Gamma(\alpha)} x^{2\alpha-1} N^{2\alpha-1} c^{\alpha} N^{-2\alpha}$$

$$= 2 \frac{\Gamma(1 - \alpha)}{\Gamma(\alpha)} c^{\alpha} x^{2\alpha-1} \cdot 1/N = R(x) \Delta x ,$$

whence

$$R(x) = 2 \frac{\Gamma(1 - \alpha)}{\Gamma(\alpha)} c^{\alpha} x^{2\alpha-1} ; \tag{21}$$

eqn. (18) yields

$$C_k = 2 \frac{\Gamma(\alpha)}{\Gamma(1 - \alpha)} x^{1-2\alpha} N^{1-2\alpha} c^{1-\alpha} N^{2\alpha-2}$$

$$= 2 \frac{\Gamma(\alpha)}{\Gamma(1 - \alpha)} c^{1-\alpha} x^{1-2\alpha} \cdot 1/N = C(x) \Delta x ,$$

whence

$$C(x) = 2 \frac{\Gamma(\alpha)}{\Gamma(1 - \alpha)} c^{1-\alpha} x^{1-2\alpha} . \tag{22}$$

Eqns. (21) and (22) represent the final result of the rather laborious manipulations of the preceding pages: the network element in Fig. 2 whose generalized impedance is

$$Z(z) = f\, z^{-\alpha}, \qquad f = \frac{\tau_o^{1-\alpha}}{\varepsilon_s - \varepsilon_\infty}, \tag{23}$$

corresponds to a semi-infinite, continuous and non-uniform *RC*-cable having a distributed resistance given by f times the resistance of eqn. (21) and a distributed capacitance that is $1/f$ times the capacitance of eqn. (22). We observe that either $R(x)$ or $C(x)$ becomes indefinitely large at the origin according as $0 < \alpha < \frac{1}{2}$ or $\frac{1}{2} < \alpha < 1$, respectively.

The formal transcription of the foregoing result into a diffision problem is not difficult: $R(x)$ becomes a coordinate dependent diffusion coefficient, $C(x)$ a continuously variable parameter connecting the time and coordinate dependent "driving force" $V(x,t)$ to the concentration of charge $Q(x,t)$. Analogous parallels may be drawn to viscosity (diffusion of momentum) or the conduction of heat. In general, the possibility of connecting the phenomenological description of relaxation processes with these preeminently dissipative physical phenomena is much more satisfactory than their formal description in terms of distribution functions, which bear no obvious relation to other relevant physical processes.

However, specifically having interpreted a frequently occurring type of relaxational behaviour as a diffusion phenomenon, we are confronted with the problem of how to explain the significance of the coordinate dependent parameters corresponding to eqns. (21) and (22). Such further interpretation of the diffusion model falls outside the domain of the phenomenological theory. It would be of considerable interest because of the wide-spread occurrence of the circular arc plot: not only the relaxational behaviour of many dielectrics but also that of some paramagnetic ([VAN DEN HANDEL], [VAN DER MAREL]) and viscoelastic [NOLLE] systems is satisfactorily described by this type of diagram.

In some dielectrics the loss factor is small and practically constant over a large range of frequencies ([KAUZMANN], [GARTON], [MÜLLER, 1953]). Gross extensively discussed transient behaviour of viscoelastic systems in which the rate of creep is proportional to t^{-m} ($0 < m < 1$) over a large interval of the time axis [GROSS, 1947]. It is readily shown that these phenomena are two aspects of the same type of relaxational behaviour, viz. that of the present diffusion model. Clearly, this model can not represent a physical system over the *entire* frequency or time axis. It is to be expected that only minor changes in its parameters are necessary to yield a diffusion model that shows the same charac-

teristic behaviour in large but finite regions of these axes. Our method for deriving the diffusion analogy has the obvious disadvantage of not yielding information about the kind and magnitude of these changes. In general, ladder-type networks as models for relaxational behaviour are far more difficult to obtain than the distribution functions; moreover, the qualitative relationships between the spectra and the characteristic functions, discussed in the preceding and present Chapters, are not known for the continued fraction representations.

Chapter 5

THE PHYSICAL BACKGROUND OF RELAXATION PROCESSES

Although the preceding phenomenological theory is useful for the description and correlation of the various types of linear relaxation processes, it can only partially contribute to their interpretation, since, except for the functional relation between the two time dependent parameters X and Y of Sect. 3.1, the theory ignores all other information about the systems in which the processes take place. In this respect the phenomenological theory may be compared with thermodynamics or electric network theory, inasmuch as these branches of science are also concerned with a limited set of macroscopic parameters of the systems they describe.

When providing a physical background for relaxational behaviour we must obviously be prepared to lose much of the generality of the preceding theory, since more specific properties of the systems must be taken into account. Therefore, no attempt has been made in this Chapter to give even a small sample of the numerous theories put forward to explain relaxational behaviour in terms of other physical processes. Instead, we will discuss a few subjects illustrative for some points specifically mentioned in the preceding Chapters. The first subject to be discussed is mechanical damping due to the so-called thermoelastic effect [PÄSLER].

A straight elastic bar or fibre, clamped at one end, vibrates transversely when the other end is deflected from its equilibrium position and released. If the surrounding medium is a gas, the damping of the vibration is found to be proportional to the pressure; hence, such a fibre (usually made from quartz) can be used as a manometer. At pressures lower than 10^{-3} to 10^{-8} mm Hg, however, it is found that the damping ceases to be proportional to the pressure and approaches a constant limiting value. Even in quartz, which is generally regarded as an almost perfectly elastic solid, the residual damping, although small, can be easily measured. (The time in which the amplitude decreases to half its ini-

tial value is of the order of 10^3 sec for an unloaded fibre 50 mm long and .1 mm thick.)

The residual damping can be entirely explained in terms of a macroscopic effect, thermoelasticity: when the fibre is deflected from its straight equilibrium position, the material on the convex side is elongated and that on the concave side is compressed. Since almost all solids, namely those with a positive coefficient of thermal expansion, decrease or increase their temperature when they are adiabatically subjected to a positive or negative strain, respectively, the temperature of the convex side will be lower and that of the concave side higher than the equilibrium value. Clearly, the actual compression and elongation do not take place under either adiabatic or isothermal, but rather under intermediate (polytropic) conditions: at very high frequencies the processes will be almost adiabatic, at very low frequencies almost isothermal.

In the oscillating system, i.e., the fibre or bar together with possibly attached masses to determine the frequency, there is a continual interconversion of kinetic and elastic energy. In addition, twice in each cycle a small amount of elastic energy is *reversibly* converted into heat at one side of the material and the opposite process takes place at the other side. On account of the resulting temperature gradient an *irreversible* flow of of heat takes place which explains the observed energy losses.

A quantitative analysis of thermoelastic damping has been given by Zener; therefore, this kind of damping is often called the Zener effect. The analysis shows the effect to be characterized by an infinite sequence of relaxation times of which only the largest has practical significance. This relaxation time and the magnitude of the damping are found to be determined by the elastic modulus, Poisson's modulus, the coefficient of thermal expansion, the specific heats c_p and c_v, the thermal diffusivity, and the *shape* of the system. Excellent agreement exists between the theoretically predicted and experimentally observed values ([Berry], [Zener]).

The shapes of the energy storage and loss curves are easily understood from the preceding qualitative analysis. With increasing frequency the processes become increasingly adiabatic, i.e., the temperature differentials in the system become more pronounced. Application of the principle of van 't Hoff-le Chatelier shows that, irrespective of the sign of the coefficient of thermal expansion, the changes of temperature are such as to counteract the forces by which they are caused. Therefore, the dynamic rigidity of the bar or fibre increases with frequency and gradually approaches a constant limiting value corresponding to purely adiabatic straining.

The nature of the loss curve may be understood by observing

that, at very low frequencies, the processes are practically isothermal, so that thermal leakage, and hence energy dissipation, is insignificant. At very high frequencies the temperature gradient approaches its maximum value; hence, the average energy loss in an interval of time long compared to the reciprocal frequency also approaches a maximum value. During one cycle, however, the temperature gradient has reversed before appreciable flow of heat takes place, so that the energy loss per cycle vanishes. At some intermediate frequency there is an optimal combination of adiabaticity and time available for the flow of heat which leads to a maximum value of the energy dissipation per cycle.

Thermoelastic damping was presented here as a consequence of a rather special type of deformation producing inhomogeneous strains in elastic solids. This type of damping should always occur, however, when different time dependent strains occur side by side in a system, whether solid, liquid, or gaseous. Such inhomogeneous strains are present, e.g., in a train of longitudinal sound waves in matter. Thermal conductivity absorption of sound, as the effect is then called [MARKHAM *et al.*], is an important effect in gases. In liquids and solids it is usually a secondary phenomenon.

Another type of thermoelastic damping in solids is found in deformation of polycrystalline materials. Here even macroscopically homogeneous strains lead to different stress-strain behaviour in adjacent crystallites because of their elastic anisotropy.

The preceding subject is an example of a satisfactory explanation of a very general type of mechanical relaxation in terms of a well-known macroscopic dissipative process. The next subject to be discussed is not a mechanism but rather an interpretation of viscoelastic phenomena from a point of view somewhat different from that of the first Chapter.

In Chapters 1 and 3 viscoelasticity was presented as a departure from ideal linear elastic behaviour. As early as 1867, however, Maxwell pointed out that ideal viscosity of liquids and ideal elasticity of solids (where *ideal* denotes exact proportionality of the shear stress to the shear rate or angle of shear, respectively) may be regarded as two extremes of the same behaviour. The similarity is succinctly expressed by the Maxwell-element discussed in Sect. 1.3. Maxwell postulated the force-deformation relation governing this series combination of an ideal spring and an ideal dashpot (transcribed as a relation between shear stress and angle of shear) to apply to any solid and liquid. A liquid is characterized by a very small time constant of the element, i.e., it behaves almost like an ideal dashpot. If, on the other hand, the relaxation time is extremely

large, the element is almost an ideal spring and it represents the elastic behaviour of solids. In other words, the experimentally observed inability of liquids at rest to sustain a shear stress is not an absolute attribute of the liquid state, but rather a relative one with respect to the time scale of the experiment, and strained elastic solids are able to sustain stresses for a very long time, but not indefinitely. Maxwell's views on viscosity and elasticity could not be experimentally confirmed at the time they were formulated. His ideas led to a valuable first order approximation, however, for the description of plastic behaviour; the equation

$$\text{shear modulus} = \text{relaxation time} \times \text{viscosity}$$

(cf. our equation (1.4.20)), for systems characterized by a single relaxation time, is known as the *Maxwell relation*.

In 1939 Kuhn extended Maxwell's theory to systems described by discrete or continuous relaxation time spectra [KUHN, 1939]. His formulation of the generalized theory is essentially contained in the equations of Chapt. 1 pertaining to relaxation (as contrasted with retardation) processes.

For ordinary liquids and solids Maxwell's interpretation appears unnecessarily complicated, since the predicted extreme values of the relaxation times fall outside the experimentally accessible time scale. It is invariably observed, however, that an increase of temperature causes the relaxation times to decrease. For substances with a sharp melting point this does not usually suffice to make the relaxation times accessible to measurement, since there is a discontinuous transition from very high to very low time constants when such a substance melts. On the other hand, many materials, such as glasses and many high polymers, are characterized by a continuous transition region between the liquid and solid state. For these substances the discussion of the mechanical properties within the transition region from the point of view of Maxwell's theory is instructive ([KUHN, 1939], [ALFREY, 1948], [STAVERMAN-SCHWARZL, 1956]).

Although Maxwell's ideas are historically of great importance their explicit use is not essential for the axiomatic formulation of the modern theory of viscoelasticity; they explain why, until recently, the description of viscoelastic behaviour in terms of the relaxation family of functions was considered to be the obvious choice.

We will now discuss a representative molecular interpretation of relaxational behaviour, viz. Debye's theory of dielectric dispersion and loss.

In Debye's model for dielectric relaxation in polar liquids the following assumptions are made about the molecules and their interactions [DEBYE] : (i) the molecules are spherical dipole carriers in rotatory Brownian motion; (ii) the motion takes place in a continuous viscous medium; (iii) the internal field acting on the dipoles is the Lorentz field.

Clearly, the first assumption represents an idealization of the actual shape and thermal motion of the particles; since the electric fields are supposed to be uniform, translatory motion of the molecules may be ignored.

The homogeneous viscous medium plays a double role in the model, first as the causative agent for the Brownian motion , i.e., as a heat bath in which the individual particles are immersed, and second as the origin of the energy dissipation in dielectric loss. The apparent contradiction between these two aspects of the mechanical interaction of the molecules is resolved by assuming the angular displacements in the Brownian movement and the times in which they take place to be considerably smaller than, respectively, the displacements brought about by the electric field and the time intervals in which this field changes appreciably.

The assumption that the field acting on the dipoles is the Lorentz field implies a neglection of the electric short-range interaction of the dipoles.

The electric polarization of the above model in a suddenly applied electric field consists of a practically instantaneous *electronic* and *atomic* polarization and a retarded polarization due to the gradual development of a slight preferential orientation of the dipoles in the direction of the field. For the quantitative discussion of the orientational polarization we represent the spatial orientation of each dipole by a point on the surface of a unit sphere, the *configuration space* of the system of dipoles. The resulting ensemble of representative points is conveniently described by means of a distribution function, defined as the density of points in a solid angle $d\Omega$:

$$dN = f \, d\Omega \, . \tag{1}$$

An argument similar to the well-known interpretation of diffusion as a random walk process readily shows the distribution function for the field free system to be governed by the diffusion equation in configuration space

$$\frac{\partial f}{\partial t} = \nabla_{\Omega} (D \nabla_{\Omega} f) \, . \tag{2}$$

$\frac{\partial f}{\partial t} = \nabla \cdot \left(\frac{kT}{\zeta} \nabla f - f M \right)$

[CHANDRASEKHAR]. In the presence of an internal field E' the diffusion equation becomes the *Smoluchowski equation*

$$\frac{\partial f}{\partial t} = \nabla \cdot (D \nabla f - \frac{M}{\zeta} f) \ . \tag{3}$$

In (3) D and ζ are the diffusion and internal friction coefficients, respectively, related by

$$D = kT/\zeta \ , \tag{4}$$

and the quantity M is the torque exercised by the field on the dipoles:

$$M = - \mu E' \sin \theta \tag{5}$$

for dipoles of magnitude μ making an angle θ with the field. Since θ is the only relevant coordinate in the following relations, we introduce

$$d\Omega(\theta) = 2\pi \sin \theta \, d\theta \tag{6}$$

as the domain in configuration space containing the representative points of all the dipoles making angles between θ and $\theta + d\theta$ with the direction of the field. The distribution function belonging to the domain $d\Omega(\theta)$ is governed by

$$\frac{\partial f}{\partial t} = \frac{D}{\sin \theta} \frac{\partial}{\partial \theta} \{ \sin \theta \, (\frac{\partial f}{\partial \theta} + \frac{\mu E' \sin \theta}{kT} f) \} \ . \tag{7}$$

Eqn. (7) describes the behaviour of the dielectric in and *near* equilibrium and is the starting point for Debye's theory.

Substitution of $\partial f / \partial t = 0$ into the Smoluchowski equation yields

$$dN = \frac{N}{4\pi} A \exp \left(\frac{\mu E' \cos \theta}{kT} \right) d\Omega(\theta) \tag{8}$$

for the number of representative points in $d\Omega(\theta)$ if the dielectric is in equilibrium. Since $\mu E'$ is usually much smaller than kT, the Boltzmann factor in (8) may be replaced by the first two terms of its power series expansion in E'. The resulting distribution function

$$f(\theta) = \frac{N}{4\pi} (1 + \frac{\mu E'}{kT} \cos \theta) \tag{9}$$

yields the well-known linear relation

$$p_{av} = \frac{\mu^2}{3 \, kT} E' \tag{10}$$

for the average contribution per dipole to the orientation polarization [BÖTTCHER].

If we only admit non-equilibrium distribution functions of the type

$$f(\theta, t) = \frac{N}{4\pi}\{1 + \frac{\mu\, C(t)}{kT}\cos\theta\} \tag{11}$$

(corresponding to small deviations from equilibrium in time only) where $C(t)$ is a function of $E'(t)$, we obtain

$$p_{av}(t) = \frac{\mu^2}{3\,kT} C(t)\ . \tag{12}$$

According to (12) the dielectric is linear if the relation between $E'(t)$ and $C(t)$ is linear. Introduction of (11) into the diffusion equation (7) indeed yields the linear ordinary differential equation

$$\frac{dC}{dt} = -\,2\,D\,\{C(t) - E'(t)\} \tag{13}$$

for $C(t)$, provided that a term containing the product $E'(t).C(t)$ is omitted. The solution of equation (13) for arbitrary $E'(t)$ is found to be the superposition integral

$$C(t) = \int_0^\infty E'(t-t')\, g(t')\, dt' \tag{14}$$

where

$$g(t) = 2\,D\,e^{-2Dt}\ . \tag{15}$$

Hence

$$p_{av}(t) = \frac{\mu^2}{3\,kT}\int_0^\infty E'(t-t')\, g(t')\, dt'$$

$$= \alpha_{\mu op}\, E'(t) \tag{16}$$

with

$$\alpha_{\mu op} = \frac{\mu^2}{3\,kT}\,(1 + \tau^*\frac{d}{dt})^{-1} \tag{17}$$

(cf. Sect. 1.3); the parameter

$$\tau^* = 1/2\,D = \zeta/2\,kT \tag{18}$$

is called the *intrinsic* relaxation time of the dielectric.

If E' is the Lorentz field, Debye's model represents a dielectric characterized by a single macroscopic relaxation time, which is not the same as τ^*, however. The relation between τ and τ^* may be obtained from the following equations for the steady state behaviour of the dielectric (cf. Sect. 2.1, [BÖTTCHER], and [VON HIPPEL]):

$$D(i\omega t) = \varepsilon_o \, \varepsilon_r(i\omega) \, E(i\omega t) = \varepsilon_o \, E(i\omega t) + P(i\omega t) \, , \qquad (19)$$

where $P(i\omega t)$ is the steady state polarization of the dielectric, i.e., the induced dipole moment per unit volume; this quantity is related to the microscopic quantities by

$$P(i\omega t) = N_1 \, \{\alpha_{ea} + \alpha_\mu(i\omega)\} \, E'(i\omega t) \, , \qquad (20)$$

where N_1 is the number of particles per unit volume, α_{ea} the sum of the electronic and atomic polarizabilities, and (cf. (17))

$$\alpha_\mu(i\omega) = \frac{\mu^2}{3 \, kT} \frac{1}{1 + i\omega\tau^*} \, ; \qquad (21)$$

the Lorentz field is related to the external field by

$$E'(i\omega t) = \frac{\varepsilon_r(i\omega) + 2}{3} E(i\omega t) \, . \qquad (22)$$

Combination of eqns (19) – (22) yields

$$\frac{\varepsilon_r(i\omega) - 1}{\varepsilon_r(i\omega) + 2} = \frac{N_1}{3 \, \varepsilon_o} \left(\alpha_{ea} + \frac{\mu^2}{3 \, kT} \frac{1}{1 + i\omega\tau^*}\right) = \frac{N_1}{3 \, \varepsilon_o} \alpha(i\omega). \qquad (23)$$

The plot of Im $\alpha(i\omega)$ against Re $\alpha(i\omega)$ is clearly a semi-circle in the $\alpha(z)$-plane. Im $\alpha(i\omega)$ attains its maximum value at a frequency $\omega_c^* = 1/\tau^*$. The $\alpha(i\omega)$-plot is obtained from the ordinary Cole-Cole plot by conformal mapping of the $\varepsilon_r(z)$-plane on the $\alpha(z)$-plane by the function

$$\frac{3 \, \varepsilon_o}{N_1} \frac{\varepsilon_r - 1}{\varepsilon_r + 2} \, . \qquad (24)$$

Two important conclusions may be drawn from this relation between the two diagrams: (i) the Cole-Cole plot of a Debye dielectric is a semi-circle if the internal field is the Lorentz field; (ii) a necessary and sufficient condition for other internal fields to yield a semi-circular Cole-Cole plot is that the left side of eqn. (23) be a bilinear function of ε_r (cf. Sect. 2.2).

Quantitative evaluation of eqn. (23) shows the intrinsic and macroscopic relaxation times to be related through

$$\tau^* = \frac{\varepsilon_r(\infty) + 2}{\varepsilon_r(0) + 2} \tau \, . \qquad (25)$$

The ratio τ/τ^* may be quite large; for water it is about 13.

Since the Lorentz field is identical with the electric field inside a dielectric sphere in a uniform external field, such a sphere, characterized by

$$\varepsilon(i\omega) = \varepsilon_\infty + \frac{\varepsilon_s - \varepsilon_\infty}{1 + i\omega\tau} \, ,$$

is found to have the steady state polarizability

$$\alpha(i\omega) = \alpha_\infty + \frac{\alpha_s - \alpha_\infty}{1 + i\omega\tau^*} .$$

Evidently τ^* is not necessarily a molecular parameter.

Criticism of the above theory has mainly been levelled at the wrong point, namely at Debye's supposition, made for the purpose of estimating the magnitude of τ^*, that Stokes's relation for the drag on a macroscopic sphere of radius r rotating in a medium of viscosity η,

$$\zeta = 8\,\pi\eta\, r^3 ,$$

may be substituted for ζ into eqn. (18). The use of the Stokes relation does yield relaxation times of the right order of magnitude, but should not be taken too seriously. Rather, one should regard the Debye theory as an essentially correct approach to the interpretation of dielectric relaxation in which the friction factor ζ is a molecular parameter not simply related to the macroscopic viscosity of the medium [KIRKWOOD]. The weak point of the theory, however, is the use of the Lorentz internal field formula.

Numerous attempts have been made to improve the Debye model by combining it with Onsager's expression for the internal field [POWLES]. This expression accounts, as a first order approximation, for the short-range interaction of the dipoles. As far as the author is aware, these extensions of the Debye theory have in common that the basic Smoluchowski equation is not modified to include the electric interaction which the use of the internal field expressions implies. In one theory this led to the absurd prediction that the Cole-Cole diagram should lie completely outside the semi-circle through ε_s and ε_∞ [BOLTON].

Another approach to the molecular interpretation of relaxation processes is that of reaction rate theory. The application of this theory to relaxational behaviour is suggested by the frequently observed exponential temperature dependence

$$\tau = \tau_o\, e^{A/T} \qquad (26)$$

of relaxation times.

Because of this temperature dependence energy storage and loss factors measured at one frequency and variable temperature can often be plotted in a diagram which is somewhat similar to the conventional Cole-Cole diagram ([STARK], [GUILLIEN]). However, since eqn. (26) may fail to represent the actual temperature

dependence of τ, or alternatively, different parts of a spectrum may be governed by equations of this type with different parameters, the shape of the diagrams thus obtained may differ considerably from that of the "true" Cole-Cole plots.

From the point of view of reaction rate theory, the exponential temperature dependence of τ indicates that at some stage in the physical mechanism underlying relaxational behaviour molecules or other structural units involved have to wait until they have acquired, by thermal fluctuations, an appreciable amount of energy in excess of the average thermal energy in the system. The implications of reaction rate theory for relaxation processes have been extensively discussed in Kauzmann's publication on dielectric relaxation as a chemical rate process [KAUZMANN].

The main objection against the reaction rate interpretation of relaxation processes is that it treats dissipative behaviour in terms of equilibrium thermodynamics and transition probabilities; this treatment offers no clear insight in the nature of the energy losses. Although Kauzmann criticizes the Debye theory, the use of the Smoluchowski equation is probably the more fundamental of the two methods of approach to a molecular understanding of relaxational behaviour. For, in 1940 Kramers has shown that the formalism of chemical rate theory may be obtained from a model of particles in Brownian motion in a potential field consisting of two holes separated by a barrier. In the limit of vanishing friction this model yields expressions equivalent to those of reaction rate theory. When the friction factor is large the model leads to the Smoluchowski equation ([KRAMERS, 1940], [CHANDRASEKHAR], [BRINKMAN]). Recently the Kramers model has been successfully applied to the interpretation of viscoelastic behaviour in high polymers [BRINKMAN-SCHWARZL].

As an application of the ideas of reaction rate theory to a specific mechanical relaxation process we may mention the molecular interpretation of the *Snoek effect*, observed in solid solutions of, e.g., carbon and nitrogen in α-iron or other cubic body centered metals ([SNOEK], [DIJKSTRA]). The internal damping of mechanical oscillations in these systems can be explained as the diffusion of the solutes between interstitial octahedral lattice sites. A strain in the direction of one of the axes of the unit cell causes a dilatation of the corresponding octahedra and hence a preferential migration of the interstitial atoms to these energetically favoured positions. In the course of the migration the foreign atoms have to slip through energetically unfavourable positions, i.e., they have to cross an energy barrier. The observed relaxation time of the damping is in close agreement with the known average jump rate of the interstitial

atoms, which is of the order of one sec^{-1} at room temperature. The temperature dependence of τ is accurately described by eqn. (26). The magnitude of the damping is so closely proportional to the concentration of foreign atoms that this quantity may be determined from relaxation measurements.

We conclude this account of microscopic theories by mentioning the formal interpretation of some relaxation processes in terms of internal heat conduction. For instance, sound absorption in molecular gases can be partly attributed to the lag in the adjustment between the translational and rotational or vibrational degrees of freedom of the molecules. The situation is conveniently described by associating different temperatures with the energies of the corresponding subsystems (which implies equilibrium within them). The entropy production due to the heat exchange between the subsystems readily accounts for the energy dissipation inherent in sound absorption. Quantitative analysis of this model leads to discrete relaxation times, in close agreement with experiment [KNESER].

Similar considerations have been applied to the molecular interpretation of paramagnetic relaxation [GORTER].

It is remarkable that almost all microscopic theories put forward to explain relaxation processes predict discrete distribution functions, usually with one single predominant relaxation time. One of the few exceptions is Fuoss and Kirkwood's theory for dielectric relaxation of solutions of linear macromolecules in non-polar solvents [FUOSS-KIRKWOOD]. This theory yields a symmetrical logarithmic distribution function; the corresponding loss curve has been shown to be in close agreement with that of the circular arc plot ([COLE, 1955], [BÖTTCHER]). In general, however, it may be stated that at present continuous spectra remain essentially unexplained.

Accordingly, no conclusive answer can be given yet to the question of whether or not the spectra are the functions most closely connected with the molecular background of the phenomena. In the preceding Chapters we repeatedly mentioned this question and mainly found evidence for the negative answer. In the present Chapter, however, we found that a number of molecular mechanism *are* associated with single relaxation times. Probably, this result of some molecular considerations has led to the wide-spread belief that the distribution functions have direct molecular significance. There are, of course, more aspects to this controversial subject than we have been able to discuss in this thesis. Thus, in the mechanical and dielectric behaviour of macromole-

cules it sometimes happens that a distinct peak in the distribution functions corresponds to the presence of a certain substituent. Then, such a peak has a direct molecular significance, but the distinction between the macroscopic and intrinsic relaxation times implies that the data of this peak are not necessarily those of its molecular counterpart. In other systems, however, no such clear cut correspondence between the properties of the distribution functions and of the system is apparent. In these cases, chemical and physical modulation of the systems may lead to a better understanding of the physical background of the phenomena. In investigations of this sort the distribution functions are, according to the discussion of Sect. 4.2, the most suitable macroscopic functions to consider because of their sensitivity to slight changes in the observed relaxational behaviour.

SAMENVATTING

Dit proefschrift geeft de resultaten weer van een onderzoek op het gebied van de fenomenologie van lineaire nawerkende systemen. Deze systemen hebben gemeen, dat twee van de tijd afhankelijke parameters, waarvan het product de dimensie energie heeft, door een lineaire operatorbetrekking met elkaar verbonden zijn. De nadere omschrijving van deze betrekking, die op vele manieren kan plaatsvinden, vormt het onderwerp van de eerste twee hoofdstukken en van een deel van het derde hoofdstuk.

Hoofdstuk 1 behandelt ten dele de reeds bekende theorie van lineair visco-elastische stoffen. Meer dan gebruikelijk is echter de, uit de electrische netwerktheorie bekende, beschrijving door middel van de Laplace-transformaties van de grootheden toegepast. Ook wordt vrij uitvoerig ingegaan op het dualisme in de beschrijving, die het gevolg is van de mogelijke – en grotendeels willekeurige – keuze tussen karakteristieke grootheden, gebaseerd op de elasticiteits-modulus of op de slapheids(*compliance*)-operator. Dit dualisme vindt men terug in de fenomenologie van alle lineaire nawerkingsprocessen; bij gebrek aan een betere nomenclatuur is het verschil in dit proefschrift aangeduid door de benamingen *relaxatie-* en *retardatiegedrag*.

In hoofdstuk 2 wordt de behandeling van de theorie, ditmaal toegepast op nawerkende diëlectrica, voortgezet. Het gebruik van gerationaliseerde electrische grootheden leidt hier tot volledige identiteit van de fenomenologie van nawerkende mechanische en diëlectrische systemen. De toepassing van de mechanische theorie op nawerkende diëlectrica is weliswaar herhaaldelijk in de literatuur genoemd, maar tot dusver nog niet in de huidige expliciete vorm gepubliceerd. Als nieuw resultaat moge de interpretatie van het Cole-Cole-diagram als conforme afbeelding van de positieve imaginaire as van het complexe frequentie-vlak genoemd worden.

Hoofdstuk 3 begint met een korte bespreking en classificatie van enige andere systemen waarop de lineaire nawerkingstheorie van toepassing kan zijn. Het blijkt dat de plaats van de parameters in de, voor de processen karakteristieke, energiedifferentiaal bepalend is voor het onderscheid tussen retardatie- en re-

laxatie-processen. In de tweede paragraaf van dit hoofdstuk worden de bekende Kronig-Kramers-relaties besproken. Paragraaf 3.3 is gewijd aan een bespreking van de integraalvergelijking van Stieltjes, de sleutelformule van de theorie der lineaire nawerkingsprocessen. Deze integraalvergelijking verbindt de complexe functies (zoals de analytische voortzetting van de complexe permittiviteit) met de, voor nawerkende systemen karakteristieke, nawerkingsfrequentie-verdelingsfuncties of -spectra. Aangezien ook in de recente literatuur nog misverstanden over het wezen van deze complexe functies blijken voor te komen, leek een uitvoerige behandeling van dit onderwerp gerechtvaardigd. De bespreking is gebaseerd op een aanschouwelijke twee-dimensionale potentiaalanalogie, die nog niet eerder in de betreffende literatuur genoemd is. Vervolgens wordt de klassieke omkeerformule voor de Stieltjesvergelijking afgeleid, die nagenoeg identiek is met de door Fuoss en Kirkwood gegeven formule ter berekening van de verdelingsfuncties uit de afhankelijkheid van de verliesfactor van de frequentie.

Hoofdstuk 4 heeft tot onderwerp het verband tussen de verdelingsfuncties en de voor meting toegankelijke grootheden van lineaire nawerkende systemen. In 4.2 wordt aan de hand van een numeriek voorbeeld aangetoond dat het Cole-Cole-diagram (en dus de frequentieafhankelijkheid van energieopslag- en verliesfactor), meer dan men zich doorgaans realiseert, ongevoelig is voor variaties in de verdelingsfuncties. De volgende paragraaf behandelt enige beperkende bepalingen voor het gedrag van Cole-Cole-diagram, verlies- en energieopslagkrommen. Nieuw zijn hier de gegevens over het gedrag van het Cole-Cole-diagram aan de uiteinden, in het bijzonder als resonantie-relaxatie optreedt. De wijze van behandelen is grotendeels gebaseerd op de eigenschappen van het diagram als conforme afbeelding en op het potentiaalbeeld voor de Stieltjesvergelijking. Deze twee resultaten uit de voorgaande hoofdstukken vinden eveneens uitgebreid toepassing in 4.4, waarin enige recente methoden voor de numerieke berekening van de verdelingsfuncties uit meetresultaten zijn samengevat. Aan het slot van het vierde hoofdstuk wordt een kettingbreukontwikkeling gegeven voor de complexe permittiviteit van de grote groep diëlectrica, die door een cirkelboogvormig Cole-Cole-diagram gekenmerkt zijn.

In het laatste hoofdstuk wordt een overzicht gegeven van enige, o.a. moleculaire, physische processen, die in de literatuur voorgesteld zijn ter verklaring van het bijzondere gedrag van nawerkende systemen.

REFERENCES

T. ALFREY, Quarterly Appl. Math. 2, 113-9 (1944).
3, 143-50 (1945).

T. ALFREY and P. DOTY, J. Appl. Phys. 16, 700-13 (1945).

T. ALFREY, *Mechanical Behavior of High Polymers*, New York, 1948.

H. BATEMAN, *Partial Differential Equations of Mathematical Physics*, New York, 1944.

B. S. BERRY, J. Appl. Phys. 26, 1221 (1955).

H. W. BODE, *Network Analysis and Feedback Amplifier Design*, New York, 1945.

H. C. BOLTON, J. Chem. Phys. 16, 486-9 (1948).

C. J. F. BÖTTCHER, *Theory of Electric Polarisation*, Amsterdam, 1952.

H. C. Brinkman, Physica 22, 29-34, 149-55 (1956).

H. C. BRINKMAN and F. SCHWARZL, Discussion of the Faraday Society, Amsterdam, April 1957, *to be published.*

C. BROT, M. MAGAT and L. REINISCH, Koll. Zs. 134, 109-42 (1953).

S. CHANDRASEKHAR, Revs. Mod. Phys. 15, 1-89 (1943).

R. V. CHURCHILL, *Modern Operational Mathematics in Engineering*, New York, 1944.

K. S. COLE and R. H. COLE, J. Chem. Phys. 9, 341-51 (1941).

R. H. COLE, J. Chem. Phys. 23, 493-9 (1955).

P. CORNELIUS and H. C. HAMAKER, Philips Research Repts. 4, 123-42 (1949).

R. COURANT and D. HILBERT, *Methoden der mathematischen Physik*, Vol. I, Berlin, 1924.

G. C. DANIELSON and C. LANCZOS, J. Franklin Inst. 233, 365-80, 435-52 (1942).

D. W. DAVIDSON and R. H. COLE, J. Chem. Phys. 19, 1484-90 (1951).

P. Debye, *Polar Molecules*, New York, 1945.

F. K. DU PRÉ, *Thesis*, Leiden, 1940.

L. J. DIJKSTRA, Philips Research Repts. 2, 357-81 (1947).

H. EISENLOHR, Koll. Zs. 138, 57-8 (1954).

H. FRÖHLICH, *Theory of Dielectrics*, Oxford, 1949.

R. M. FUOSS and J. G. KIRKWOOD, J. Am. Chem. Soc. 63, 385-94 (1941).

C. G. GARTON, Trans. Far. Soc. 42A, 56-60 (1947).

S. Goldman, *Frequency Analysis, Modulation and Noise*, New York, 1948.

C. J. Gorter, *Paramagnetic Relaxation*, Amsterdam, 1947.

E. Goursat, *Cours d'Analyse Mathématique*, Vol. II, p. 266, Paris, 1925.

E. H. Grant, T. J. Buchanan and H. F. Cook, J. Chem. Phys. 26, 156-61 (1957).

B. Gross, J. Appl. Phys. 18, 212-21 (1947).
19, 257-64 (1948).

B. Gross, *Mathematical Structure of the Theories of Viscoelasticity*, Paris, 1953.

B. Gross, Koll. Zs. 134, 65-72, 73-84 (1953).
138, 65-8 (1954).

E. A. Guggenheim, *Thermodynamics*, p. 375, Amsterdam, 1949.

R. Guillien, Ann. Univ. Saraviensis 2, 61-74 (1953).

D. R. Hartree, *Numerical Analysis*, Oxford, 1955.

E. Hiedemann and R. D. Spence, Zs. Physik 133, 109-23 (1951).

I. I. Hirschman and D. V. Widder, *The Convolution Transform*, Princeton, 1955.

C. D. Hodgman, *Handbook of Chemistry and Physics*, Cleveland, 1955.

J. C. Jaeger, *An Introduction to the Laplace Transformation*, London, 1955.

H. Jeffreys and B. Jeffreys, *Methods of Mathematical Physics*, Cambridge, 1956.

Th. von Kármán and M. A. Biot, *Mathematical Methods in Engineering*, New York, 1940.

W. Kauzmann, Revs. Mod. Phys. 14, 12-44 (1942).

G. Kegel, Koll. Zs. 135, 125-33 (1954).

J. G. Kirkwood, J. Chem. Phys. 14, 180-201 (1946).

H. O. Kneser, Koll. Zs. 134, 20-32 (1953).

H. A. Kramers, Atti Congr. Int. Fis. Como, 545-57 (1927).

H. A. Kramers, Physica 7, 284-304 (1940).

R. Kronig, J. Opt. Soc. Am. 12, 547-57 (1926).

W. Kuhn, Zs. physik. Chem. 42B, 1-38 (1939).

W. Kuhn, O. Künzle and A. Preismann, Helv. Chim. Acta 30, 307-28, 464-86 (1947).

J. R. Macdonald and M. K. Brachman, Revs. Mod. Phys. 28, 393-422 (1956).

W. Magnus and F. O. Oberhettinger, *Formeln und Sätze für die speziellen Funktionen der mathematischen Physik*, Berlin, 1948.

J. J. Markham, R. T. Beyer and R. B. Lindsay, Revs. Mod. Phys. 23, 353-411 (1951).

N. W. McLachlan, *Complex Variable Theory and Transform Calculus*, Cambridge, 1953.

J. Meixner, Koll. Zs. 134, 3-20 (1953).

J. MEIXNER, Zs. Physik 139, 30-43 (1954).
J. MEIXNER, Zs. Naturforschung 9a, 654-63 (1954).
J. MEIXNER, Math. Nachr. (1957 or 1958), *in print*.
F. H. MÜLLER, Koll. Zs. 134, 85-101 (1953).
A. W. NOLLE, J. Polymer Sci. 5, 1-54 (1950).
C. OPPENHEIM, J. chim. phys. 48, 376-80 (1951).
M. PÄSLER, Koll. Zs. 129, 65-72 (1952).
O. PERRON, *Die Lehre von den Kettenbrüchen*, Leipzig, 1913.
E. G. PHILLIPS, *Functions of a Complex Variable*, London, 1951.
J. G. POWLES, J. Chem. Phys. 21, 633-7 (1953).
F. C. ROESLER and J. R. A. PEARSON, Proc. Phys. Soc. B57, 338-47 (1954).
F. C. ROESLER, Proc. Phys. Soc. B58, 89-96 (1955).
F. C. ROESLER and W. A. TWYMAN, Proc. Phys. Soc. B58, 97-105 (1955).
TH. G. SCHOLTE, *Thesis*, Leiden, 1950.
F. SCHWARZL, Physica 17, 830-41, 923-30 (1951).
F. SCHWARZL and A. J. STAVERMAN, Physica 18, 791-8 (1952).
F. SCHWARZL and A. J. STAVERMAN, Appl. Sci. Res. A 4, 127-41 (1953).
F. SCHWARZL, Proc. 2nd Int. Congr. Rheology, 197-201 (1954) *).
I. N. SNEDDON, *Functional Analysis. Handbuch der Physik*, Vol. II, 198-348, Berlin, 1955.
I. N. SNEDDON, *Special Functions of Mathematical Physics and Chemistry*, Edinburgh 1956.
J. L. SNOEK, Physica 8, 711-33 (1941).
J. L. SNOEK, Physica 9, 862-4 (1942).
A. SOMMERFELD, *Vorlesungen über theoretischen Physik*, Vol. II, *Mechanik der deformierbaren Medien*, Wiesbaden, 1947.
A. SOMMERFELD, *Vorlesungen über theoretischen Physik*, Vol. III, *Elektrodynamik*, Wiesbaden, 1948.
R. V. SOUTHWELL, *Relaxation Methods in Theoretical Physics*, Oxford, 1946.
H. STARK, Nature 166, 436 (1950).
A. J. STAVERMAN and F. SCHWARZL, *Die Physik der Hochpolymeren*, Vol. IV. Edited by H. A. Stuart. Berlin, 1956.
T. J. STIELTJES, *Oeuvres Complètes*, Vol. II, 402-566, Groningen, 1918.
J. A. STRATTON, *Electromagnetic Theory*, New York, 1941.
D. TER HAAR, Physica 16, 719-37, 738-52 (1950).
E. C. TITCHMARSH, *Introduction to the Theory of Fourier Integrals*, Oxford, 1937.
C. J. TRANTER, *Integral Transforms in Mathematical Physics*, London, 1951.

*) Edited by V. G. W. Harrison.

J. VAN DEN HANDEL, *Advances in Electronics and Electron Physics*, Vol. VI. (Editor L. Martin) New York, 1954.
L. C. VAN DER MAREL, Koll. Zs. 134, 32-38 (1953).
E. VOLTERRA, Proc. 2nd Int. Congr. Rheology, 73-78, London, 1954 *).
A. R. VON HIPPEL, *Dielectrics and Waves*, New York, 1954.
H. S. WALL, *Analytic Theory of Continued Fractions*, New York, 1948.
D. V. WIDDER, *The Laplace Transform*, Princeton, 1948.
C. ZENER, *Elasticity and Anelasticity of Metals*, Chicago, 1948.

*) Edited by V. G. W. Harrison.

Op verzoek van de Faculteit der Wis- en Natuurkunde volgen hier enige persoonlijke gegevens.

Na het behalen van het einddiploma H.B.S.-B in 1942 aan de Gemeentelijke H.B.S. te Leiden begon ik mijn scheikundestudie in october van dat jaar aan de Gemeentelijke Universiteit te Amsterdam. Nadat in mei 1943 verder studeren door oorlogsomstandigheden onmogelijk was geworden, werd de studie in juli 1945 aan de Rijksuniversiteit te Leiden voortgezet. Het candidaatsexamen F in de Wis- en Natuurkunde legde ik af in april 1948.

In juli 1952 legde ik het doctoraalexamen af, met hoofdrichting physische chemie (hoogleraar Dr. C.J.F.Böttcher), bijvak theoretische natuurkunde (hoogleraar Dr. H.A.Kramers, na diens overlijden Dr. J.Korringa, lector).

In de periode 1947-51 heb ik verscheidene malen tijdelijke assistentschappen vervuld aan de afdeling physische scheikunde. Van october 1951 tot mei 1954 was ik belast met de leiding van het candidatenpracticum physische scheikunde, eerst als candidaatassistent, na mijn doctoraalexamen als hoofdassistent. Per 1 januari 1956 werd ik benoemd tot wetenschappelijk ambtenaar.

In mei 1954 werd onder leiding van de hoogleraar Dr. C.J.F. Böttcher met het onderzoek aangevangen, waarvan in dit proefschrift een deel van de resultaten wordt beschreven.

Gaarne wil ik deze gelegenheid benutten om mijn erkentelijkheid tot uitdrukking te brengen aan Prof. R.H.Cole (Brown University) en aan Prof. J.Meixner (Technische Hochschule Aachen) voor stimulerende discussies over het onderwerp van dit proefschrift. Ook dank ik Prof. L.E.Steiner (Oberlin College) voor de bereidwilligheid waarmee hij de eerste vier hoofdstukken gezuiverd heeft van wat schrijver dezes achtte goed Engels te zijn.

Bijlage academisch proefschrift
J.Schrama, Leiden 1957.

STELLINGEN

1

De methode van Fuoss en Kirkwood ter berekening van het nawerkingstijdspectrum uit de frequentieafhankelijkheid van de verliesfactor is slechts in enkele gevallen bruikbaar.

R.M.Fuoss en J.G.Kirkwood, J.Am.Chem.Soc. 63, 387-8 (1941).

2

De uitspraak van Macdonald en Brachman over de pariteit van verliesfactor en frequentieafhankelijk deel van de reële permittiviteit van diëlectrica, beschreven door het cirkelboogvormige Cole-Cole-diagram, is onjuist.

J.R.Macdonald en M.K.Brachman, Revs.Mod.Phys. 28, 405 (1956).

3

De eigenwaarden van de door Rouse gebruikte matrix zijn de wortels van een polynoom, dat nauw verwant is aan enige van de door Heilbronner besproken polynomen. Tussen deze polynomen en de Tschebycheff-polynomen bestaan eenvoudige betrekkingen, die het berekenen van de wortels vergemakkelijken.

J.P.Rouse, J.Chem.Phys. 21, 1276 (1953).
E.Heilbronner, Helv.Chim.Acta 36, 170-88 (1953).
B.van der Pol en Th.J.Weyers, Physica 1, 78-96 (1934).

4

Zeer waarschijnlijk leidt het voorschrift, dat Crane en Rydon geven voor de bereiding van 2-acetoxyaethylamine, niet tot deze verbinding, doch tot N(2-hydroxyaethyl)acetamide.

C.W.Crane en H.N.Rydon, J.Chem.Soc., blz. 530 (1947).

5

Bij het meten van de diëlectrische eigenschappen van vaste stoffen, die in vloeibare toestand in de meetcel gebracht zijn, dient men bijzondere aandacht te besteden aan het vermijden van discontinuïteiten in de inhoud van de cel.

6

De beschouwingen van Skrabal over de gedefiniëerdheid van enige grootheden in de reactiekinetica zijn aanvechtbaar.

A. Skrabal, Monatshefte 87, 613-6 (1956).

7

De hypothese van Fajans omtrent de grotere polariseerbaarheid van ionen van de overgangselementen, ter verklaring van de afwijkende vormingswarmten van verbindingen van deze elementen, is onnodig ingewikkeld.

J.C. Bailar, The Chemistry of Coordination Compounds, New York, 1956.
A.E. van Arkel, Molecules and Crystals in Inorganic Chemistry, London, 1956.

8

Bij het zuiveren van organische oplosmiddelen voor spectrofotometrische doeleinden dient aandacht geschonken te worden aan het verwijderen van opgeloste zuurstof.

A.U. Munck en J.F. Scott, Nature 177, 587 (1956).

9

Het door Lüscher, Pfister, de Zeeuw en anderen voorgestelde gebruik van kleurentests is als psychodiagnostische methode aan bedenkingen onderhevig.

M. Lüscher, Psychologie der Farben, Basel, 1949.
M. Pfister, Die Farbpyramidentest, Psychol. Rundschau, 1, 192 (1949-50).
J. de Zeeuw, Dissertatie Leiden, 1957.

10

Er bestaat een merkwaardige discrepantie tussen de mate van nauwkeurigheid, waarmee in het maatschappelijk leven geldbedragen worden aangegeven, en de nauwkeurigheid van de physische metingen, die voor het verkrijgen van de meeste van deze getallen moeten zijn verricht.